

UC Berkeley

UC Berkeley Previously Published Works

Title

Engineered Transport in Microporous Materials and Membranes for Clean Energy Technologies

Permalink

<https://escholarship.org/uc/item/1nb0c4hb>

Journal

Advanced Materials, 30(8)

ISSN

0935-9648

Authors

Li, Changyi
Meckler, Stephen M
Smith, Zachary P
et al.

Publication Date

2018-02-01

DOI

10.1002/adma.201704953

Copyright Information

This work is made available under the terms of a Creative Commons Attribution-NonCommercial-NoDerivatives License, available at <https://creativecommons.org/licenses/by-nc-nd/4.0/>

Peer reviewed

Engineered Transport in Microporous Materials and Membranes for Clean Energy Technologies

Changyi Li, Stephen M. Meckler, Zachary P. Smith, Jonathan E. Bachman, Lorenzo Maserati, Jeffrey R. Long, and Brett A. Helms*

Many forward-looking clean-energy technologies hinge on the development of scalable and efficient membrane-based separations. Ongoing investment in the basic research of microporous materials is beginning to pay dividends in membrane technology maturation. Specifically, improvements in membrane selectivity, permeability, and durability are being leveraged for more efficient carbon capture, desalination, and energy storage, and the market adoption of membranes in those areas appears to be on the horizon. Herein, an overview of the microporous materials chemistry driving advanced membrane development, the clean-energy separations employing them, and the theoretical underpinnings tying membrane performance to membrane structure across multiple length scales is provided. The interplay of pore architecture and chemistry for a given set of analytes emerges as a critical design consideration dictating mass transport outcomes. Opportunities and outstanding challenges in the field are also discussed, including high-flux 2D molecular-sieving membranes, phase-change adsorbents as performance-enhancing components in composite membranes, and the need for quantitative metrologies for understanding mass transport in heterophasic materials and in micropores with unusual chemical interactions with analytes of interest.

1. Introduction

Improving the efficiency of membrane-based separations is critical to the advancement of many clean-energy technologies, including gas and chemical separations, carbon capture and sequestration (CCS), water desalination, dehumidification, fuel-cell technology, and electrochemical energy storage (EES). Schemes to engineer highly selective species transport across microporous membranes have progressed considerably in the past decade due to the advent of microporous membrane components with controlled pore architectures and pore chemistries (Figure 1). Here we provide a critical assessment of how the pore architecture and pore chemistry of microporous materials dictate analyte selectivity or specificity. We also discuss emerging opportunities to increase membrane permeability and selectivity, e.g., using high-flux 2D molecular-sieving membranes or phase-change composites. Furthermore, given the composite character of many membrane designs, we

identify a critical need for quantitative metrologies for understanding mass transport and mass transfer across heteromaterial interfaces and in micropores with unusual chemical interactions with analytes of interest. The emerging perspective is that, in contrast to conventional absorptive or adsorptive strategies requiring energy-intensive regeneration procedures, microporous membranes can achieve high fluxes of the desired permeant at markedly lower energetic costs, e.g., to improve gas and chemical separations;^[1] they can often be implemented in a continuous process, consisting of a low-cost, integrated unit with a smaller footprint than the incumbent technology. Microporous membranes also allow electrochemical devices, including fuel cells (FCs) and batteries, to be operated without active material crossover owing to the transport selectivity of their pore architectures, improving the energy efficiency of those devices and ensuring their longevity.

Microporous membrane components considered here feature persistent free-volume elements (i.e., pores) less than 2 nm in diameter, which discriminate between analytes based on size and chemistry. Microporous membranes can either be single component or composites of several materials, of which at least one is microporous. The rigidity of their architectures


Dr. C. Li, Dr. J. E. Bachman, Prof. J. R. Long
Department of Chemical and Biomolecular Engineering
The University of California
Berkeley, CA 94720, USA

S. M. Meckler, Prof. J. R. Long
Department of Chemistry
The University of California
Berkeley, CA 94720, USA

Prof. Z. P. Smith
Department of Chemical Engineering
The Massachusetts Institute of Technology
Cambridge, MA 02139, USA

Dr. L. Maserati, Prof. J. R. Long, Dr. B. A. Helms
Materials Sciences Division
Lawrence Berkeley National Laboratory
1 Cyclotron Rd, Berkeley, CA 94720, USA
E-mail: bahelms@lbl.gov

Dr. B. A. Helms
The Molecular Foundry
Lawrence Berkeley National Laboratory
1 Cyclotron Rd, Berkeley, CA 94720, USA

 The ORCID identification number(s) for the author(s) of this article can be found under <https://doi.org/10.1002/adma.201704953>.

DOI: 10.1002/adma.201704953

influences, and sometimes enforces, size selectivity; thus, low framework mobility is often required. In these instances, the coupled motion of the microporous host material does not directly mediate the transport of guest analytes. As a result, transport selectivity and flux can be decoupled from the intra- and intermolecular mechanical flexibility of the microporous materials, thereby allowing for independent optimization of membrane performance attributes.

The primary classes of microporous materials are (1) inorganics (e.g., zeolites);^[2] (2) hybrids (e.g., metal-organic frameworks, MOFs);^[3] (3) carbons (e.g., carbon nanotubes^[4] and carbon molecular sieves, CMSs);^[5] and (4) organics (e.g., microporous polymers^[6,7] and organic nanotubes).^[8] While significant attention has been paid to the adsorptive^[9] and catalytic^[10–12] properties of high surface area microporous materials, here we will discuss how their unique architectures impact transport selectivity for gases, liquids, and ions. Furthermore, we will address how transport outcomes are affected by both nanoconfinement within free-volume elements and pore-analyte interactions. The emerging perspective, regardless of the type of transport process, is that the unique shape-persistent architectures of these materials permit molecular diffusive permeabilities that are orders of magnitude faster than molecular diffusion in liquids or dense materials, and in rare cases, even faster than bulk kinetics while restricting the passage of other components of the analyte mixture.

2. Microporous Materials with Controlled Pore Architectures and Pore Chemistries

2.1. Zeolites and Related Inorganic Molecular Sieves

Zeolites are microporous aluminosilicate framework solids^[19] that exhibit well-ordered and periodic arrangements of matter and empty space (**Figure 2**). Related inorganic molecular sieves include silicalites,^[20] metallosilicates,^[21] and metallophosphates.^[22] Though discovered in the 1700s,^[23] zeolites did not find widespread industrial use for nearly two centuries.^[24,25] Indeed, the molecular-sieving effect was not recognized in zeolites until 1925.^[26] Today, hundreds of zeolites are available with uniform pore sizes ranging from 3 Å to more than 1 nm. Strict size and shape selectivity^[27] have not only made them attractive molecular sieves for selective transport but also led to their broad adoption as adsorbates^[28] and heterogeneous catalysts, particularly the so-called “Big Five” (FAU, MFI, MOR, BEA, and FER types).^[12,29] Typical zeolite syntheses are carried out under hydrothermal conditions using silicates and aluminates. Variations of temperature, cations, reaction time, and pH, among other parameters, dictate framework outcomes.^[25] Typically, the chemical makeup determines the structure of the zeolites. Occasionally, minor pore size adjustments are possible. For instance, zeolites 3A, 4A and 5A are all derived from zeolite A and incorporate different guest counterions: K⁺, Na⁺, and Ca⁺, respectively.^[30] Their incorporation into a membrane could take the form of a solid dispersion or in situ synthesis on a membrane by way of seeded growth.^[31] Recently, membrane design using zeolite nanosheets (ns) and inorganic nanotubes has also been investigated.^[32]



Changyi Li received his Ph.D. from the University of California, Berkeley, in 2015, and his B.S. from the California Institute of Technology in 2010, both in chemical engineering. His research interest is in engineering materials for selective transport.



Stephen M. Meckler received his B.S. in chemistry from The Pennsylvania State University (2013) and is currently a Ph.D. candidate in physical chemistry at the University of California, Berkeley. His research interests are in the chemical design of microporous polymers, crystals, and composites thereof for clean-energy technologies.



Brett A. Helms is a Staff Scientist at the Molecular Foundry, Lawrence Berkeley National Laboratory. His research program there is devoted to understanding architecture–property relationships in micro- and mesostructured systems assembled from organic, polymeric, and nanocrystalline components, with relevance to clean-energy technologies. Prior to beginning his independent career, he completed his Ph.D. in chemistry at the University of California, Berkeley, under the direction of Prof. Jean M. J. Fréchet (2000) and postdoctoral work at the Technische Universiteit Eindhoven with E. (Bert) W. Meijer (2007).

relevance to clean-energy technologies. Prior to beginning his independent career, he completed his Ph.D. in chemistry at the University of California, Berkeley, under the direction of Prof. Jean M. J. Fréchet (2000) and postdoctoral work at the Technische Universiteit Eindhoven with E. (Bert) W. Meijer (2007).

2.2. Metal-Organic Frameworks

MOFs^[33] are hybrid microporous materials composed of organic linkers joined together at inorganic nodes to form an extended 3D network (**Figure 2**). These crystalline materials are made up of two types of building blocks or secondary building units (SBUs)—metal-containing SBUs and organic SBUs. The metal-containing SBUs, which could be a metal ion or a cluster, act as nodes that are connected by polytopic organic linkers. In addition to forming architectural topologies that can be isomorphic to zeolites at an expanded scale (as is the case with

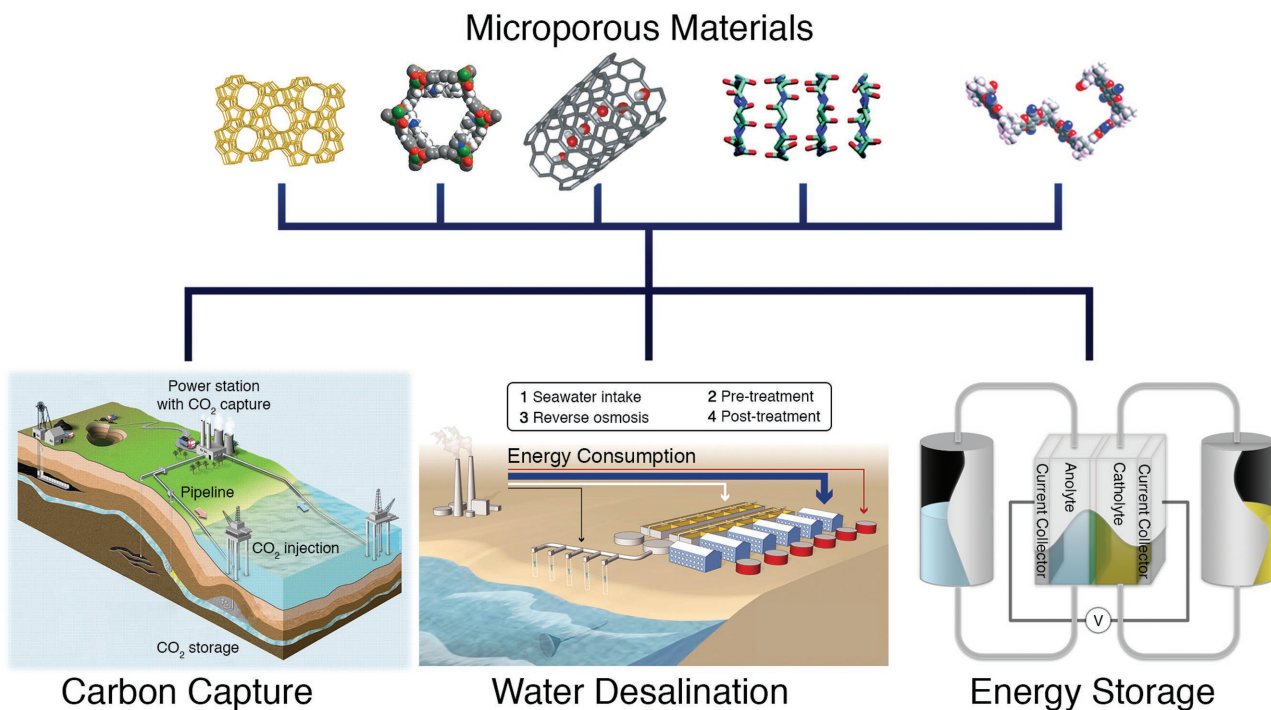


Figure 1. Microporous materials are leading a step change in clean-energy technologies ranging from carbon capture and water desalination to electrochemical energy storage. Microporous membrane components span zeolites, MOFs, carbon nanotubes, organic nanotubes, and intrinsically microporous polymers. The carbon capture image: Reproduced with permission.^[13] Copyright 2009, AAAS. Water desalination image: Reproduced with permission.^[14] Copyright 2011, AAAS. MOF image: Reproduced with permission.^[15] Copyright 2015, Nature Publishing Group. Carbon nanotube image: Reproduced with permission.^[16] Copyright 2001, Nature Publishing Group. Organic nanotube image: Reproduced with permission.^[17] Copyright 2014, The Royal Society of Chemistry. Microporous polymer image: Reproduced with permission.^[18] Copyright 2010, The Royal Society of Chemistry.

zeolitic imidazolate frameworks or ZIFs),^[34] organic linkers can be designed to yield MOFs of more exotic topologies or nets.^[35]

Like zeolites, MOFs feature periodic arrangements of micropores, or in some instances mesopores, depending on the organic linker. They are also amenable to postsynthetic modifications to fine-tune interactions with analytes.^[36] The diversity of architectures in this class of microporous materials is remarkable, with examples pushing the bounds of specific surface area (up to 7000 m² g⁻¹)^[37] and porosity (up to 90%).^[38] MOFs can adsorb and facilitate reactions for molecules that are too bulky for zeolites and other inorganic molecular sieves, and SBUs can be engineered synergistically to mediate analyte–pore-wall interactions.^[39,40] These properties have been exploited for gas storage/adsorption,^[41] catalysis,^[10] sensing,^[42] and other types of selective transport.^[43,44]

Replacing the metal centers in MOFs with polytopic organic moieties yields covalent organic frameworks (COFs), e.g., as pioneered by Yaghi and co-workers.^[46] COFs have attracted much attention but, although a small number of COF membranes have been reported,^[47] they have yet to be used extensively in selective transport. Nonetheless, COFs have found early successes in gas storage^[48] and electronic charge storage.^[49] Interested readers are directed to a relevant review on these topics.^[50]

2.3. Carbon Nanostructures

Carbon nanotubes are a mainstay of nanoscience and nanotechnology.^[51] They exhibit unique electrical,^[52] thermal, and mechanical^[53] properties, and are also molecular-sieving materials in their own right. Catalysts, precursors, and process conditions can be tuned to control nanotube diameters, either as single-walled or multiwalled nanostructures.^[54] While a variety of routes have been reported to modify carbon nanotubes on the exterior or the openings,^[55] there are as yet no strategies to functionalize their interior space. Instead, they remain a continuous and atomically smooth hydrophobic surface that is capable of promoting faster-than-bulk, frictionless kinetics via specular reflection of analyte molecules.^[56] In addition to having a confined geometry for molecular sieving, carbon nanotubes also have shown promise in chemically distinguishing between analytes, ranging from ions^[57] to macromolecules.^[58] Microporous graphene is a promising 2D membrane material with greater opportunities for pore-wall functionalization.^[59] As its potential in this field is only just emerging, we discuss its properties at length toward the end of this review (Section 5.2).

Whereas carbon nanotubes and porous graphene are exemplars of 1D and 2D microporous carbon nanostructures, respectively, CMSs are 3D. By pyrolyzing a polymer precursor, microporous carbonaceous architectures emerge with high surface area, small

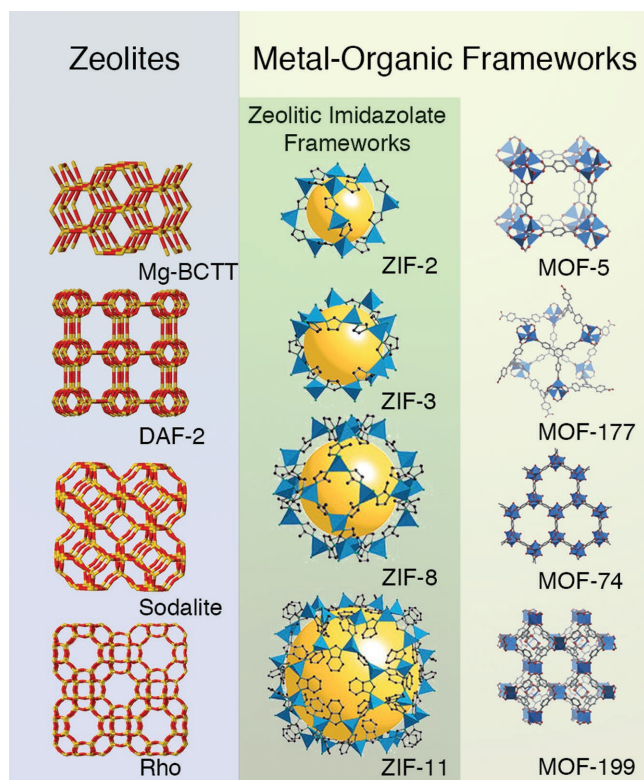


Figure 2. Structural diversity is a hallmark of both zeolites and MOFs, as demonstrated by the various structures and topologies presented here. ZIFs and their isomorphous counterpart zeolites are listed together for comparison. Zeolite structures: Generated using the Database of Zeolite Structures. [19c] MOF structures: Reproduced with permission. [45] Copyright 2008, Elsevier. ZIF structures: Reproduced with permission. [34] Copyright 2006, National Academy of Sciences.

pores (<1 nm), and narrow pore-size distributions.^[60,61] Most CMSs are derived from polyimides,^[62] such as Matrimid^[63,64] or Kapton.^[60,63,65] Other polymer precursors have included poly(furfuryl alcohol),^[66] phenol-based resins,^[67] and poly(vinyl chloride) copolymers.^[68] Both precursor chain packing and pyrolyzing procedure influence the final micropore architecture.^[69] Unlike zeolites or MOFs, however, these shape-persistent microporous materials are random arrangements of matter and empty space. Through the stochastic stacking, the microvoids enable molecular sieving in membranes tailored for gas separations.^[5,70,71]

2.4. Organic Nanotubes

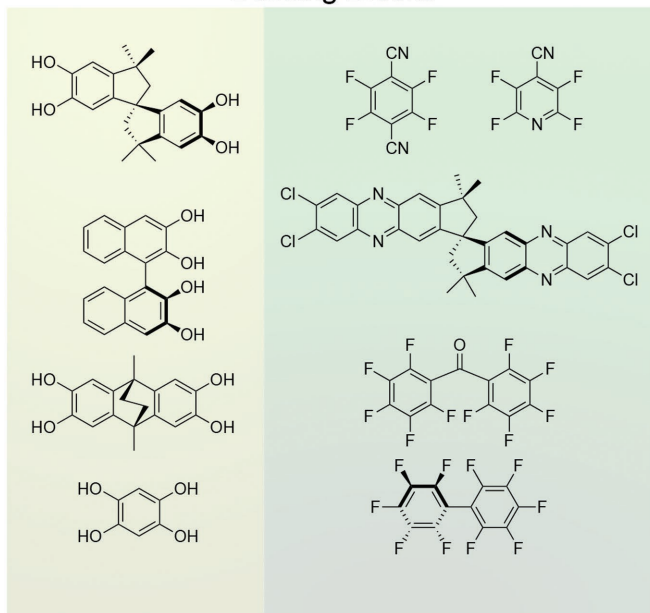
Organic nanotubes are like carbon nanotubes, prototypical microporous 1D nanostructures. Unlike carbon nanotubes, however, they are assembled from molecular components—either from wedge-like molecules (e.g., dendrimers,^[72] guanosine quartets, or their related analogues,^[73] etc.) or from discrete macrocycles (e.g., carbon nanohoops,^[74] arylene ethynyls,^[75] or cyclic peptides)^[76]—via noncovalent interactions, such as π - π stacking or hydrogen bonding. The structural diversity of organic nanotubes is vast. The size of their aperture can range from $\approx \text{\AA}$ to $\approx \text{nm}$, which is subject to precise synthetic

control; the length of organic nanotubes, on the other hand, strongly depends on the strength of the noncovalent interactions and the assembly strategy. Uniquely, both their exteriors and interiors^[77,78] can be modified with chemical functionality to enhance transport selectivity. Not surprisingly then, advances in synthetic methods have thus far focused on understanding these molecular structure–transport–selectivity relationships, rather than on practical aspects associated with scale-up, as might be required for membrane-based separations. In some instances, organic nanotubes benefit from exterior functionalization to align the nanotubes within a matrix (e.g., a mesostructured block copolymer film), allowing for facile membrane casting from solution.^[79] Given their ability to regulate transport, organic nanotubes have been explored as transmembrane protein analogs.^[80] Aside from bioinspired membrane applications, they have also been used as sensors.^[81]

2.5. Microporous Polymers

In organic polymers, micropores naturally arise from imperfect packing of highly rigid and amorphous macromolecular structures. Whereas conventional polymers have dynamic microporosity due to thermally activated segmental chain motion (a physical characteristic more aptly defined as free volume), in recent years, researchers have engineered void-forming elements at the molecular level. In these cases, segmental chain dynamics have been significantly reduced, thereby resulting in materials that would be defined more classically as microporous (**Figure 3**). For microporous organic polymers such as poly(1-trimethylsilyl-1-propyne) (PTMSP), 34% fractional free volume (FFV)^[82] has been reported. PTMSP features a bulky trimethylsilane group on the backbone while maintaining a rigid sp^2 -hybridized carbon main chain. Likewise, polymers of intrinsic microporosity (PIMs) achieve high FFV by introducing kinks into an otherwise rigid polymer backbone, which results in frustrated chain packing in the solid state.^[83] For PIM-1, FFV approaches 20% and consists primarily of micropores.^[84] Conjugated microporous polymers generate porosity via a similar principle of maintaining rigidity to disrupt packing. For polymers that are considered dense, there are generally two ways to introduce porosity chemically—reductive or additive. The reductive strategy is more prevalent and yields pores through triggered condensation of chemical moieties appended to the polymer. Thermally rearranged (TR) polymers^[85] derive their microporosity in this manner, often times in a two-step process: first, monomers are polymerized into a processable precursor material; second, a thermal treatment is applied, which activates contracting rearrangement or partial decomposition of the precursor, revealing the micropores. CMSs can be considered as an extreme of this case; one key difference, however, is that TR polymers can be formed without undergoing pyrolysis. The additive path, on the other hand, creates voids by chemically wedging spacers between polymer chains, often accomplished by crosslinking^[86] (e.g., hyper-crosslinked polymers). In general, these polymers are processable in their non-crosslinked forms as large-area, flexible films. They often serve as a highly permeable matrix for composites incorporating other molecular-sieving components. The ease of processing and low

a Polymers of Intrinsic Microporosity Building Blocks



b Thermally-Rearranged Polymers Building Blocks

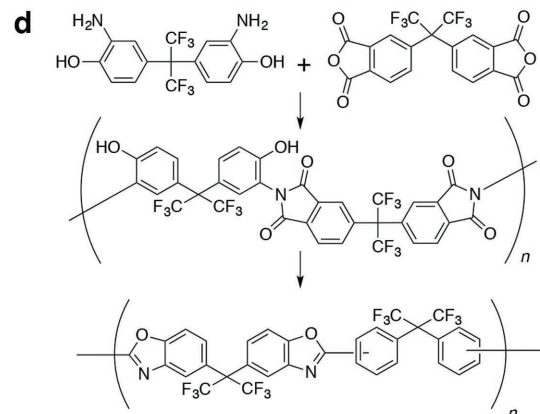
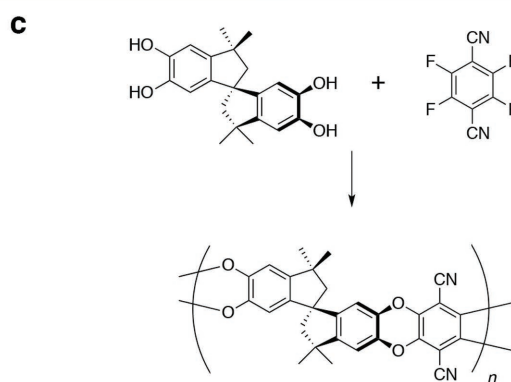
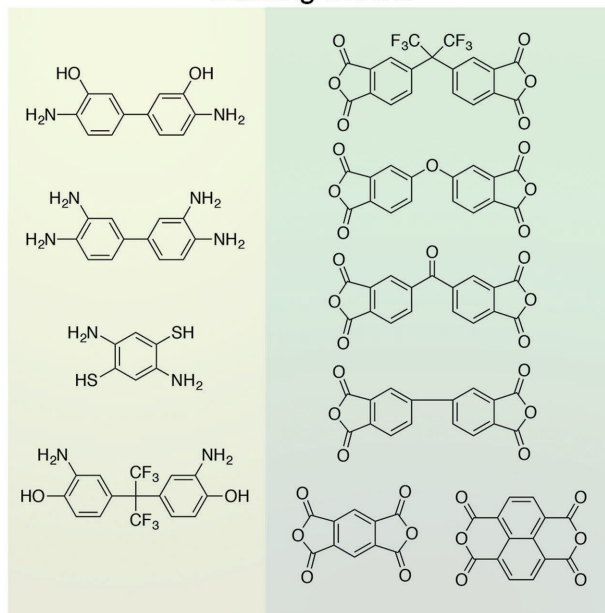


Figure 3. a) Monomer selection for PIMs. b) Monomer selection for TR polymers. c) PIM synthesis via step-growth polymerization. d) TR polymer synthesis via step-growth polymerization and subsequent thermal rearrangement.

cost of these microporous polymers have led to their adoption across many technology areas, including gas separation,^[83,85,87] desalination,^[88] and energy storage.^[84]

3. Fundamentals of Transport in Microporous Membranes

Some general descriptions are useful in understanding transport across microporous membranes used in various applications. First, analyte molecules in the feed contact the membrane. The analyte then enters the membrane, either dissolving into the membrane bulk or occupying pore free volume. Then, the analyte diffuses across the membrane driven by a chemical potential gradient. Flux is determined by the ability of the analyte to fit within the confines of the pore (size exclusion) and its interactions with the pore walls (chemical selectivity). Finally, the analyte desorbs at the downstream side

of the membrane, establishing a steady-state chemical potential gradient. In this section, we provide a brief overview of the chemical and physical forces influencing transport in microporous materials, the models used to understand their transport characteristics, and the design principles used to apply them to next-generation separations.

3.1. Size Selectivity and Chemical Selectivity

In the design of new membrane materials, two primary design parameters are available: (1) in the $\approx \text{\AA}$ size regime, chemical control over the pore-wall functionality determines the energetics of pore-analyte interactions, and (2) at the nanoscale, pore size and shape determine the barriers to analytes entering and moving between pores. Often, these axes of control are orthogonal. Consider the case of isorecticular MOFs. Pore size can be tuned by changing the length of the organic ligands.^[40]

Conversely, through careful choice of ligand, postsynthetic modification, or cation exchange, frameworks with very similar pore architectures but vastly different pore-wall chemistries are accessible.^[89] As we demonstrate in the following subsection, the size and chemistry of the pores are often considered together when modeling transport, which is most easily understood as a function of the speed and frequency with which analytes traverse the membrane. Nonetheless, these concepts are useful for establishing design principles for the advancement of membrane technology. Ultimately, as all separations necessarily operate on chemical and physical differences between the analytes being separated, those analyte properties determine the respective relevance of pore size and chemistry on membrane performance.

Chemical selectivity in membrane applications is most applicable when the analytes differ substantially in polarizability, electrostatic charge, Lewis acidic/basic character, etc. Increasing the favorability of interactions between membrane materials and a given analyte will typically increase the flux of that analyte. On one extreme, membranes can form reversible bonds with the higher-flux analyte. If the rate of analyte exchange on the reactive sites is sufficiently fast, the effective concentration of that particular analyte is markedly increased, increasing both selectivity and productivity in a process called facilitated transport.^[90] However, if the analyte interacts too strongly with particular moieties in the matrix, transport across the potential well of the bound state is disfavored, slowing transport. Another strategy is to block the transport of certain analytes by designing repulsive pore–analyte interactions.^[91] This process is seen in the use of electrostatically charged membrane matrices for ion exclusion, which is discussed in Section 4.3.

Pore-size control for size-exclusion separations can be quite effective with even small differences in analyte size when the matrix exhibits appropriate *in situ* pore dimensions. For example, gaseous propane and propylene can be separated through molecular sieving in the MOF ZIF-8 despite having very similar van der Waals diameters (4.16 and 4.03 Å, respectively).^[92,93] This example is also illustrative of the importance of pore dynamics in molecular-sieving applications. The crystal structure of ZIF-8 suggests a selective pore aperture of only 3.6 Å, but Zhang et al. demonstrated that natural fluctuations in the crystal structure permit fast diffusion of analytes up to ≈4.1 Å in diameter.^[92] As such, size exclusion as a design principle must be considered within the relevant operating conditions of the separation. Common methods for pore-size characterization, such as crystallography and adsorption isotherms, do not necessarily account for pore-dimension fluctuations with changes to solvent environment, temperature, flexibility, etc.^[94,95] Understanding analyte size also requires careful treatment. In the simple case of dilute gaseous analytes, multiple measures of size exist that sometimes suggest conflicting results (building on the propane/propylene example, the kinetic diameter of propane is the smaller of the two while the opposite trend holds for the van der Waals diameters).^[92] As system complexity increases, the permeating species sometimes includes noncovalent aggregates. In redox-flow battery membranes, analyte sizes are estimated as the radius of gyration of the analyte molecule/ion and its solvent shell, which are quantified using either scattering, electrochemical, or diffusion-ordered NMR spectroscopy (DOSY) methods, or

alternatively, computationally using *ab initio* or semiclassical molecular dynamics (MD) simulations, which also allow desolvation energies to be calculated.^[96] A complementary approach to engineering pore architectures is to alter the size of the analyte. In some applications, analyte size can be controlled through oligomerization, polymerization, or the introduction of bulky chemical functionalities without compromising analyte functionality, improving membrane performance with no change to the matrix itself.^[97]

Throughout the discussion of microporous membrane applications in clean-energy technologies (Section 4), these design principles are carefully considered in turn with respect to the demands of each use case.

3.2. Transport Fundamentals

The first consideration for transport in microporous materials is distinguishing solution diffusion from molecular sieving. Molecular sieving occurs when the pore size and persistent shape exclude a given species; transport is impossible for that analyte. For analytes that do enter the membrane, permeation in bulk materials, particularly those with low free volume, is commonly viewed from the standpoint of the solution-diffusion model^[98]

$$P = \bar{D} \times \bar{S} \quad (1)$$

where P is permeability, and \bar{D} and \bar{S} are concentration-averaged effective diffusion and solubility/sorption coefficients, respectively. Within this model, transport is envisioned to occur via three discrete steps. First, the analyte dissolves into the matrix, diffuses across the film, and then desorbs at the downstream interface. Therefore, for a binary system of species i and j , selectivity, α , can be achieved for materials that exhibit differences in molecular diffusion rates or thermodynamic partitioning

$$\alpha_{i/j} = \frac{\bar{D}_i}{\bar{D}_j} \times \frac{\bar{S}_i}{\bar{S}_j} \quad (2)$$

Basic permeation characteristics of microporous materials can be understood in the context of a simple model. Consider gases traveling in the yz plane through a microporous material that has within a given unit cell (dimensions $L_y \times L_z$) a pore ($L_{py} \times L_{pz}$) separated from other pores in a 1D channel by narrow windows with width L_{wy} and length L_{wz} .^[99] At low pressures, the system enthalpy is described by the chemical potential of the analyte in the free volume, which is dominated by adsorption in the pores. The Henry constant, used here to quantify solubility, is thus

$$H = \frac{\beta V_p}{V} e^{-\beta U_p} \approx \frac{\beta L_{pz}^2}{L_y L_z} e^{-\beta U_p} \quad (3)$$

where V_p is the pore volume, V is the unit cell volume, β is the inverse product of absolute temperature and the Boltzmann constant, and U_p is the chemical potential of an analyte molecule in the pore. As the chemical potential of analyte molecules

in the windows is high, its effect on the system can be neglected. The diffusion constant as determined using the steady-state approximation is

$$D = \frac{1}{4} |v_a| \frac{L_{wy} L_z^2 e^{-\beta U_w}}{L_{pz}^2 e^{-\beta U_p}} \quad (4)$$

where v_a is the average particle velocity at a given temperature and U_w is the chemical potential in the windows. Permeability, the product of solubility and diffusivity, is then

$$P = D \cdot H = \frac{\beta |v_a| L_{wy} L_z}{4 L_y} e^{-\beta U_w} \quad (5)$$

While not all of the assumptions used in constructing this model hold for many real systems, especially when interactions between analytes are strong, it nonetheless demonstrates some interesting relations useful in membrane design. If the volume fraction of the pores increases, the Henry coefficient increases while the diffusion coefficient decreases (and vice versa), affecting no change on the permeability, while increases to the window diameter improve permeability by increasing the diffusion coefficient. Changes to the pore chemistry resulting in more favorable pore-analyte interactions improve solubility but impede diffusion. Similar changes to the window chemistry, however, have little impact on adsorption and can be used to tune diffusion. In practice, most changes to the matrix structure will change the pore-analyte and window-analyte interactions to a similar degree, meaning more favorable matrix-analyte interactions will improve permeability through solubility while having little impact on diffusion.

While the solution-diffusion model is generally successful in describing permeability and selectivity trade-offs in materials such as polymers, microporous materials with persistent free volume consistently show transport properties exceeding those defined by this model.^[87] In general, transport through some of these materials can still be described within the framework of the solution-diffusion model, but in significantly rigid and contorted structures, such as glassy porous polymers, amorphous carbons, and zeolites, transport can depend on a combination of transport mechanisms including solution-diffusion transport, molecular sieving, surface diffusion, and Knudsen diffusion (Figure 4).^[98,100,101]

Analyte diffusion in these cases is mediated by local collisions. When those collisions are most frequently with rigid pore walls, e.g., with low-pressure gases in mesoporous materials, Knudsen diffusion is the dominant transport mechanism.^[99] As solubility in this case is roughly the same for all analytes, differences in flux are considered to originate from diffusivity differences, which in turn result from the velocity with which molecules bounce off the pore walls. As these velocities are well described using a Maxwell distribution, the diffusion coefficient is a function of pore diameter, membrane temperature, and analyte mass

$$D_i^k = \frac{2r}{3} \sqrt{\frac{8RT}{\pi M_i}} \quad (6)$$

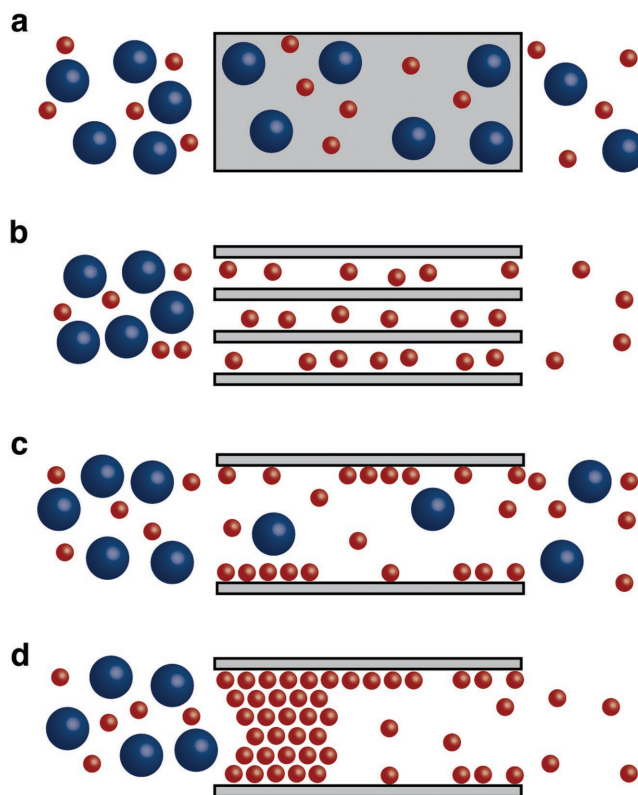


Figure 4. Comparison of diffusion mechanisms in polymers and microporous materials. a) Solution-diffusion transport, b) molecular sieving, c) surface diffusion and Knudsen diffusion, and d) capillary condensation.

where D_i^k is the Knudsen diffusion of species i , r is the radius of the capillary, R is the gas constant, T is the temperature of the membrane, and M_i is the molar mass of species i .^[102]

In amorphous carbons, where sorption into microporous sites is particularly strong, Ash et al. first observed that the preferred diffusion mechanism was a hopping-type mechanism known as surface diffusion (cf. Figure 4c).^[103] Strong sorption interactions can further influence diffusion through processes such as capillary condensation for gas mixtures, which describes the blocking of adsorption sites by condensable gases (cf. Figure 4d). For strongly adsorbing gases, capillary condensation can result in inverted or enhanced gas-phase selectivities when testing gas mixtures instead of pure gases.^[104] These types of observations are rare for polymer systems but have been observed in PTMSP and TR polymers.^[101,105]

As pore shapes become well ordered, such as those found in crystalline coordination solids, a process known as single-file diffusion can also be observed. This process is similar to capillary condensation and surface diffusion in amorphous carbons and microporous polymers but is significantly more selective due to the uniformity of precisely well-defined 1D channels.^[106] In nature, these types of restricted transport mechanisms are found for water transport in aquaporins;^[107] analogous transport behavior is predicted and, in some cases, experimentally observed for thin-walled carbon nanotubes^[108] and zeolites.^[109]

When analyte collisions are most frequent with solvent molecules or other analytes, the effective diffusion coefficient is described using a series of dimensionless factors accounting for pore geometry

$$D_e = \frac{D\varepsilon\delta}{\tau} \quad (7)$$

where D_e is the effective diffusion coefficient through the membrane, D is the diffusion coefficient in the medium filling the pores, ε is the porosity (<1), δ is the constrictivity (≤ 1), and τ is the tortuosity (>1).^[110] The parameter δ describes resistance to flow from increased viscosity through narrow pore apertures, and the parameter τ describes resistance to flow resulting from the winding paths analytes take through the membrane. While porosity can be measured directly using a number of common techniques, including gas adsorption^[111] and ellipsometric porosimetry,^[112] tortuosity and constrictivity are typically empirical, although advanced X-ray tomography for the direct measurement of tortuosity has been demonstrated.^[113]

3.3. Modeling Transport through Microporous Materials

As predictive and mechanistically informative models of specific membrane systems are desirable to direct membrane design, many such descriptions of individual transport systems have been developed. Such theoretical formalisms governing the transport of gases through microporous materials are well developed and illustrative of the types of considerations one must address carefully with analytes generally. We begin our discussion of gas transport in microporous polymers by first considering models used to describe gas dissolution into glassy polymers. The simplest of these is the dual-mode model^[114]

$$C = k_D p + C'_H \frac{bp}{1+bp} \quad (8)$$

where C is the concentration of a penetrant in the polymer, k_D is the Henry's law partition coefficient, C'_H is the Langmuir capacity constant, b is the Langmuir affinity constant, and p is pressure. Sorption coefficients are defined as the secant slope of sorption isotherms

$$\bar{S} = \frac{C}{p} = k_D + C'_H \frac{b}{1+bp} \quad (9)$$

For rubbery elastomers, sorption of nonswelling penetrants can be described using only the parameter k_D .^[115] However, for glassy polymers, an additional, Langmuir-type contribution to sorption becomes manifest in experimental isotherms. The dual-mode model captures this behavior by envisaging two distinct "sites" for sorption in amorphous glasses: (1) sorption into Henry's law sites and (2) sorption into Langmuir sites. From a molecular perspective, the dual-mode model does not possess true physical meaning, as there is no proven experimental evidence that supports the presence of discrete sorption sites in glassy polymers.^[116] From the perspective of statistical thermodynamics, far more meaningful and truly predictive models

for describing gas dissolution into rubbery polymers (Sanchez-Lacombe)^[117] and glassy polymers (nonequilibrium lattice fluid, NELF)^[118] have been developed. Nevertheless, parameters evaluated from the dual-mode model provide some insight into the potential advantages of using microporous polymers for membrane-based separations. Most importantly, higher total sorption in polymers can be achieved when operating in the glassy state, and higher sorption corresponds to higher permeation rates as predicted by the solution-diffusion model.

The nonequilibrium morphology of high free volume and microporous polymers permits significantly more sorption into glassy polymers than their corresponding elastomers. The reader should note that the term "free volume" and "microporous" both relate to open spacing within the polymer matrix devoid of electron density. However, "free volume" is a term used to indicate stochastically fluctuating gaps in the free space of the polymer, whereas "microporous" is used to indicate long-lasting, persistent gaps that are significantly immobilized and considered relatively intransient.^[119] From the framework of the dual-mode model, the ratio of nonequilibrium to equilibrium sorption can be described at infinite dilution as a ratio of the dual-mode fitting parameters, $C'_H b/k_D$. **Figure 5** demonstrates that cooling poly(ethylene terephthalate) (PET) below its glass transition temperature (T_g) produces significant nonequilibrium free volume that is responsible for increased CO_2 sorption.^[120] For polymers often classified as microporous, such as PTMSP, TR polymers, and PIM-1, the ratio of nonequilibrium to equilibrium sorption for CO_2 at 35 °C often falls within the range of 5–20, indicating that the dominant mechanism of sorption in these polymers is derived from their microporous nature.^[121–123]

While excess free volume often correlates with increased sorption, the same is not true for sorption selectivity. In general, polymers often characterized as microporous follow the same trends for solubility selectivity as their low free-volume counterparts,

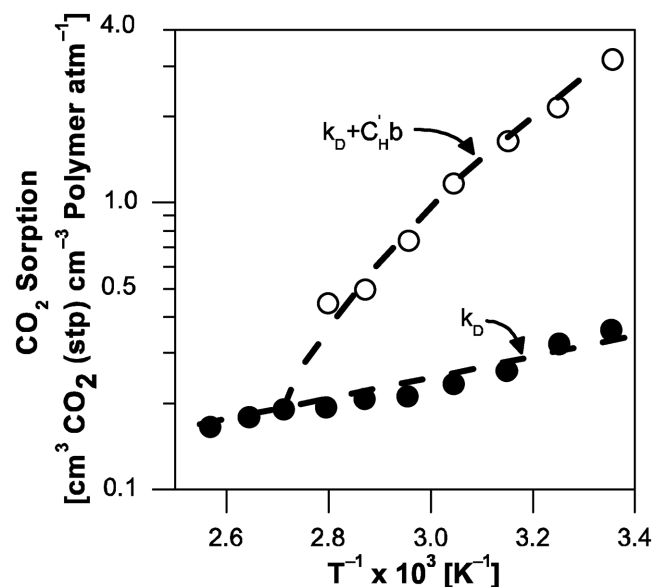


Figure 5. Contributions to CO_2 sorption from equilibrium sorption (k_D) and from excess free volume ($C'_H b$) above and below the glass transition temperature for PET. Reproduced with permission.^[120] 1978, John Wiley & Sons, Inc.

including PTMSP,^[121] TR polymers,^[123,124] and PIMs.^[125] These correlations are upheld for a range of FFVs, including 20–24% for PIM-1,^[126] 26.3% for TR-1-450,^[85,127] and 32–34% for PTMSP.^[126] From the standpoint of the dual-mode model, the origins of this invariance in sorption selectivity in the face of significant differences in total sorption correspond to the energetics of gas sorption in the glassy state. The parameter C'_H only begins to manifest itself as the polymer is cooled below its glass transition temperature. When plotted against inverse temperature on a semilog Van't Hoff plot, C'_H exhibits a strong nonlinear dependence. In contrast, an analogous plot of the affinity constant, b , versus inverse temperature reveals linear Van't Hoff type behavior.^[120,128] Thus, relative sorption affinities, which are characteristic of b , are invariant to free volume and microporosity.

In contrast to sorption selectivities, diffusion rates and diffusion selectivities are strongly influenced by polymer structure and fractional free volume or microporosity. For illustrative purposes, consider the separation of H_2 from CH_4 . H_2 has a kinetic diameter of 2.89 Å compared to 3.8 Å for CH_4 , a difference of less than 1 Å.^[129] For poly(dimethyl siloxane) (PDMS; $T_g = -123$ °C), an elastomer, H_2/CH_4 diffusion selectivity is only 6,^[130,131] whereas H_2/CH_4 diffusion selectivity for a glassy polyimide (benzophenone-3,3',4,4'-tetracarboxylic dianhydride-*para*-4,4'-oxydianiline, or BTDA-*para*-ODA; $T_g = 266$ °C) is 280.^[132] However, PDMS, the most permeable rubbery polymer known,^[130] has an H_2 diffusivity of 1.4×10^{-4} cm² s⁻¹ compared to only 3.6×10^{-7} cm² s⁻¹ for that of BTDA-*para*-ODA. This comparison highlights a general trend. Gas diffusion in low free-volume glassy polymers, such as BTDA-*para*-ODA, is significantly reduced due to immobilization of polymer chain segments. However, for high free-volume, microporous glassy polymers, significant non-equilibrium free volume allows for lower activation energies of diffusion, thereby permitting high diffusion rates. For example, PTMSP has an H_2 diffusion coefficient of 2.6×10^{-4} cm² s⁻¹ and an H_2/CH_4 diffusion selectivity of 7.6,^[121] properties that surpass both the diffusion rate and diffusion selectivity of PDMS (i.e., $D = 140$ cm² s⁻¹, and $D_{H_2}/D_{CH_4} = 6$).^[130]

In polymer systems, the mechanism of gas diffusion has classically been described in analogy to molecular diffusion of liquids using Eyring's transition-state theory.^[133] Eyring describes diffusion as a process that occurs through "holes" or gaps in the lattice framework that occasionally open into voids large enough to permit diffusive displacement between lattice sites. Diffusion of these holes, D , can therefore be statistically described by a relationship proposed by Cohen and Turnbull^[134]

$$D = A \exp \left[\frac{-\gamma v^*}{v_f} \right] \quad (10)$$

where A is a temperature-independent preexponential factor, v_f is the volume of the transient holes, or free-volume elements, γ is a numerical factor to account for overlapping free-volume elements, and v^* is the molecular volume of the diffusing diluent (or analyte). The basic form of this relationship, which was further expanded to describe polymer-diluent systems by Fujita^[135] predicts a few basic correlations for molecular diffusion in polymers. Specifically, faster diffusion occurs for smaller molecules and for larger or interconnected free-volume elements. Free volume is often determined through group

contribution methods^[136] or through spectroscopic characterization such as positron annihilation lifetime spectroscopy.^[137]

Diffusion can similarly be described as an energetically activated process using an Arrhenius relationship of similar form to the equation proposed by Cohen and Turnbull^[138]

$$D = D_0 \exp \left[\frac{-E_D}{RT} \right] \quad (11)$$

where D_0 corresponds to entropic contributions to activation, E_D is the activation energy of diffusion, R is the ideal gas constant, and T is the absolute temperature. From this relationship, Meares proposed that the energy required for a molecule to make a diffusive jump correlates with the energy required to separate the surrounding media with sufficient space to accommodate the cross section of the diffusant.^[139] Regardless of whether free-volume considerations or activated diffusion considerations are used to describe the mechanism of diffusion in polymers, the slope of the upper bound relationships originally described empirically by Robeson can be fundamentally described within the framework of either of these models.^[87,140,141] These upper bound relationships describe a consistent trade-off between permeability and selectivity observed for polymer membranes.

When the analytes to be separated are more strongly interacting than dilute gases, as is the case for liquids and solvated species, the nanoscale dimensions of micropores often lead to behaviors deviating from continuum fluid dynamics, and MD simulations are necessary to model these systems.^[142,143] The distribution and diffusion of nanoconfined analytes strongly depend on analyte-analyte and analyte-matrix interactions, both of which change with time and position in the system. MD simulations can capture these complicated interactions, such as transient hydrogen-bond networks that influence the barriers to permeation, as well as other relevant properties of the system (e.g., solvent density or viscosity fluctuations).^[143] Often, these studies highlight key aspects of the system relevant to membrane performance, and analytical models that qualitatively track with the simulated results are later developed to provide a greater description of the system.^[59] Water and aqueous solutions are common subjects of these studies, as they are interesting from both basic science and application-driven perspectives. Sometimes, the models and intuitions of traditional fluid dynamics hold true in microporous transport; however, simulation is usually needed to ascertain when this is the case.

Such MD studies have been particularly useful in the context of 2D materials. While these membranes, including nanoporous graphene^[144] and graphene,^[143] achieve separations by mechanisms as simple as molecular sieving, the interplay between solvent molecules and the membrane pores produces a number of more complicated confinement effects. For example, Cohen-Tanugi and Grossman demonstrated that the chemical functionality of nanoporous graphene pore walls plays a critical role in determining water flux and selectivity over salt ions due in part to the entropic penalty of solvent confinement in the pores.^[59] When hydrogenated pore walls are replaced with hydroxylated ones, water molecules in the pores become more disordered, raising the system entropy and consequently lowering the free energy of molecules traversing the

membrane, ultimately improving water flux. Separately, introducing charged species to the pores has been shown to produce large free-energy barriers to coions.^[145] Outside of the pores, solvent in contact with the membrane surface also exhibits interesting ordering effects that influence flux. Near the hydrophobic surface of graphene, solid-like hydrogen-bond arrangements increase water density and viscosity, limiting flow across the membrane, especially for small pores.^[143] Together, these studies develop a picture of perturbed solvent behavior at the water–membrane interface, underscoring the importance of a well-developed molecular view of transport in these systems.

Nanotubes also provide confined volumes for liquid analyte transport and have thus received considerable attention from the MD community. Carbon nanotubes are the simplest case and have been studied in detail.^[146] Simulations allow for the effects of pore size, chemistry, and roughness to be studied independently. Interestingly, long and narrow nanotubes with smooth, hydrophobic pore walls are needed to promote the faster-than-bulk transport; examples of such materials are well known.^[142,147] In more structurally complex cyclic peptide nanotubes, the free energy landscape changes periodically along the length of the tube, and water molecules tend to prefer the space between cycles.^[148] As the pore diameter increases, single-file behavior gives way to bulk-like diffusion properties. Cyclic peptide nanotubes are especially exciting materials because, unlike carbon nanotubes, the interior pore-wall chemistry can be finely controlled through alterations in the amino acid sequence of the subunits.^[77] The effects of peptide substitution on diffusion and selectivity have been investigated in detail by Keten and co-workers.^[17,149] While water interacts primarily with carbonyl groups in canonical peptide nanotubes, the introduction of other functionalities (methyl, amine, etc.), experimentally demonstrated by Helms and Xu, changes the energy landscape roughness and sterically influences analyte transport.^[77] Simulated ion flow rates can be tuned by over an order of magnitude using this method. Functionalities promoting the exchange of the solvent shell, such as highly polar or sterically bulky groups, slow Na⁺ passage, while nonintrusive glycine-like hydrogen allows the ion to retain its solvent shell, promoting fast transport. Additionally, conformational freedom of the peptide cycles themselves enables coordination with analytes that would be unobtainable in traditional, rigid microporous materials.^[150]

4. The Application of Microporous Membranes to Clean-Energy Technologies

Here we provide an overview of clean-energy technologies where membrane design is central to large-scale implementation. The technologies are organized by analyte—gases, water, and ions—and, in turn, by application. Though the demands of each analyte and environment differ, some classes of microporous materials show promise across multiple applications.

4.1. Gas Transport—Carbon Capture and Other Gas Separations

With looming concern over global climate change brought about by excessive emission of greenhouse gases, CCS, the

process by which atmospheric carbon dioxide is collected and injected underground, has become a major driving force for membrane development. In the US today, over half of greenhouse gas emissions come from burning fossil fuels—mostly coal and natural gas—at source locations for electricity production and industrial use.^[151] Therefore, the most immediate way to prevent CO₂ release into the environment is by capturing it directly at these sources.

Strategies for controlling CO₂ emissions at power plants include precombustion capture, postcombustion capture, and oxy-fuel combustion (cf. **Figure 6**).^[152] Precombustion and oxy-fuel combustion strategies target CO₂ capture by purifying the fuel source or the oxidant feed, respectively. For precombustion carbon capture, the power plant fuel is predominantly H₂, derived from the separation of gasified coal syngas. For oxy-fuel combustion, coal or gas is burned in high purity oxygen, which is derived from a high-volume air separation unit, to produce high concentrations of CO₂ that can be dehydrated and compressed for sequestration. While membranes could be used in precombustion carbon capture (predominantly H₂/CO₂ separation) and oxy-fuel combustion carbon capture (predominantly O₂/N₂ separation), practically all existing and newly developed coal-fired power plants are designed with boilers specifically made for combustion of coal in air. Therefore, postcombustion carbon capture is the most practical and economic option for retrofitting currently existing and soon-to-be built power plants.^[152]

Emissions from coal-fired and natural gas power plants consist largely of CO₂ and N₂, although significant quantities of other gases are found in these mixtures (**Table 1**).^[153] The incumbent CO₂-scrubbing technology, which has been deployed commercially for natural gas sweetening since the 1930s,^[154] implements aqueous solutions of amino alcohols that capture carbon dioxide from flue gas streams.^[155] Regeneration proceeds thermally, which is energy intensive, costing up to 30% of the power plant output.^[156] Therefore, alternative separation processes that use solid-state adsorbents and gas separation membranes potentially present more energy-effective solutions.^[157]

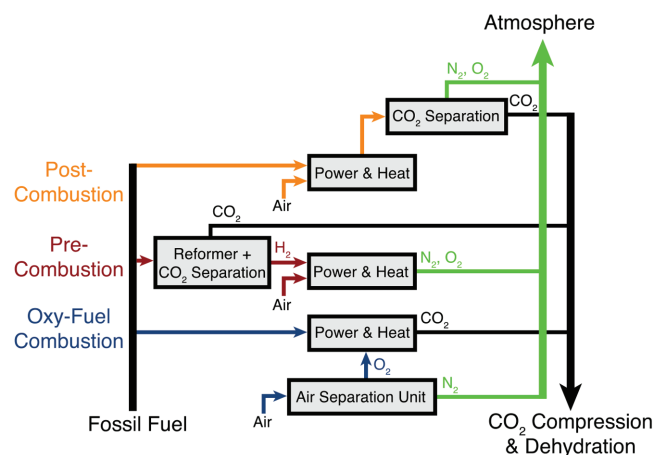


Figure 6. Potential routes for power plant decarbonization for energy production. Major gaseous components for each part of the process diagram are highlighted. Reproduced with permission.^[152] Copyright 2010, Elsevier.

Table 1. Approximate composition of flue gas from a coal-fired and natural gas power plant.^[153]

Component	Coal	Natural gas
N ₂	70–80%	74–80%
CO ₂	12–15%	3–5%
SO ₂	1800 ppm	<10 ppm
NO _x	500 ppm	50 ppm
H ₂ O	5–7%	7–10%
O ₂	3–4%	12–15%
CO	<100 ppm	<5 ppm
Hg/As	ppb	0
Particulates	10–20 mg N m ⁻¹	NA
Pressure	1 atm	1 atm

For microporous membrane materials to compete with amino alcohol solutions for postcombustion carbon capture, the design of membrane materials must be weighed carefully against the engineering process requirements. Gas separation membranes operate via a pressure driving force, so historically, their earliest industrial adaptation was for applications with preexisting, high-pressure feeds, such as the recovery of hydrogen from purge lines in petrochemical and ammonia production plants.^[158,159] The same pressurized feeds are found in emerging applications, such as natural gas sweetening, where wellhead pressures provide a natural driving force upward of 60 bar.^[160] Under these conditions, single-stage membrane systems do not require compressors, significantly shifting the economics for natural gas purification away from amine absorption. In many cases, even two-stage membrane systems coupled with an intermediate compressor to repressurize the permeate are still more economically attractive than amine absorption.^[160] On the other hand, postcombustion CO₂ capture has an intrinsic driving force of only 0.03–0.15 bar, the approximate partial pressure of CO₂ in flue gas, making this separation significantly more challenging. As a technical analogy, there is only one major application today where membranes are used to process low partial pressure gases: nitrogen generation from air, which is typically used in on-board inert gas generation systems (OBIGGS).^[159,161] To reduce compressor costs and improve N₂ recovery, these applications often use glassy polymers with low permeability but high O₂/N₂ selectivity (i.e., 6–8).^[162] However, flue gas capture is an inherently different application than nitrogen generation. OBIGGS are used in confined spaces on commercial aircraft to process limited flow rates of gas.^[163] If implemented industrially, CO₂ recovery from flue gas would be the highest flux adoption of membrane separators today. A typical 600 MW coal-fired power plant emits 11 000 tons of CO₂ per day, a flow rate that is 5–10 times larger than typical amine absorption processing facilities used for natural gas sweetening.^[152]

Because pressure differentials drive membrane gas separations, pressure-ratio limitations significantly influence the engineering design of carbon capture systems.^[164] Merkel et al. concluded that membrane systems could potentially compete with amine absorption.^[152] However, the process proposed for

their implementation is based on careful economic process optimization and design: a light vacuum (0.22 bar) would be pulled on the permeate and a low-flow sweep stream of CO₂-lean retentate would be used in a countercurrent flow module.^[152] For these pressure-ratio-limited applications, microporous polymers with moderate CO₂/N₂ selectivities (≈ 25) and high permeabilities could have significant impact. PIMs, TR polymers, and composite mixed-matrix membranes (MMMs) are attractive for this separation.^[165]

Nonpolymeric microporous membranes could also be used for postcombustion CO₂ capture. However, materials like activated carbons, considered some of the simplest nonpolymeric materials to scale up, are estimated to be at least an order of magnitude more expensive to form into membrane geometries than polymers.^[126,164] Moreover, polymer membranes deployed for commercial applications today, which process significantly lower flow rates than those required for flue gas capture, have surface areas of 1000–50 000 m² and selective layer thicknesses of ≈ 100 nm.^[162] To compete economically with state-of-the-art polymers, nonpolymeric membranes must be made from materials that can be produced at sufficient scale and formed into selective thin films; indeed, efforts in that direction are underway with selective materials, including MOFs^[166] and zeolites.^[167]

There are, of course, clean-energy chemical separations beyond those used for CCS. By some accounts, 10–15% of the total global energy expenditure goes toward chemical separations, and any technology to lower that cost has the potential to significantly reduce anthropogenic carbon dioxide emissions.^[1] Microporous membranes have been investigated for many such separations, as discussed in the following subsections.

4.1.1. Microporous Single-Component Systems for CCS and Gas-Phase Chemical Separations

Polymer membranes with microporous character have shown promising separation efficiency for several industrially relevant gas pairs. PIMs are particularly noteworthy in this regard (i.e., as upper bound membrane materials). Since the mobility of the polymer backbone is not the limiting kinetic process in mediating gas transport, optimization of the membrane transport properties in turn calls for the rigidification of the backbone, to the point of minimizing the number of rotatable bonds. PIMs have evolved from ladder polymers, typically bearing either kinked bicyclic or spirocyclic aromatic monomers along their backbone,^[83] to rigid polymers that are fully constrained and decorated with bulky groups.^[168] PIMs have demonstrated superior performance in separating CO₂/CH₄ and other gas pairs:^[169–171] methanol-treated PIM-1 membranes have demonstrated CO₂ permeabilities as high as 11 200 Barrer.^[172] Moreover, tetrazolate derivatives of PIM-1 (e.g., TZPIM-1 or TZPIM-2) offer CO₂/N₂ selectivity approaching 30.^[170] PIMs are likely to continue to push the bounds of the Robeson permeability-selectivity trade-off, provided monomer-level structural motifs directing pore network architectures advance significantly beyond present designs.^[7,18,173,174]

Thermally rearranged polymers have also found success in improving efficiency and productivity for gas separation

membranes. First reported by Park et al. in 2007,^[85] TR polymers are formed from a solid-state reaction of poly(hydroxyimide)s, where the hydroxyl group is *ortho*-positioned to the diamine monomer. These polyimides, which can be cast as films, are heated, typically to temperatures between 350 and 450 °C, thereby inducing an intramolecular cyclization reaction between the hydroxyl group and the imide carbonyl to form polybenzoxazoles.^[127,175] Once converted, these polymers become insoluble in their casting solvent, possibly due to intermolecular crosslinking reactions, which endows these materials with excellent plasticization resistance.^[105] Because these reactions take place in the solid state, slight variations in the synthesis of the polyimide precursors significantly influence transport behavior for the resulting TR polymer.^[176] For example, modifying the hydroxyl group on the polymer backbone to larger *ortho*-positioned functional groups can be used to effectively engineer free volume and free-volume distribution in these materials, resulting in significant improvements in permeability.^[177,178]

TR polymers first showed promising transport properties and plasticization resistance for CO₂/CH₄ separation,^[85] but additional studies suggest that TR polymers could find use in CO₂/N₂,^[173] O₂/N₂,^[173] and olefin/paraffin separations.^[179] Of practical interest, TR polymers are derived from solution processable polyimide precursors, a class of polymers currently deployed by Air Liquide and Ube for industrial gas separation membranes, so TR polymers have a logical pathway to industrial deployment using currently available membrane formation methods.^[162] Of note, TR polymers have already been formed into hollow-fiber geometries.^[180]

Of particular interest is understanding and tuning the free-volume architecture of TR polymers. Initial reports indicated a sharpening of the free-volume distributions due to a coalescence of free-volume elements during thermal rearrangement,^[85] but additional studies have reported other potential phenomena, such as the formation of bimodal free-volume distributions,^[176,181] or more traditional free-volume trade-off behavior such as unimodal free-volume distributions that follow upper bound type limitations.^[179] The origins of these competing and complex morphologies of TR polymers likely relate to slight differences in polymer preparation methods. As described in the theoretical section of this paper, transport in these microporous-like materials occurs predominantly through their nonequilibrium packing morphology, so the method by which they are prepared has direct implications on their performance.

Two major challenges deterring industrial deployment of TR polymers and PIMs relate to their mechanical brittleness and susceptibility to physical aging, respectively. For TR polymers, when conversion temperatures up to 450 °C are required, samples often become brittle.^[85] To overcome these mechanical issues, researchers have investigated methods for lowering the thermal rearrangement temperature to avoid potential polymer backbone degradation. To do so, precursor polyimides have been synthesized with lower glass transition temperatures, which can rearrange at lower temperatures.^[178] Alternatively, more flexible backbone functionalities, such as spirobisindane units similar to those in PIMs, have been incorporated into the polymer backbone.^[182] Additionally, alternative precursors,

such as poly(hydroxyamide)s, which undergo thermal rearrangement at temperatures closer to 250 °C, have been formed.^[175,183] While mechanical properties can be improved with these modifications, the true microporous nature of TR polymers, as indicated by detectable Brunauer–Emmett–Teller (BET) surface areas, is typically only found for samples converted near their degradation point.^[85] Therefore, improvements in mechanical properties are often met by reductions in transport performance. Thus, in the future, TR polymers would benefit significantly from a more holistic understanding of which types of thermally rearrangeable bonds, beyond the limited set now available, should be incorporated into the polymer backbone to yield useful properties for efficient gas separation membranes.

A similar conundrum exists in the formation of PIMs. PIMs achieve outstanding size-sieving capabilities by reducing polymer chain mobility, which often results in adverse mechanical properties (e.g., brittleness). PIM-1 is a notable exception and has a characteristic tensile strength and elongation at break in the range of 45.1–47.1 MPa and 7.2–11.2%, respectively,^[184,185] which represent mechanical properties that begin to approach those of commercially available membrane polymers.^[186] In many instances, structural modifications to the PIM backbone, such as copolymerizing trifluoromethyl and phenolsulfone groups^[184] or copolymerizing dinaphthyl groups,^[187] can improve selectivity while maintaining upper bound performance relative to PIM-1. However, these modifications result in concomitant losses in mechanical properties. Conversely, structural modifications to the PIM backbone designed to improve ductility, such as adding tetraoxide thianthrene,^[187] shift transport performance away from the upper bound. Postsynthetic modifications to PIM-1, such as the addition of carboxylic acid functionality, are also known to reduce film ductility.^[185] Some of the most promising improvements in transport properties are for ethanoanthracene PIMs containing Tröger's base (e.g., PIM-EA-TB).^[171] Replacing ethanoanthracene with triptycene-based functionality (e.g., PIM-Trip-TB) improves mechanical properties. However, like the aforementioned examples, these changes in mechanical properties correspond to with a decrease in upper bound performance.^[188]

Physical aging is another concern for the industrial deployment of microporous polymers. Physical aging is the slow relaxation of nonequilibrium glassy polymers to their equilibrium packing state.^[189] This relaxation phenomenon is accelerated for high free-volume materials and for polymers close to their glass transition temperatures (T_g). Perhaps most critically, physical aging is significantly pronounced for thin polymer films, which have higher surface-area-to-volume ratios than thick films.^[190] PTMSP has been studied extensively for these effects. Initially, thick films on the order of tens to hundreds of micrometers thick showed 6–27-fold reductions in permeability after 4 years, a loss that correlated with reduced diffusivity.^[191] Additional studies revealed that the aging rate for PTMSP is significantly accelerated for films $\approx 1 \mu\text{m}$ thick or thinner.^[192,193] Similar to PTMSP, thick PIM films show significant aging effects after only 1 d,^[171] and more pronounced aging has been measured for a variety of PIM structures over much longer periods of time.^[188,194] While reductions in permeability are not as significant for PIMs and

TR polymers compared to those of PTMSP, possibly due to the greater rigidity of PIM and TR polymer backbones, 220 nm thick PIM-1 shows an 80% reduction in oxygen permeability over 40 d,^[193] and 1.4–1.8 μm thick partially converted TR polymer samples derived from HAB-6FDA show between 55% and 65% reductions in oxygen permeabilities over the same timeframe. Predicting long-term transport performance for thin films of microporous polymers will be essential for their industrial acceptance.

Other microporous polymers, such as conjugated microporous polymers, have achieved some success as well,^[195] and the reader is directed to a relevant review for more detailed discussions.^[196]

CMS membranes, or simply carbon membranes, were first investigated by Barrer in the early 1960s.^[103,104,197] Though derived from polymeric precursors, CMS membranes boast performance metrics that can exceed those of polymer membranes. By their sieving behavior, these membranes achieve advantageous diffusion selectivities and significantly larger sorption capacities compared to those of pure polymers, resulting in higher permeabilities. This type of behavior has been demonstrated for separations practiced in industry, particularly O₂/N₂ and CO₂/CH₄ separations,^[198] and for emerging applications, such as propylene/propane^[199] and ethylene/ethane separations.^[200] However, it is estimated that carbon membranes will cost 10–100 times more than polymer membranes,^[164] and perhaps the greatest challenge is forming carbon membranes that are stable to condensable gases and water vapor.^[126] In addition to transport properties, these economic and practical processing considerations need to be addressed when designing carbons for industrial membrane applications. A broader selection of carbon materials and their application in gas separations can be found in recent reviews.^[5,70]

4.1.2. Multicomponent Systems—Composite Membranes for CCS and Gas-Phase Chemical Separations

An attractive means of enhancing membrane properties beyond those of single component membranes is to employ composites, which are combinations of two or more components that interact synergistically to improve gas separation performance. Compositing has primarily been considered in the context of MMMs consisting of a permselective filler phase dispersed into a polymer matrix. The filler phase in an MMM is often a zeolite,^[201–203] MOF,^[204–209] silica,^[210] CMS,^[211,212] or carbon nanotube.^[213] The MMM approach has major advantages, as well as challenges, when compared to pure component systems. In many instances, composites have improved separation performance over neat polymer membranes, as well as better processability compared with pure component systems such as CMS membranes or neat MOF membranes. Major challenges with the approach include developing composites that are defect free, mechanically robust, and have high permeance.

The primary advantage that composites have over neat polymers is their gas separation performance, as there are numerous examples of membranes with gas separation performance that exceed the Robeson upper bound for neat polymers. There are two primary mechanisms by which the filler phase of a mixed-matrix system imparts improved separation performance on the membrane, including diffusive enhancements (or size-sieving) and adsorptive enhancements. Although transport through the filler phase does not necessarily follow the solution-diffusion model, it can still contribute to the overall solubility or diffusivity of various components in the membrane. In this way, fillers can act primarily as diffusive-selective particles, or sieves, or as solubility-selective particles or adsorbents. To see how each of these approaches might be leveraged for a separation, it is first necessary to compare the physical properties of commonly targeted gas molecules. **Table 2** lists the relevant physical properties of gas molecules commonly considered for gas separations.

The differences in the molecular properties for gas pairs can be leveraged to conduct a separation. In more traditional, thermal-based separations, the differences in condensability, or boiling point, are leveraged. In membrane-based separations, a molecule's ability to diffuse is related to its kinetic diameter and its adsorptive partitioning is related to properties such as dipole moment (μ), quadrupole moment (Θ), and polarizability (α). For example, C₂H₄/C₂H₆ mixtures are particularly challenging to separate because these two molecules have similar boiling points and kinetic diameters, while in contrast, H₂/C₃H₈ mixtures are relatively simple to separate using thermal, diffusive, or adsorptive mechanisms.

When targeting a specific gas pair and choosing materials for a composite membrane, it is important to keep in mind the mechanism that will enable the separation. While there are many examples of fillers employed in the literature, we can compare specific examples of how sieving fillers are used to improve olefin/paraffin or CO₂-based separations.

Diffusivity-Based Enhancements: The most prevalent way to impart permselectivity in a composite is through the addition of diffusive-selective, or size-sieving, particles. This approach has been widely used to enhance the selectivity for CO₂/CH₄, CO₂/N₂, H₂/CO₂, and C₃H₆/C₃H₈ separations. Specifically, the sieve leverages differences in the kinetic diameter between the two permeating components to achieve selectivity. The sieve then has an intrinsic permeability and selectivity of its own, and that

Table 2. Relevant physical properties of light gases.^[44]

Gas	Kinetic diameter [Å]	Boiling point [K]	Dipole moment, μ [10 ⁻¹⁸ esu m]	Quadrupole moment, Θ [10 ⁻²⁶ esu m ²]	Polarizability, α [10 ⁻²⁵ cm ³]
CO ₂	3.3	216.6	0	4.30	29.11
N ₂	3.64–3.80	77.4	0	1.52	17.403
H ₂	2.83–2.89	20.3	0	0.66	8.042
CH ₄	3.76	111.7	0	0	25.93
C ₂ H ₄	4.16	169.4	0	1.50	42.52
C ₂ H ₆	4.44	184.6	0	0.65	44.3–44.7
C ₃ H ₆	4.68	225.5	0.37	0	62.6
C ₃ H ₈	4.3	231.0	0.084	0	62.9–63.7

is imparted to the composite membrane proportionally to the volume fraction of sieve in the composite. The resulting permeability of a composite that contains sieving particles is given by the Maxwell relationship, which is widely used to predict the permeability of composites^[214]

$$P_{\text{MMM}} = P_p * \left[\frac{P_s + 2P_p - 2\phi(P_p - P_s)}{P_s + 2P_p + \phi(P_p - P_s)} \right] \quad (12)$$

where P_{MMM} is the permeability of the composite, P_p and P_s are the permeabilities of the polymer phase and sieve phase, respectively, and ϕ is the volume fraction of the film that is occupied by the sieve phase. This relationship is useful for determining the intrinsic properties of the sieve phase and can allow for the determination of composite properties at various sieve loadings.

One of the main challenges with forming composites using sieving particles is in finding a filler phase that has a pore diameter that can discriminate effectively between the two permeating gas molecules while in the polymer matrix. Two prominent examples of this effect being successfully implemented for $\text{C}_3\text{H}_6/\text{C}_3\text{H}_8$ and CO_2/CH_4 separations are by Zhang et al.^[203] and Rodenas et al.,^[207] respectively. In the case of $\text{C}_3\text{H}_6/\text{C}_3\text{H}_8$ separations, it was found that a zeolitic imidazolate framework (ZIF-8) provides exceptional selectivity between these two molecules based on their kinetic diameters. ZIF-8 is comprised of Zn^{2+} ions linked through methyl-imidazolate units into a sodalite-type MOF. This material was shown not to have any specific adsorptive affinity for propylene over propane, yet when used to form an MMM exhibits significantly enhanced permeation properties. **Figure 7** shows the adsorption isotherms of ZIF-8 as well as the permeation properties of the composite membranes.

As shown in **Figure 7**, the improved permeability and permselectivity for ZIF-8 MMMs do not originate from an adsorption mechanism. Similarly, the rate of adsorption data does not suggest significantly higher diffusivity for C_3H_6 over C_3H_8 in neat ZIF-8. While the permeability of olefins and paraffins in ZIF-8 elegantly matches the Maxwell model, the intrinsically high permselectivity found for ZIF-8 for $\text{C}_3\text{H}_6/\text{C}_3\text{H}_8$ separations could not have been predicted by measuring equilibrium adsorption isotherms and rates of adsorption

alone; indeed, diffusion kinetics are key compared to the thermodynamic partitioning.^[92]

Solubility-Based Enhancements: While sieving filler materials increase diffusive selectivity by leveraging differences in analyte kinetic diameters, MMM fillers can also tune the solubility component of permeability to improve permselectivity. This approach has been successfully employed to improve the selectivity for CO_2/N_2 ,^[206] CO_2/CH_4 ,^[209,215] and $\text{C}_2\text{H}_4/\text{C}_2\text{H}_6$ ^[204,216] separations. There are numerous porous materials that have been developed that show very high adsorptive selectivities for CO_2 -based and $\text{C}_2\text{H}_4/\text{C}_2\text{H}_6$ separations. Most notable are MOFs with coordinatively unsaturated metal centers^[217] as well as various types of porous materials that have amine functionality.

To elaborate further, we will consider a system that was used to improve all three of these separations, namely $\text{M}_2(\text{dobdc})$ ($\text{M} = \text{Mg}, \text{Mn}, \text{Co}, \text{Ni}, \text{and Zn}$) MOF nanocrystals embedded within polyimides. Improving $\text{C}_2\text{H}_4/\text{C}_2\text{H}_6$ separations using $\text{M}_2(\text{dobdc})$ was demonstrated by Bachman et al.,^[204] and this improvement was shown to occur through an adsorption-enhanced mechanism. Most neat polymers exhibit permselectivity for C_2H_4 over C_2H_6 based on a complex trade-off between diffusion and solubility selectivity. Diffusion selectivity favors the smaller C_2H_4 molecule, but sorption selectivity slightly favors the more condensable C_2H_6 molecule. Therefore, from the exclusive perspective of solubility selectivity, neat polymers operate at a fundamental disadvantage for a $\text{C}_2\text{H}_4/\text{C}_2\text{H}_6$ separation. Interestingly, the limited sorption-based selectivity can be improved significantly through the incorporation of highly selective nanocrystals of $\text{M}_2(\text{dobdc})$, which preferentially interact with C_2H_4 over C_2H_6 . This preferential olefinic binding leads to composite films that are selective for C_2H_4 in both solubility and diffusivity (**Figure 8**). Similarly, improving CO_2 permselectivity by incorporating $\text{M}_2(\text{dobdc})$ was achieved by Bae and Long,^[206] where the coordinatively unsaturated metal sites in $\text{Mg}_2(\text{dobdc})$ allowed for improved solubility selectivity and thus permselectivity when combined with the polyimide, 6FDA-DAM (**Figure 9**). Similar phenomena were demonstrated for CO_2/CH_4 separations using $\text{Ni}_2(\text{dobdc})$ nanoparticle fillers in a number of polymer matrices.^[209] For all three of these separations, the highly selective $\text{M}_2(\text{dobdc})$ MOFs have improved permselectivity in composite membranes via adsorption enhancement. Going forward, improvements to

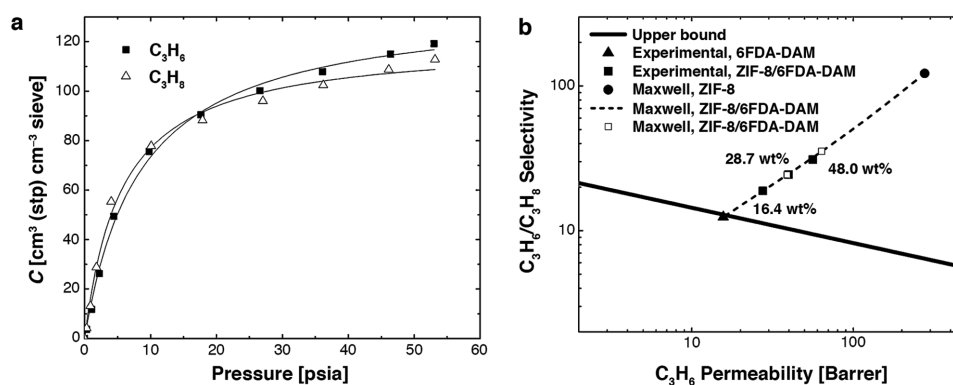


Figure 7. Adsorption and separation performance of ZIF-8 and composite membranes. a) Adsorption isotherms of C_3H_6 and C_3H_8 in ZIF-8 and b) membrane performance on the $\text{C}_3\text{H}_6/\text{C}_3\text{H}_8$ upper bound for various loadings of ZIF-8 as well as the corresponding Maxwell predictions. Reproduced with permission.^[208] Copyright 2012, Elsevier.

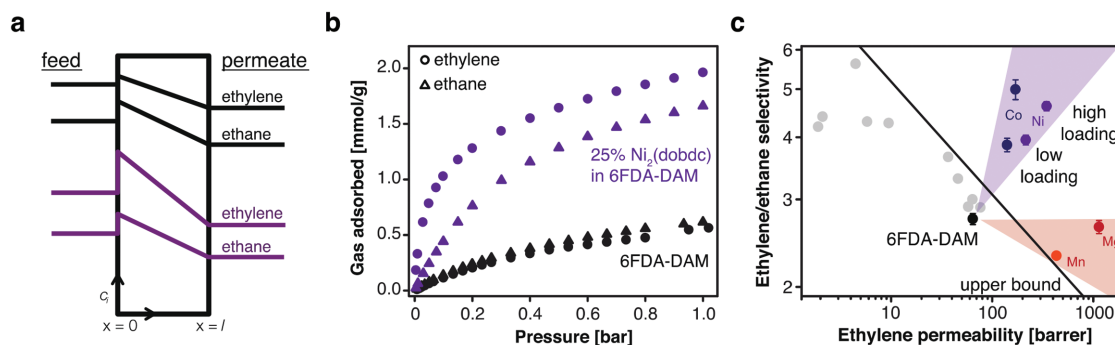


Figure 8. Adsorption-enhanced composite membranes for C_2H_4/C_2H_6 separation. a) By increasing the relative concentration gradient for ethylene across the membrane using the adsorptive selectivity in the MOF, there is a greater driving force for mass transport across the film. b) The ethylene and ethane isotherms in neat 6FDA-DAM, as well as the composite with 25 wt% $Ni_2(dobdc)$, indicating the large increase of gas adsorbed into the film as well as an ethylene adsorptive selectivity due to incorporation of the adsorbent. c) The resulting permselectivities at 2 bar and 35 °C for variants of $M_2(dobdc)$ ($M = Mg, Mn, Co, \text{ and } Ni$). MOF content in each membrane by weight are 10% and 33% for $Co_2(dobdc)$, 6% and 25% for $Ni_2(dobdc)$, 23% for $Mg_2(dobdc)$, and 13% for $Mn_2(dobdc)$. Reproduced with permission.^[204] Copyright 2016, Nature Publishing Group.

adsorption-enhanced membranes can be achieved through the development of more selective adsorbents.

In addition to the attractiveness of adsorption enhancement for tailoring performance in composite membranes, it should also be noted that $M_2(dobdc)$ /polyimide blends demonstrate an unusual, advantageous interface effect.^[204] Incorporating the MOF into the polymer creates an effectively crosslinked, insoluble matrix. These membranes exhibit plasticization resistance typical of crosslinked polymers without suffering from the usually associated decrease in permeability. This result demonstrates that properly matched polymer and filler surface functionalities can produce interfaces that inherently improve performance, creating a composite greater than the sum of its parts.

4.2. Aqueous Transport

4.2.1. Desalination

Access to potable water is a pressing issue in many parts of the world. In coastal communities, seawater desalination is being

implemented at increasingly larger scales. Desalination is also needed in other geographical areas, where water is confined to salted aquifers.^[218] Reverse osmosis is the leading desalination technology in terms of overall capacity, and a reliable polymer membrane has been key to its success. Thin film composite membranes are featured prominently in reverse osmosis. These are typically made of an aromatic polyamide thin film (typically 0.1–0.3 μm) atop a thick polysulfone support layer ($\approx 40 \mu m$). In practice, an additional support layer ($\approx 100 \mu m$) is needed to uphold the structural integrity of the membrane.^[219]

The permeability/selectivity trade-off observed in gas separation is also applicable to membranes for water desalination under the framework of the solution-diffusion model (Figure 10).^[220,221] Here, membrane polymer chain dynamics control water and salt permeability and selectivity. Microporous membranes, single-component or composite, featuring more shape-persistent micropores may provide advantages in future designs. For example, decoupling membrane-analyte interactions for aqueous transport has been achieved using carbon-nanotube-based membranes, leveraging their interior surface to promote frictionless transport for water molecules

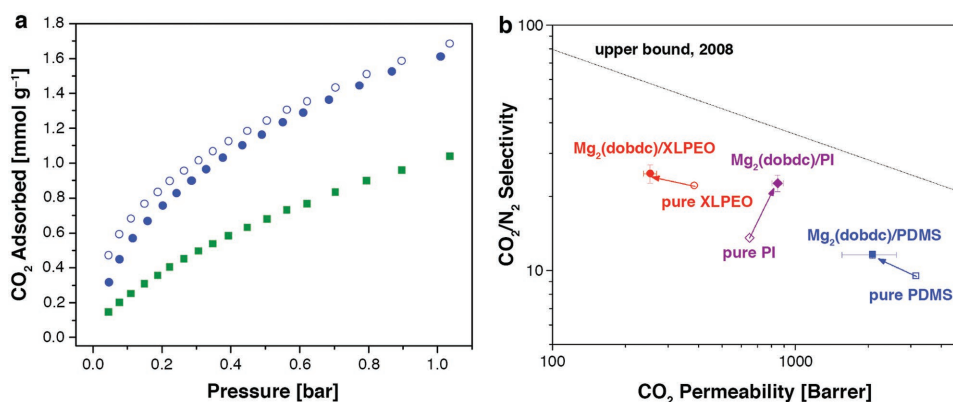


Figure 9. Adsorption-enhanced CO_2/N_2 separations using $Mg_2(dobdc)$. a) Equilibrium adsorption isotherms in neat 6FDA-DAM (green squares), 10% $Mg_2(dobdc)$ in 6FDA-DAM (blue circles, filled), and the predicted amount adsorbed based on the pure component isotherms (blue circles, open). b) Performance of various $Mg_2(dobdc)$ composites on the CO_2/N_2 upper bound. Reproduced with permission.^[206] Copyright 2013, the Royal Society of Chemistry.

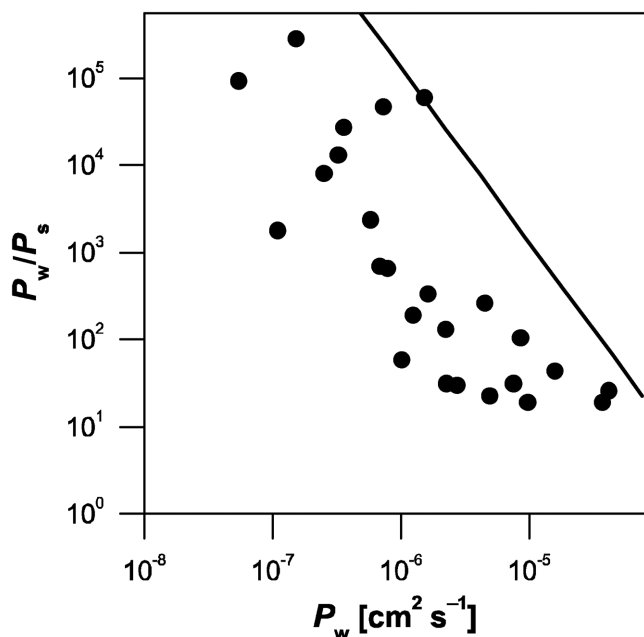


Figure 10. The permselectivity trade-off plot for reverse osmosis. Reproduced with permission.^[220] Copyright 2014, Elsevier.

in both simulation^[222,223] and experiment;^[224,225] additionally, the micropore orifice efficiently prevents hydrated ion translocation.^[223,226] Zeolite–polymer composite and even some MOF–polymer composite membranes have been investigated for reverse osmosis applications with the porous crystals providing pathways for fast transport of water molecules.^[227] In these composites, interfacial voids pose a significant problem and warrant further attention moving forward.

Related membranes are also garnering early successes in forward osmosis applications for desalination, wastewater treatment, and water reclamation.^[228] While reverse osmosis relies on an applied pressure to drive water against the osmotic pressure, forward osmosis allows water to flow spontaneously across the membrane from a low concentration feed solution into a high concentration draw solution. By thoughtfully designing the composition of the draw solution, the water passing across the membrane can be reclaimed. Commonly, the feed is salt water from a natural source, and the draw solution uses solutes that can easily be removed, leaving potable water behind. Thermolytic solutes that evolve gases at high temperatures and salts that precipitate upon cooling have been investigated for this application, as have tandem forward osmosis–reverse osmosis and forward osmosis–nanofiltration systems.^[229]

Forward osmosis membranes are often composite structures configured with a thin, dense selective layer on one or more nonselective support layers. Regarding the selection of microporous selective layers, Song and Xu used MD simulations to evaluate various carbon nanostructures for this application.^[230] Notably, CNTs exhibited similar fluxes for water yet greater ion rejection than porous graphene; both compare favorably to reported values for existing forward osmosis technologies. Composite zeolite–polymer selective layers have also been investigated to some success, though few examples exist in the literature.^[231] As this application is still an emerging

area of exploration for microporous materials, we anticipate significant growth in the next few years in new microporous selective layers for forward osmosis.

4.2.2. Pervaporation—Dehydration of Organic Liquids

Pervaporation is a process by which a mixture of liquids on one side of a membrane selectively diffuses across the membrane to vaporize at low pressure on the downstream side. The most common commercial application is the dehydration of organic liquids.^[232,233] Because crude renewable biofuels are produced in fermentation reactors as primarily aqueous solutions of alcohols, efficient dehydration techniques are needed to separate the combustible alcohol from this mixture.^[234] Unlike conventional distillation techniques, pervaporation is not limited by the formation of a water–alcohol azeotrope. While dense films with separation performance governed by the solution-diffusion mechanism are predominantly used for pervaporation, a selection of inorganic and hybrid membranes has emerged with behavior that deviates from this mechanism, including supported zeolite membranes, prepared by nucleation and growth of zeolites directly on an inorganic support.^[235] Thus, while polymer-based membranes presently dominate the market, recently commercialized zeolite membranes for pervaporation may eventually overtake them.^[236] The water is separated primarily through size selectivity, although counterexamples of hydrophobic zeolite membranes that preferentially transport the larger organic molecules due to chemical selectivity also exist.^[232]

New classes of microporous materials are being adopted as pervaporation membranes. PIM-1 is one example, and it has shown promise both as a neat membrane and as part of a composite. Early studies by Adymkanov et al. show that the strongly hydrophobic character of PIM-1 selectively permits the passage of alcohols over water, and alcohol permeability decreases with increasing molecular diameter.^[237] Carboxylated PIM-1 (cPIM-1), with a greater hydrophilicity than the unmodified polymer, has been demonstrated as an effective permeability enhancer in high selectivity, low permeability polyimide pervaporation membranes.^[238] In these systems, water permeates faster than alcohols. Blending 20% cPIM-1 into Matrimid and several other polyimides increases water permeability nearly twofold in separations from 1-butanol, with no measurable reduction in selectivity; however, higher cPIM-1 loadings lead to severe loss in selectivity.^[239] Blends of higher cPIM-1 content swell considerably in the alcohol solutions, lowering the barrier to butanol diffusion.

MOF-based MMMs have also been investigated for alcohol dehydration.^[240] Membrane improvements are noted in this system due both to the adsorptive selectivity imparted by hydrophobic MOFs, such as ZIF-8, and to changes in polymer chain mobility due to interactions with the filler material. Marti et al. have recently demonstrated that neat films of the MOF SIM-1, made by chemically grafting individual crystals into a continuous membrane with ethylenediamine, act as an effective molecular sieve to separate water from water–ethanol mixtures.^[241]

It should be noted that pervaporation is also applied to anhydrous liquid–liquid separations. The rising prevalence of

organophilic sieving materials, particularly zeolites and MOFs, has made this approach more viable.^[242] For example, silicalite-1-based membranes have shown efficacy in separating xylene isomers via pervaporation.^[243] Many examples of neat MOF pervaporation membranes used in this context have also been reported.^[244]

4.2.3. Dehumidification—Indoor Air Conditioning

Maintaining a comfortable indoor environment for building occupants is an energy-intensive process that may take up to 60% of the total energy consumption for a building.^[245] Dehumidification is an integral part of air conditioning systems. Conventional dehumidification cools humid indoor air to collect the condensed water before reheating the dry air to the indoor temperature level for recirculation.^[246] Liquid-to-air membrane energy exchangers are an alternative membrane-based approach to dehumidification. Here, water transports through a porous membrane into a liquid desiccant, which can be regenerated with waste heat elsewhere in the building. Techno-economic analyses of membrane-based dehumidifying systems can be found elsewhere.^[246,247] While membranes presently used are generally macroporous or mesoporous,^[248] a few notable examples of microporous composite^[249] and single-component^[250] membranes are showing promise. Though still a nascent area of membrane science that impacts one of the major sources of energy consumption, there may be relatively straightforward solutions with existing platforms such as PIMs, TR polymers, or CNT membranes (i.e., those that leverage friction-free water transport within microporous voids).^[224]

4.3. Ion Transport

4.3.1. Aqueous Ion Transport—Fuel Cells and Electrochemical Energy Storage

Renewable generation and storage^[251] of electrical energy are critical to a sustainable future. To this end, FCs offer on-demand energy generation by converting chemical potential energy into electrical energy. The source of chemical energy in fuel cells is either H₂ or an alcohol, such as methanol or ethanol. Hydrogen fuel cells can achieve a zero-emission rating when the hydrogen fuel is generated using renewable energy sources. EES, on the other hand, is increasingly being paired with systems featuring intermittent energy generation, including wind and solar. Doing so allows for multihour power delivery, frequency regulation, load shifting, and other advantages depending on the rate capability of the chemistry and scale of the system. For both FCs and EES, membrane technology is a critical determinant of system performance. The membrane is responsible for selective ion transport and other functions. Since the operations of these electrochemical devices occur in aqueous and nonaqueous settings, across wide temperature ranges and under extremes of chemical reactivity, there is not a universally applicable membrane platform. Instead, membranes are developed to balance system needs for conductivity, selectivity, and structural integrity.

In approaching the design of ion-transporting membranes for FCs and EES, it is important to first consider the fundamental aspects governing ion transport in polymeric materials. Poly(ethylene oxide),^[252] or PEO, ubiquitous as a component in solid polymer electrolytes, conducts cations through reversible coordination to a charge neutral polymer backbone.^[253] Solid and gel (or plasticized) polymer electrolytes are simply formulated by dissolving salts in PEO, or its derivatives, alongside other additives.^[91] Polyelectrolytes, on the other hand, feature a charged backbone or side chain alongside mobile counterions. The mobile counterions experience a repulsive electrostatic field from charges residing on the polymer, or Donnan exclusion, which results in perfect ion-transport selectivity. Nonetheless, these interactions, similar to strongly adsorptive interactions in gas separation, slow down the rate of ion transport, embodied by the ionic conductivity in this case. In doing so, the mobility of the ions is coupled to the polymer segmental chain dynamics, which are at least an order of magnitude slower than the bulk ionic mobility.^[91] With that in mind, shape-persistent microporous membranes are increasingly attractive targets for engineering transport selectivity without sacrificing ionic conductivity. By deploying a microporous framework as the sieving elements, three desirable membrane attributes can be conferred: selectivity can be enforced through size exclusion without necessarily using charged moieties featuring strong interactions, minimized membrane–analyte interactions decouple ion motion from the sieving material (rigidity and inertness can be deliberately introduced for dimensional and chemical stability), and high conductivity can be realized with frictionless pore walls with additional transport enhancement possible through confinement effects.

4.3.2. Aqueous Proton Transport—Proton Exchange Membrane Fuel Cell

Aqueous proton transport is a key process in proton exchange membrane (PEM) fuel cells.^[254] This fuel-cell chemistry is not affected by unwanted active-material crossover; therefore, we will only discuss mechanically robust microporous membranes with high rates of proton conduction. Protons exhibit unusually high diffusion rates compared to Na⁺ and K⁺ ions^[255] due to the formation of large-scale hydrogen-bond networks where lone electron pairs are coordinated to hydrogen atoms. However, unlike an ice crystal, the liquid structure is dynamic and can incur various defects. One of these defects is the ionic defect, where the O–H vibration is sufficiently large to release the proton to a neighboring water molecule, effectively creating a hydroxide ion, OH[−], and a hydronium ion, H₃O⁺. A hydronium ion solvated by three water molecules is called the Eigen^[256] cation, and a proton coordinated between two water molecules is called the Zundel^[257] cation. These are the principal complexed proton carriers or vehicles in bulk water. Protons can diffuse by virtue of their carrier's motion, a mechanism aptly called vehicular transport (**Figure 11**). Transport can also occur through fluctuations in the hydrogen-bonding network structure when an excess proton is transferred to an appropriately aligned neighboring water molecule. This process is called the Grotthuss mechanism,^[258] named after the 19th century

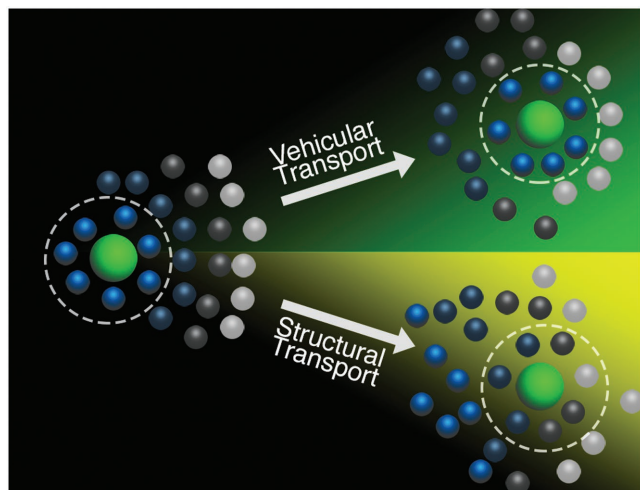


Figure 11. Mechanistic considerations governing ion transport in liquid media. In vehicular transport (top), the ion retains its solvation shell as it moves through the medium. In structural transport (bottom), the solvent molecules in the first solvation shell exchanges with bulk solvent molecules.

scientist who first hypothesized it.^[259] Through a multitude of simulation methods, Markovitch et al. have determined that the multistep proton-transfer process in bulk water goes through an Eigen–Zundel–Eigen transition (Figure 12).^[260] The process is initiated by a rotating Eigen cation. As a result, the proton hopping mechanism is limited by the molecular rotation time-scale. While vehicular transport is general to all ions in both aqueous and nonaqueous environments, Grotthuss transport is only present in hydrogen-bonded networks and is the cause of the unusually high proton diffusion in water. Detailed review of the ab initio simulations on the proton-transfer processes^[261] and emerging insights into their nuances^[262] can be found elsewhere.

The rate-limiting step in proton transfer is molecular rotation and alignment while in the Eigen form of the cation. As confinement is imposed upon the water molecules, the bulkier

isotropic Eigen cation is destabilized, giving way to the Zundel form as the only possible cation complex.^[263] The directional nature of the hydrogen bonds in a confined space implies that the water molecules are well aligned for proton transfer via the Zundel–Zundel pathway (Figure 12).^[255,264] The proton diffusion is thus enhanced by an order of magnitude^[263] due to the removal of the rate-limiting step. This process serves as the motivation for the use of microporous materials in proton transport as confining frameworks and structured proton-transfer mediators.

Though intrinsically not a microporous material, Nafion and related perfluorosulfonic acids (PFSAs) are the standard bearers of proton exchange membranes. Nafion and other PFSAs feature a perfluoropolyether backbone and hydrophilic sulfonic acid side chains of variable length and loading. These polymers undergo microphase separation upon hydration, leading to a bicontinuous network^[265] featuring a mechanically robust phase and a hydrophilic ion-conducting phase. As water is the primary medium in which proton transport takes place within the hydrophilic phase, bulk-like proton diffusion at $\approx 7.8 \times 10^2 \text{ S cm}^{-1}$ is observed in these microenvironments and has been studied extensively through experiments^[266] and simulations.^[267]

Nafion and PFSAs are not ideal membranes for fuel cells. Higher temperatures ($>80 \text{ }^\circ\text{C}$) are desirable for fuel-cell efficiency due to enhanced catalytic activity; however, the critical role water plays in proton conduction in PFSAs also signifies that the loss of hydration at higher temperature is detrimental to membrane performance. Considering this, some microporous materials offer promising alternatives to PFSAs. Their persistent micropores can not only emulate the liquid-infiltrated state but also impose the effect of nanoconfinement, leading to improved proton conductivity.

Carbon nanotubes present a simple model system where improved proton transfer has been observed when in confinement. Brewer et al.^[263] used empirical valence bond method to simulate the diffusivity of protons under confinement. A tenfold improvement in proton diffusivity was observed despite diminished vehicular transport behaviors in carbon nanotubes with diameters less than 5 Å. Dellago et al.^[268] showed in their

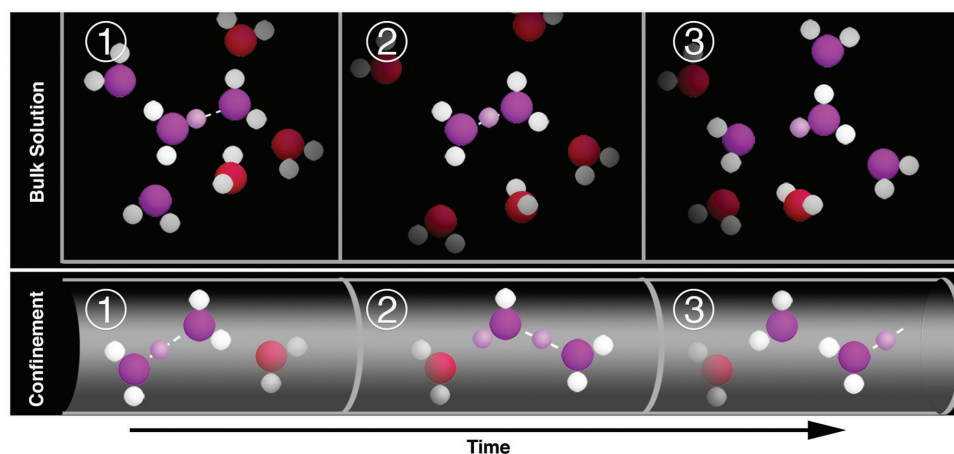


Figure 12. Aqueous proton transport in bulk (top) and confinement (bottom) at three key instances in chronological order. In bulk, proton transfer undergoes the Eigen–Zundel–Eigen mechanism. On the other hand, only the Zundel–Zundel mechanism is observed in confinement. Oxygen atoms participating in the proton complexes and the corresponding excess protons are highlighted.

Car–Parrinello MD simulation that the diffusion coefficients of protons are more than 40 times higher in a (6,6) carbon nanotube (≈ 8 Å in diameter) than they are in bulk.^[269] Furthermore, Voth and co-workers showed that proton transfer in a (6,6) carbon nanotube takes place exclusively via the Zundel–Zundel process, a sign of confinement-assisted conductivity enhancement.^[264] The delocalized excess proton structure referenced therein, $H_7O_3^+$, was corroborated by a recent path-integral MD simulation,^[255] a gradual departure from the discrete description based solely on individual Eigen and Zundel complexes. In the context of PEM fuel cells, carbon nanotubes have not been used as a proton exchange membrane yet, but have been extensively investigated as a catalyst support. However, carbon-nanotube-based proton- and electron-conducting membranes have been reported. Wu et al.^[270] pioneered epoxy-based carbon nanotube membranes, generated by microtoming an epoxy–nanotube composite. Pilgrim et al.^[271] fabricated thicker epoxy membranes with oriented nanotubes. These nanotubes were grown as a thick forest, which was infiltrated with epoxy as the membrane matrix postsynthesis. The demonstrated proton-transfer rate is approximately half of that of a Nafion membrane, still with room for improvement. Given the synthetic capabilities^[272] and membrane precedents,^[224,270,273] a carbon-nanotube-based proton exchange membrane leveraging confinement-induced high proton-transfer rate may still be within reach.

Nanotubes can also be constructed from bottom-up approaches from organic macrocycles via self-assembly. Though examples of proton transport exist for arylene ethynylene^[274] and dendritic dipeptide,^[275] they have not moved beyond the lipid bilayer vesicle platform and are not amenable to energy-related applications. Another notable class of organic nanotubes is cyclic peptides. Hypothesized in 1974^[276] and first synthesized in 1993,^[76] cyclic peptides have sustained two decades of development. Proton transport was among the first properties investigated, also using a vesicle platform.^[277] The class of materials has since then extended its applicability into ion channels in a biooriented context.^[278] However, in energy technology, membranes require greater dimensional stability than lipid bilayers. Xu et al.^[79] used hierarchical assembly to achieve such a sub-nanometer microporous polymeric membrane by bringing together a block copolymer, a homopolymer, and cyclic peptide macrocycles. The macrocycles are covalently attached to chains of poly(ethylene oxide), which interface favorably with the hydrophilic block of polystyrene-*b*-poly(methyl methacrylate). The system undergoes self-assembly, sequestering the polymer-covered nanotubes in the lumens of cylindrical-morphology block copolymers. The nanotubes are shown to conduct protons much more effectively than the bare membranes. Even though the current material's selection cannot withstand the harsh conditions imposed by PEM fuel cells, the synthetic diversity that it can display could control liquid water structure with unprecedented specificity.^[17,149]

MOFs have also garnered attention for their unusual ability to facilitate anhydrous proton transport, directly addressing the shortcomings of Nafion and PFSA at high temperature.^[279] Shimizu and co-workers^[280] and Kitigawa and co-workers^[281–283] demonstrated that the installation of acidic functionalities within the cavities of MOFs enables the direct mediation of proton transfer in the absence of water (Figure 13). Both aryl

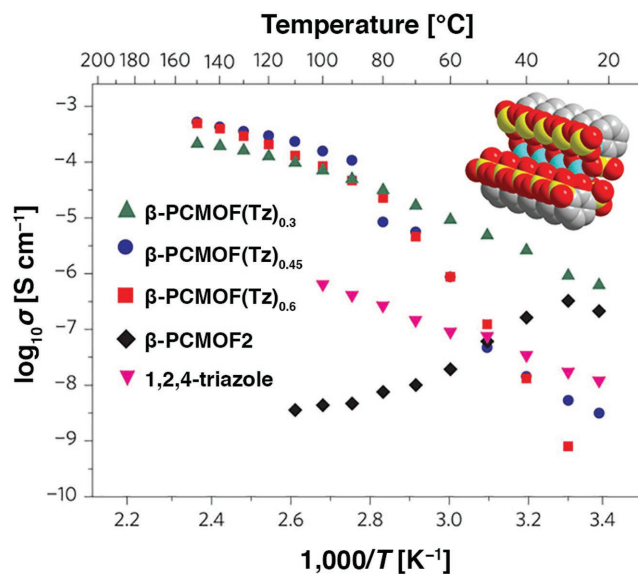


Figure 13. Anhydrous proton conduction in β -PCMOF2 by scaled introduction of 1*H*-1,2,4-triazole. Conductivity of the triazole-infused complexes maintains a monotonic increase in proton conductivity as temperature rises above 100 °C, demonstrating anhydrous proton transfer. Reproduced with permission.^[280] Copyright 2009, Macmillan Publishers Ltd.

sulfonates and aryl phosphonates^[284] within the framework serve as strongly acidic groups that facilitate proton transport. This functionalization was accomplished either through the use of sulfonated or phosphonated ligands^[281] or through post-synthetic modification.^[285] These sites, along with infiltrated water depending on the relative humidity, act as proton hopping sites, enabling proton conductivity typically in the range of 1×10^{-3} S cm^{-1} by promoting structured proton transfer.^[281,286] For high-temperature operations, water can be substituted for less volatile proton hopping mediators such as 1*H*-1,2,4-triazole.^[287] The introduction of these azaheterocyclic mediators enabled proton conduction at 150 °C, well above the boiling point of water.^[280] Exceptional conductivity can be achieved at more than 1×10^{-2} S cm^{-1} by lubricating the framework or weakening the water–framework interaction.^[282] An alternative proton conduction strategy involves the use of a guest proton conductor in a micropore, such as imidazole.^[283] For interested readers, more detailed reviews on proton-conducting MOFs operating under various states of humidity can be found elsewhere.^[288,289]

4.3.3. Nonaqueous Ion Transport—Electrochemical Energy Storage

Membranes play a critical role in many emerging technologies for electrochemical energy storage for aviation, transportation, and the grid. Membranes electronically isolate the cathode from the anode and allow the working ion of the battery to diffuse between them during cycling. Importantly, many of the energy-storage chemistries in these devices involve active materials that are either dissolved, dispersed, or suspended in the supporting electrolyte, including metal–air batteries, metal–sulfur batteries, and redox-flow batteries. In such systems,

membranes should prevent active-material crossover while minimizing resistance to ionic conduction, which ensures maximal utilization of the active materials in a given cell. Failure to prevent active-material crossover lowers the energy efficiency of the cell due to shuttling of active materials between electrode compartments (i.e., due to an internal chemical short). Once comingled, active materials—particularly in their charged state—can also cross-annihilate, giving rise to an unacceptable degree of capacity fade.

Commercially available membranes based on mesoporous polyolefin separators^[290] are nonselective in that both the working ion of the battery and the charge-storing actives can traverse the membrane. These membranes are thus unsuitable for the aforementioned batteries. A number of alternative strategies have been explored, including modified Nafion membranes,^[291] ceramic membranes,^[95,292] and coated polyolefin separators.^[293] Not surprisingly, these are costly additions to the cell. Ion-exchange membranes have also not been as effective as desired, often due to chemical degradation or poor electrolyte compatibility. On the other hand, microporous membranes present an exciting new development that is on track to meet both cost and performance requirements.^[294] Their implementation in advanced energy-storage concepts and systems raises new and interesting questions as to the role of membrane pore architecture and chemistry on ion conduction and ion selectivity. Given the wide range of organic solvents and supporting electrolyte salts typically encountered in these systems,^[295] it remains an outstanding challenge to codify structure–transport relationships in microporous materials and membranes for working ions of interest, such as Li^+ , Na^+ , K^+ , Mg^{2+} , tetraalkylammonium cations, BF_4^- , PF_6^- , FSI^- , TFSI^- , methanesulfonate, trifluoromethanesulfonate, etc. However, in recent reports noting performance gains, there is an overwhelming reason to do so in the near future.^[96,296,297]

Whereas our understanding of ion transport in aqueous systems is mature, less mechanistic detail is available for ion transport in nonaqueous electrolytes and considerably less is known regarding nonaqueous ion transport within a micropore or in a membrane with structurally complex and percolated ion-transduction paths in 3D.

To date, solvent-stabilized Li-ion dynamics have been explored in select battery-relevant solvents such as ethylene carbonate^[298–302] and propylene carbonate.^[299,300] For example, Borodin and Smith^[302] have posited that there are two diffusion mechanisms at play—vehicular diffusion and structural diffusion (Figure 11). Vehicular diffusion, as discussed in the context of proton transport, refers to ions that diffuse with their solvation shell intact. Transport of alkali (and alkali-earth) ions in carbonate solvents—and likely other solvents including etheral (e.g., THF, 1,3-dioxolane, or glymes), nitriles (e.g., acetonitrile, benzonitrile, or succinonitrile), amides (e.g., DMF, NMP, or DMAc), and sulfoxides (e.g., DMSO or sulfolane)—is predominantly by vehicular diffusion. Structural diffusion, on the other hand, denotes a scenario where migration of the ion and its solvation shell are not concerted. Quaternary ammonium cations and anions that are weak Lewis bases (e.g., TFSI^- , BF_4^- , or PF_6^-) primarily experience structural diffusion in nonaqueous electrolytes. Fast exchange of the solvation shell around a given ion will see structural diffusion contributing a greater amount to the overall diffusion. For battery electrolytes that coordinate strongly and selectively to one of the ions (e.g., to alkali metal cations), the size of that solvated ion is effectively larger; in these instances, counterions without this explicit solvent shell tend to diffuse faster (e.g., BF_4^- ion^[300] or the PF_6^- ion).^[298] Coordination chemistry thus plays a large part in determining the mechanism of diffusive ion transport in electrolytes.^[298–300] Moving forward, it will be important to understand how such mechanisms evolve when transport is confined to a micropore, where the pore dimensions are commensurate with the size of solvated ions.

Early efforts in confining nonaqueous ion transport to a micropore were described by Long et al. in MOF-based solid electrolytes for Li^+ ions^[303,304] and Mg^{2+} ions^[305] (Figure 14). In the case of the former, lithium alkoxides were introduced to $\text{Mg}_2(\text{dobdc})$ MOFs (i.e., Mg-MOF-74), which have arrays of open-metal coordination sites lining their 1D channels. These metal sites are Lewis acidic and thus readily bind to the alkoxide base, which reduces the binding strength of that species to the lithium ion. These MOF-based solid electrolytes exhibited a lithium-ion conductivity of $1 \times 10^{-5} \text{ S cm}^{-1}$ at ambient temperature. The addition of LiBF_4 further increased the ionic

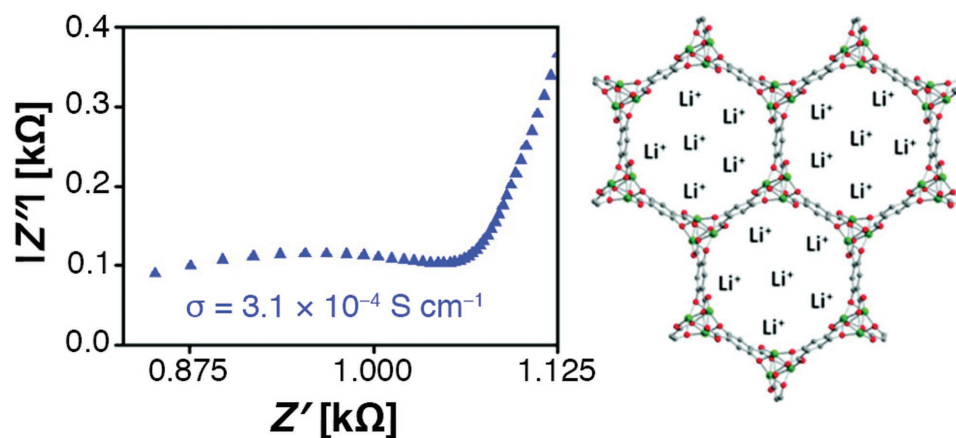


Figure 14. EIS spectra of lithium-ion conduction in $\text{Mg}_2(\text{dobdc})$ with 0.35 equivalent of LiO^iPr and 0.25 equivalent of LiBF_4 . Reproduced with permission.^[303] Copyright 2011, American Chemical Society.

conductivity by an order of magnitude.^[303,306] Interestingly, this is one of the first examples where the micropore chemistry directly participated in the ion-conduction mechanism, where the mobility of the anion was minimized by immobilizing it on the framework and thereby enable solid electrolytes with high Li^+ transference numbers. MOF solid and hybrid electrolytes have been featured in several recent reviews^[289,307] and have inspired the design of analogous porous aromatic framework solid electrolytes.^[308]

While these studies in MOF solid electrolytes begin to touch on a new foundation to build ion-transporting membranes for energy-storage devices, as we noted earlier, the electrochemical cell may also require of these membranes a strict blocking ability for the active materials. Ongoing studies in ion-selective and even ion- or molecular-sieving membranes are beginning to map forward a material development strategy across a variety of platforms, including microporous polymers, MOF, and ZIF selective layers on macroporous supports, and porous carbon membranes (e.g., graphene oxide).

Two related chemistries where each of these platforms have been used effectively in a battery include lithium–sulfur and lithium–polysulfide. For either, inefficiencies in the cell arise when soluble polysulfides—intermediates in the electrochemical interconversion of S_8 and Li_2S —cross the membrane and thereby incur a shuttling current. This shuttling current generally results in an infinite charge cycle for the cell. Competitive with shuttling, a chemical reaction between these wayward polysulfides and the surface of the lithium-metal anode yields a lithium sulfide surface film, which increases cell impedance, decreases sulfur utilization, and ultimately shortens cycle life.

Polysulfide-blocking membranes based on graphene oxide (GO) have shown notable performance enhancements in lithium–sulfur cell performance, including longer cycle life.^[296] Presently, the resistance of GO membranes continues to limit current density, suggesting avenues for future development that might include better control over the pore architecture and pore chemistry. More recent work using ZIFs as selective layers on macroporous supports appears to resolve some of these challenges.^[309] Nevertheless, understanding better how to

control ZIF film thickness with minimal defects on a variety of porous substrates, inorganic or polymeric, will continue to advance this work beyond its present capabilities.

Microporous polymer membranes, particularly those based on PIMs, offer a unique approach to simultaneously manage working-ion conduction and polysulfide blocking. They are also low cost and processable over large areas as is needed for commercialization of any membrane technology. As shown by Li et al., the molecular dimensions of solvated polysulfides are close to or above the exclusion limit of PIM membranes that feature sub-nanometer pore dimensions.^[96] The first quantitative measurements of polysulfide crossover rates and their diffusive permeability across polymer membranes were also published in that study: 500-fold reductions in polysulfide diffusive permeability were achievable with PIM-1 membranes as compared to Celgard 2325 separators. When these polysulfide-blocking PIM membranes were implemented in lithium–polysulfide hybrid flow cells, an energy density of 100 Wh L^{-1} was sustainable after 50 cycles whereas cells employing nonselective Celgard membranes were defunct (**Figure 15**).

One of the outstanding challenges in implementing PIM membranes in more energy-dense lithium–sulfur batteries relates to their chemical evolution in the cell, which influences their polysulfide-blocking ability. More specifically, polysulfides are both nucleophilic and reducing to many chemical species or functional groups (on a polymer). Recent work in Doris et al. has shown that polysulfides react with the cyano groups on PIM-1 to yield lithiated thioamides, which causes changes in the membrane architecture such that they become more permissive to polysulfide crossover as they age chemically.^[310] Crosslinking strategies offer a solution to these changes in pore chemistry and pore architecture, although they do not inhibit the reaction. In future schemes, it may be necessary to replace the cyano groups altogether. The structural diversity in which PIMs can be synthesized suggests that this approach is feasible in principle. It may be that computational screens for polymer reactivity to various active materials that make contact with the membrane would reduce the number of polymers likely to be needed or tested. Such screens may take advantage of recent

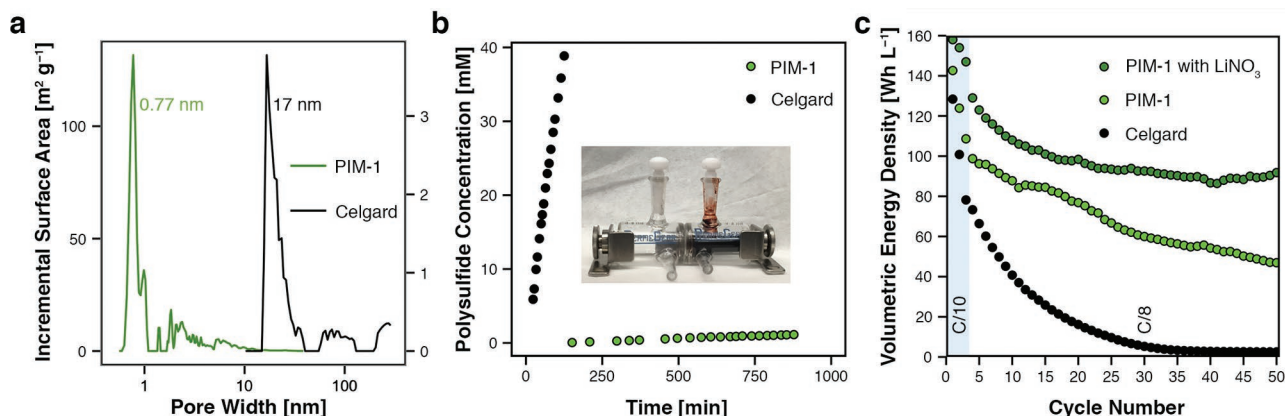


Figure 15. a) Pore-size distributions of PIM-1 and Celgard 2325. PIM-1 has primarily micropores while Celgard has mesopores. b) The crossover rates of lithium polysulfides as performed in an H cell. The microporosity of PIM-1 is capable of screening out the majority of lithium polysulfides, significantly delaying the unwanted species crossover. c) Significant improvement in capacity retention by replacing Celgard with PIM-1. Additional capacity gain is possible when PIM-1 is used in conjunction with the anode-protecting additive LiNO_3 . Reproduced with permission.^[96] Copyright 2015, American Chemical Society.

materials genome tools to accelerate the identification of the usable design space.^[311] For example, materials genomics screens recently identified a redox-active PIM that could be chemically transformed by reducing lithium polysulfides, such that on contact, the ion-transport selectivity of the membrane improved its polysulfide blocking ability. Such membranes are a rare example of an adaptive membrane that implements a negative feedback loop to manipulate membrane chemistry, architecture, and transport selectivity without impacting the necessary functions of conducting the battery's working ion.^[297]

One of the more forward-looking achievements for microporous membranes concerns their use in redox-flow batteries for grid-scale energy storage. As noted in Doris et al., PIM-1 membranes completely arrest active-material crossover in redox-flow batteries implementing organic active materials (Figure 16) by scaling the membrane's pore size to molecular dimensions and in turn increasing the size of the organic active materials to be above the membrane's pore-size exclusion limit.^[97] This strategy to tailor the active materials along with the membrane's pore dimensions breaks with convention on several fronts. In the past, flowable electrodes consisting of a single redox-active molecule (ROM) dissolved in electrolyte could only be used with ceramic membranes, which are expensive, difficult to scale, and power limited. Noting these problems, the field had widely adopted an alternative whereby thick macroporous separators (e.g., Daramic) were paired with mixed-electrode formulations (i.e., ROM anolytes and ROM catholytes present in both electrode compartments). Such configurations are particularly prone to Coulombic inefficiencies ($\approx 50\text{--}60\%$) and short cycle life as small molecule ROMs shuttle freely between the electrode compartments and interact with each other (i.e., cross-annihilation). Only through engineering controls it is possible to reduce (but not eliminate) crossover (e.g., high flow rates, unusual flow fields, etc.); it is unlikely that these methods scale beyond laboratory demonstrations.

The foundational concept of a size-sieving membrane for active-material sequestration in an all-organic redox-flow cell

was first introduced to the field by Moore and co-workers, where mesoporous separators (e.g., Celgard) were paired with solutions or dispersions of redox-active polymers (RAPs) or colloids (RACs), respectively.^[312] Unfortunately, to date, RAPs and RACs have proven challenging to pump through electrochemical cells at high molecular weight, at high concentrations, and at all states of charge in organic electrolyte due to an ensemble of colloidal interactions that affect their stability and performance.

A strategy that implements ROM oligomerization, as opposed to polymerization, solves many of those challenges while also retaining facile charge transfer kinetics between oligomeric active materials and the electrodes.^[313] These gains are essential for power quality, energy efficiency, cycle life, and active-material utilization. A crossover-free redox-flow cell is likely critical for this battery technology to advance beyond what is now achieved using all-vanadium redox-flow batteries. Given that the rate of active-material crossover can now be reduced $>9000\text{-fold}$ compared to traditional separators at minimal cost to ionic conductivity when PIM-1 membranes are paired with redox-active oligomeric (RAO) materials, a crossover-free cell is in sight. Indeed, the absolute rate of crossover in these cell assemblies was less than $3.0\ \mu\text{mol cm}^{-2}\ \text{d}^{-1}$ for a $1.0\ \text{M}$ concentration gradient, which exceeds industry-identified performance targets for these systems.^[294] Given that this strategy was generalizable to both high- and low-potential active materials dissolved in a variety of nonaqueous electrolytes, the versatility of microporous polymer membranes in implementing next-generation redox-flow batteries is readily apparent and is likely to dominate future endeavors.

4.4. Summary of Microporous Membrane Applications

As outlined above, the expansive use of microporous membranes across various disciplines has produced a fruitful pipeline for academic research into several commercial sectors.

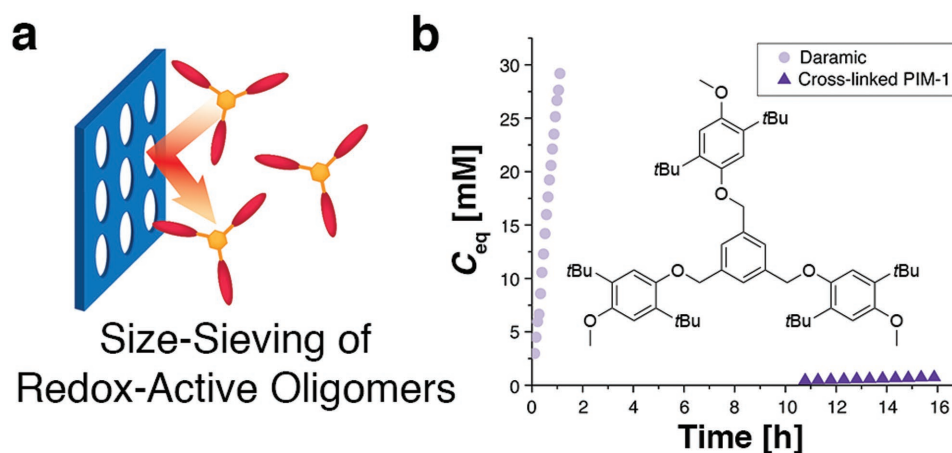


Figure 16. a) Conceptual design strategies for preventing active-material crossover in all-organic redox-flow batteries, featuring RAOs that are blocked from passing through a microporous polymer membrane by a size-sieving mechanism. b) Microporous PIM-1 membranes at work, significantly retarding the rate of crossover of a catholyte species in DME-based battery electrolyte when compared with conventional Daramic separator. Reproduced with permission.^[97] Copyright 2017, Wiley.

Table 3. Summary of promising technologies for microporous membrane adoption.

Technology	Membrane class	Notable challenges	Proximity to commercialization	Reference(s)
Gas separations	CMS membranes	Cost, stability to condensable gases, and humid feeds	Near commercialization	[126,164,198,199]
	TR polymer membranes	Poor mechanical properties	Near commercialization	[85,173,179]
	PIM membranes	Plasticization, physical aging	Near commercialization	[169–172,187]
	Mixed-matrix membranes	Interfacial defects	Near commercialization	[201–213]
Desalination	Mixed-matrix membranes	Interfacial defects	Concept	[227]
	Carbon nanotube membranes	Processability	Near commercialization	[222–226]
Forward osmosis	Carbon nanotube or porous graphene membranes	Processability	Concept	[230]
	Mixed-matrix membranes	Interfacial defects	Concept	[231]
Pervaporation	Zeolite membranes		Commercialized	[236]
	PIM membranes		Concept	[237–239]
	MOF membranes	Processability	Concept	[244]
	Mixed-matrix membranes	Interfacial defects	Concept	[241]
Dehumidification	Mixed-matrix membranes	Interfacial defects	Concept	[249]
	Graphene oxide membranes	Fragility, low selectivity at increased temperatures	Concept	[250]
Aqueous proton transport	Carbon nanotube membranes	Processability	Concept	[270,271]
	Cyclic peptide nanotube membranes	Poor stability in PEM fuel-cell conditions	Concept	[79,277]
Nonaqueous ion transport	MOF membranes	Processability	Concept	[280–284]
	MOF membranes	Processability	Concept	[303–305]
	Graphene oxide membranes	High resistance	Concept	[296]
	PIM membranes	Stability during cycling	Near commercialization	[96,310]

Highlights of this discussion and each membrane technology's outlook for commercial adoption is summarized in **Table 3**.

5. Future Directions

While the discovery of microporous materials outpaces their adoption in membrane applications, the separation demands of clean-energy technologies are complex, necessitating such activities. Within this expanding research space, we see several emerging directions for microporous membranes, applied to both existing and nascent technology areas: phase-change membrane components, engineered microporosity in 2D materials, and advanced compositing strategies all demonstrate significant promise for future innovation. Furthermore, for any of these strategies to be successful long-term, quantitative metrologies are needed to understand transport kinetics in heterophasic materials or where one of the membrane components is a phase-change material.

5.1. Phase-Change Microporous Materials

Recent scientific advances in microporous materials include the advent of responsive framework materials that undergo concerted phase transformations^[314,315] when interacting with an analyte of interest. For example, McDonald et al. demonstrated

a unique adsorption mechanism in diamine-appended MOFs of the type $M_2(\text{dobpc})$.^[15,316] As noted previously, this family of MOFs features open-metal sites that, in this case, bind to one of the amine groups in the diamine. Once the CO_2 pressure reaches a critical threshold, gas molecules insert into the nitrogen–metal bond, creating a metal-bound carbamate that ion pairs with an ammonium cation formed on the end of a neighboring diamine. This lowers the activation barrier of CO_2 insertion into the neighboring metal site, setting off a cooperative sequence of gas adsorption. CO_2 adsorption isotherms in these materials feature phase-change, step-like shapes instead of the typical Langmuir shape. Subsequently, similar behavior has been identified in the flexible MOF $\text{Co}(\text{bdp})$, which undergoes a reversible structural change between a collapsed and open structure with pressure.^[315] Despite considerable interest in these phase-change materials as selective gas adsorbents, they have not yet been adopted in any membrane formats. It is possible that their impressive selectivities and unique behavior in the presence of a given analyte could be exploited in the development of new state-of-the-art membranes with high permselectivity.

5.2. Microporous 2D Selective Layers

Microporous 2D materials are increasingly sought after to maximize permeance for selective separations. For many

microporous materials, however, 2D morphologies are difficult to obtain. Intrinsically 2D materials such as graphene are exceptional in this regard,^[317,318] but have found limited success in the laboratory as selective membranes.^[319,320] Otherwise impermeable, graphene requires treatment with high-energy ions, electrons, and photons to introduce microporosity.^[319] All of these techniques are either very limited in scale (e.g., small area) or pore density, with no control over the chemistry of the perforated pore.^[319] Significant advances in synthetic methods will be required before their advantages are realized. Nonetheless, microporous monolayer graphene and 2D materials in general are ideal sieving platforms with high selectivity and permeability (Figure 17a). Selectivity can be as sharp as the pore-size distribution is narrow. Permeability can be maximized with high pore density and negligible analyte–wall interactions. Despite these synthetic limitations, graphene-based sieving membranes have shown initial promise in gas separations^[321,322] and nanofiltration.^[318,322,323]

While graphene may be difficult to manipulate, GO carries less stringent usage conditions. GO refers to partially oxidized graphene flakes, which are produced by subjecting graphite to strongly oxidizing conditions.^[324] The limiting dimension that effects sieving is the gap between the layers, and analyte transport mainly takes place in the interlayer solvent environment (Figure 17b).^[325] The surface is composed of hydrophilic defect sites, pristine hydrophobic graphene surfaces and pores. Though pristine patches of graphene surface exist,^[326] evidence suggests that oxygen-rich hydrophilic defect sites are highest in areal density and are most likely interacting with analytes.^[327] Due to the weak interplane interactions, GO

is a rather dynamic system in the absence of cross-linking. The state of hydration,^[328] annealing conditions,^[329] and the crosslinking agents^[330] can all affect the sieving dimension. Park and co-workers have demonstrated outstanding selective permeation for few-layered GO membrane sheets on the order of 3–10 nm in thickness with transport properties that surpassed those of pure polymers.^[331] Surprisingly, these GO membranes show significantly improved CO₂/N₂ separation performance in the presence of water, a phenomenon that is ascribed to an N₂-blocking mechanism by condensed water molecules in the pores or between the layers in GO sheets.^[331,332]

It is worth noting that similar 2D materials have also been prepared to be microporous molecular sieves.^[334] They are attractive for the same reason graphene as a membrane is desirable—ultrathin membranes result in ultrafast kinetics. Recent work in 2D polymers may ultimately overcome many of the limitations encountered with preparing graphene or graphene oxide with well-defined pore dimensions and chemical functionality.^[335] Confining the growth of a microporous material to a liquid–liquid interface has been successful in generating 2D architectures, as has postsynthetic chemical or physical exfoliation of microporous materials with layered structures.^[336] For example, COFs derived from multiple building blocks have been successfully synthesized and delaminated as a 2D material with pores ranging from 1.5 to 2 nm.^[46,337] COF membranes, and likely others, are also accessed using flow techniques. Porous 2D polymers using a single monomer have also been synthesized,^[338] sometimes with the aid of metal coordination to impart control over pore structure.^[339] Alternative strategies

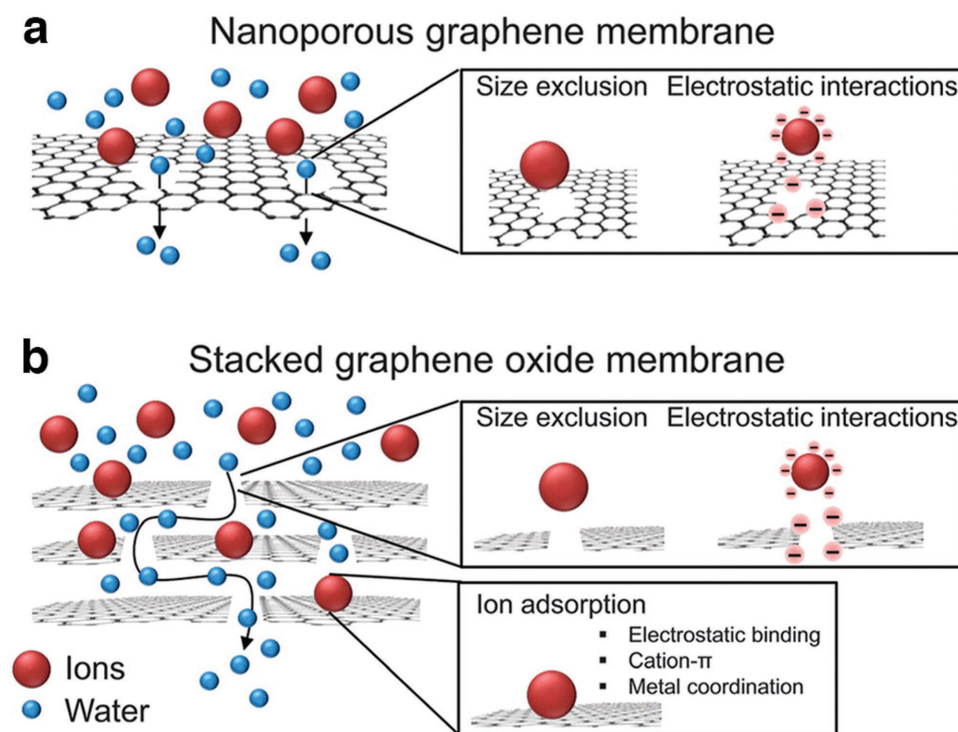


Figure 17. Transport pathways in graphene and graphene oxide membranes. Reproduced with permission.^[333] Copyright 2015, the Royal Society of Chemistry.

to using planar monomers (or COF SBUs) were recently reported by Schlüter and co-workers where building blocks were self-assembled in 3D based on π - π interactions.^[340] Pre-organization and subsequent polymerization afforded porous sheets amenable to exfoliation. In parallel to these pursuits, synthetic efforts to yield 2D zeolite sheets are beginning to show promise. Zeolites are innately 3D constructs; delamination is necessary to obtain 2D flat sheets. To date, a select few types of zeolites have been successfully exfoliated.^[341,342] Molecular sieve membranes have been fabricated using these nanosheets, via Langmuir-Schaefer deposition,^[167] as seeds for secondary growth,^[343] or simply by filtration.^[342,344] Interested readers are directed elsewhere for a detailed analysis of 2D membranes^[345] where they are being used in H_2/CO_2 ,^[346] CO_2/CH_4 ,^[207] and other separations. In these early studies, it is clear that the robustness and chemical integrity of the membrane remains a concern.

One approach to integrate 2D materials into membranes, noting those concerns, is through compositing. This approach has been shown to be successful in MMMs using both exfoliated zeolite layers as well as 2D MOF sheets. This unique geometry allows for a greater transport synergy between the sieve and the matrix than is offered by typical spherical particles, which are limited by the Maxwell model. Here, transport that can occur through the sieving layers will have a far less tortuous path through the film than the larger component. This has been successfully applied by Rodenas et al. to improve CO_2/CH_4 separations in a Matrimid matrix using 2D sheets of the MOF CuBDC (Figure 18).^[207]

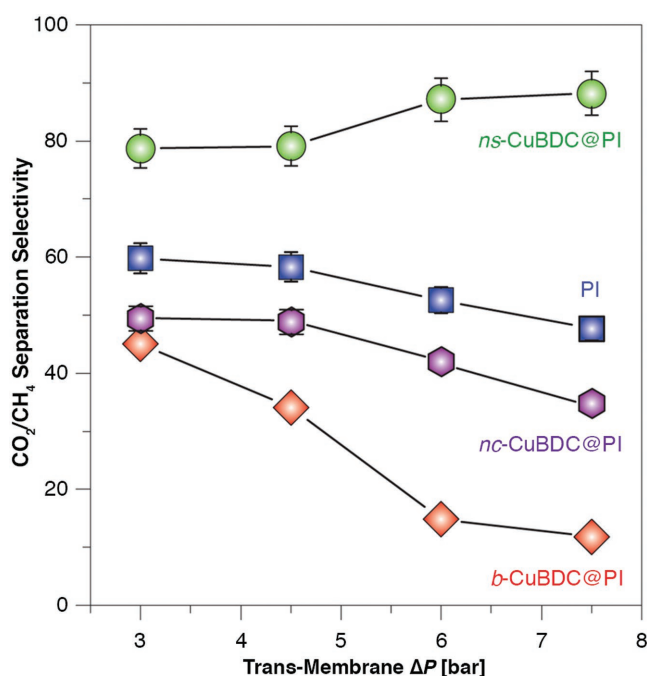


Figure 18. Separation performance of various composite membranes with different filler morphologies of CuBDC loaded into a Matrimid (PI) matrix. Nanosheet (ns) morphology showed the greatest improvement over neat PI in terms of CO_2/CH_4 selectivity. Reproduced with permission.^[207] Copyright 2015, Nature Publishing Group.

5.3. Chemistry for Controlling the Structure and Dynamics of Component Interfaces

A major shortcoming with many microporous sieving components considered in this review is their poor processability. Solid-in-solid dispersions are increasingly sought after, where microporous components are dispersed within a matrix (Figure 19a). Such dispersions feature incredibly large interfacial area between components. Poor control over these interfaces can yield a percolating network of nonselective pathways with minimal resistance, bypassing any permselective characteristics of either sieving component. In the other extreme, strong binding leads to rigidified chains and pore blockage, isolating the sieving elements from efficient transport.^[202]

These considerations call for proper interface tuning to ensure reliable adhesion between components. To this end, thermal and chemical treatments have been utilized to enhance interfacial properties. Heat restructures the polymer chain packing, leading to a densified polymer matrix, including near the interface.^[212,347,348] Separately, chemical functionalization, be it tethered to the sieving element or embodied in a small molecule codispersant, can also promote interfacial adhesion.^[347,349] Another example of interfacial engineering was for carbon nanotubes. Though technically not an MMM, carbon nanotube membranes have been fabricated leveraging the high wettability by polystyrene.^[273] The active field has been reviewed extensively.^[202,350]

In addition to zipping up these defects, an alternative strategy to minimize transport along defects would be to reduce the

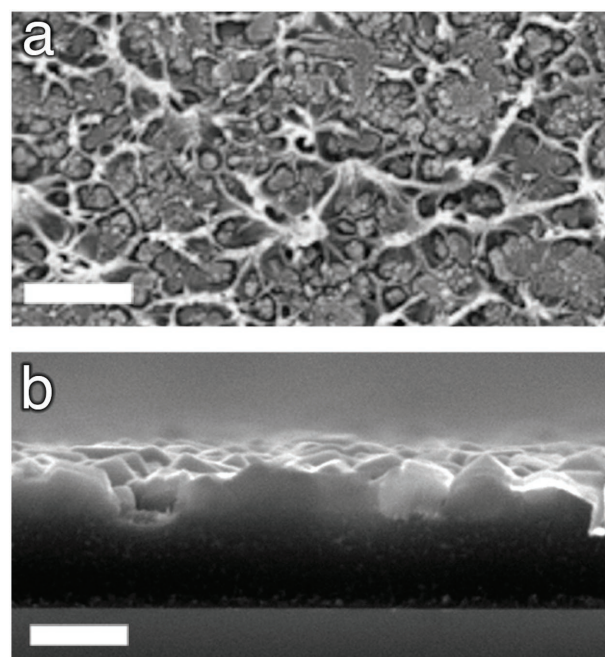


Figure 19. Differentiating compositing schemes. a) Zeolite in polymer solid dispersion MMM. Scale bar is 1 μm . Reproduced with permission.^[351] Copyright 2010, Elsevier. b) Planar ZIF on polymer membrane, grown in situ. Scale bar is 0.2 μm . Reproduced with permission.^[352] Copyright 2015, American Chemical Society.

dimensionality of the defects. By replacing a solid dispersion with a layered structure,^[353] interfacial defects are no longer a percolating 3D network but a 2D plane (Figure 19b). The added advantage of a layered structure is that the interface can be oriented orthogonal to molecular transport, thereby increasing the accessible surface area for analyte interactions. There has been significant interest in creating planar ZIF structures, such as at the interfaces of two immiscible liquids^[354] and on hollow-fiber membrane interior surfaces.^[355] The latter can be accessed through the chemical transformation of ligand-free, or “naked,” metal oxide nanocrystal^[356] thin films on an underlying support; such an approach has been used to access ultrathin ZIF-selective layers on PIM membranes.^[352]

5.4. New Metrologies for Understanding Analyte Kinetics in Heterophasic Membranes

The development of MMMs for gas, liquid, and ionic separations calls for a detailed understanding of molecular adsorption/diffusion kinetics in such composite materials. While kinetics of single component polymeric membranes^[87,140] and thermodynamics of adsorption in inorganic adsorbents are well understood,^[357] the kinetics of composite materials are only recently being considered in detail.^[358] The nontriviality in studying dynamic arises for the multicomponent nature of the membrane through which analytes travel. Transport across diffusion-enhanced composite membranes can be described using the Maxwell model, but this model neglects the influence of interfaces, especially when defect density is high. The challenge is therefore to develop investigation techniques capable of assessing the overall transport behavior, evaluating the performances of the interacting subparts of the system. Steps in this direction have been recently taken by different groups that focused on experimental measurements based on spectroscopy, scattering,^[359] or alternatively theoretical predictions^[360] to describe inner interfaces of membranes. By using these tools, a more robust chemical intuition of polymer–particle interaction^[361] could guide advancement in the field of composites.

More investigation is also required regarding gas kinetics in exotic inorganic components. The MOF community primarily reports gas adsorption at equilibrium conditions,^[44] largely overlooking adsorption kinetics, which is a highly relevant performance metric for MOFs in MMMs. While theoretical studies of analyte transport in MOFs appear in the literature, the introduction of new classes of MOF adsorbents, including the reversible phase-change MOFs described in a previous section, necessitate new theoretical models for describing gas kinetics in these systems.^[362]

6. Conclusion

In this review, we have presented leading-edge research and development of microporous materials and membranes incorporating them. Such membranes are highly sought after to address outstanding problems in clean-energy technologies related to chemical separations or sequestration. Their

attractiveness in this regard is reflective of their ability to engage in the selective transport of a broad array of analytes including gases, water, and ions in a variety of devices. The multivariate design space that is a hallmark of microporous materials has been explored in depth and will continue to see advances. However, equally important will be understanding how microporous materials engage in selective transport, including what factors contribute to optimal analyte flux and selectivity when a mixture of analytes is present. We anticipate that as different platforms are elaborated upon, particularly with respect to the chemistry and dimensionality of the analyte-discriminating component and the interface strategy with a matrix (if utilized), we will need to develop further our analytical techniques to better understand the transport kinetics dictating separation performance. Furthermore, we challenge the field to harness our ever-growing computational resources and prowess to predict which material platforms or combinations are best suited for a selective separation in a given device. It may also be useful to consider whether those same resources can guide the field as to how analytes of interest and other species in the system act upon various membrane components to evolve their structure in the course of a separation. These advances might include developing a better understanding of plasticization of a microporous polymer by gases for carbon capture or with electrolytes in a redox-flow battery. Little is known how such events at the level of atoms and molecules translate to changes in membrane pore architecture. Nevertheless, the emergence of microporous materials, be it MOFs, COFs, PIMs, or TR polymers, combined with other long-standing molecular sieves, forms a crucial toolset to tackle the separation technologies of tomorrow, one mixture at a time.

Acknowledgements

C.L. and B.A.H. were supported by the Joint Center for Energy Storage Research, an Energy Innovation Hub funded by the U.S. Department of Energy, Office of Science, Office of Basic Energy Sciences. S.M.M., Z.P.S., J.E.B., L.M., and J.R.L. were supported by the Center for Gas Separations Relevant to Clean Energy Technologies, an Energy Frontier Research Center funded by the U.S. Department of Energy, Office of Science, Basic Energy Sciences under Award No. DE-SC0001015. B.A.H. acknowledges additional support from The Molecular Foundry, which is supported by the Office of Science, Office of Basic Energy Sciences, of the U.S. Department of Energy under Contract No. DE-AC02-05CH11231.

Conflict of Interest

The authors declare no conflict of interest.

Keywords

chemical separations, energy conversion, energy storage, microporous materials, transport selectivity

Received: August 29, 2017

Revised: October 12, 2017

Published online:

- [1] D. S. Sholl, R. P. Lively, *Nature* **2016**, 532, 435.
- [2] a) C. S. Cundy, P. A. Cox, *Microporous Mesoporous Mater.* **2005**, 82, 1; b) C. S. Cundy, P. A. Cox, *Chem. Rev.* **2003**, 103, 663.
- [3] a) N. Stock, S. Biswas, *Chem. Rev.* **2012**, 112, 933; b) O. K. Farha, J. T. Hupp, *Acc. Chem. Res.* **2010**, 43, 1166; c) H. Furukawa, K. E. Cordova, M. O’Keeffe, O. M. Yaghi, *Science* **2013**, 341, 1230444.
- [4] H. Dai, *Acc. Chem. Res.* **2002**, 35, 1035.
- [5] S. M. Saufi, A. F. Ismail, *Carbon* **2004**, 42, 241.
- [6] R. Dawson, A. I. Cooper, D. J. Adams, *Prog. Polym. Sci.* **2012**, 37, 530.
- [7] N. B. McKeown, P. M. Budd, *Chem. Soc. Rev.* **2006**, 35, 675.
- [8] D. T. Bong, T. D. Clark, J. R. Granja, M. R. Ghadiri, *Angew. Chem., Int. Ed.* **2001**, 40, 988.
- [9] N. L. Rosi, *Science* **2003**, 300, 1127.
- [10] J. Lee, O. K. Farha, J. Roberts, K. A. Scheidt, S. T. Nguyen, J. T. Hupp, *Chem. Soc. Rev.* **2009**, 38, 1450.
- [11] K. Tanabe, W. Hölderich, *Appl. Catal., A* **1999**, 181, 399.
- [12] A. Corma, *J. Catal.* **2003**, 216, 298.
- [13] R. S. Haszeldine, *Science* **2009**, 325, 1647.
- [14] M. Elimelech, W. A. Phillip, *Science* **2011**, 333, 712.
- [15] T. M. McDonald, W. R. Lee, J. A. Mason, B. M. Wiers, C. S. Hong, J. R. Long, *J. Am. Chem. Soc.* **2012**, 134, 7056.
- [16] G. Hummer, J. C. Rasaiah, J. P. Noworyta, *Nature* **2001**, 414, 188.
- [17] L. Ruiz, Y. Wu, S. Ketan, *Nanoscale* **2015**, 7, 121.
- [18] P. M. Budd, N. B. McKeown, *Polym. Chem.* **2010**, 1, 63.
- [19] a) C. Baerlocher, L. B. McCusker, D. H. Olson, *Atlas of Zeolite Framework Types*, Elsevier Science B.V., Amsterdam **2007**; b) D. W. Breck, *Zeolite Molecular Sieves: Structure, Chemistry and Use*, John Wiley & Sons, New York, London, Sydney, Toronto **1974**; c) Ch. Baerlocher, L. B. McCusker, Database of Zeolite Structures: <http://www.iza-structure.org/databases/>.
- [20] E. M. Flanigen, J. M. Bennett, R. W. Grose, J. P. Cohen, R. L. Patton, R. M. Kirchner, J. V. Smith, *Nature* **1978**, 271, 512.
- [21] a) D. M. Chapman, A. L. Roe, *Zeolites* **1990**, 10, 730; b) P. T. Tanev, M. Chibwe, T. J. Pinnavaia, *Nature* **1994**, 368, 321.
- [22] a) M. E. Davis, C. Saldarriaga, C. Montes, J. Garces, C. Crowdert, *Nature* **1988**, 331, 698; b) S. T. Wilson, B. M. Lok, C. A. Messina, T. R. Cannan, E. M. Flanigen, *J. Am. Chem. Soc.* **1982**, 104, 1146; c) M. Estermann, L. B. McCusker, C. Baerlocher, A. Merrouche, H. Kessler, *Nature* **1991**, 352, 320; d) B. M. Lok, C. A. Messina, R. L. Patton, R. T. Gajek, T. R. Cannan, E. M. Flanigen, *J. Am. Chem. Soc.* **1984**, 106, 6092.
- [23] A. F. Cronsted, *Akad. Handl.* **1756**, 17, 20.
- [24] M. E. Davis, R. F. Lobo, *Chem. Mater.* **1992**, 4, 756.
- [25] A. K. Cheetham, G. Férey, T. Loiseau, *Angew. Chem., Int. Ed.* **1999**, 38, 3268.
- [26] E. M. Flanigen, in *Zeolites and Molecular Sieves an Historical Perspective*, in *Studies in Surface Science and Catalysis*, Vol. 58 (Eds: H. van Bekkum, E. M. Flanigen, J. C. Jansen), Elsevier, Amsterdam, the Netherlands **1991**, p. 13.
- [27] N. Y. Chen, T. F. Degnan Jr., C. M. Smith, *Molecular Transport and Reaction in Zeolites: Design and Application of Shape Selective Catalysis*, Wiley-VCH, New York **1995**.
- [28] S. Babel, T. A. Kurniawan, *J. Hazard. Mater.* **2003**, 97, 219.
- [29] a) W. Hölderich, M. Hesse, F. Nümann, *Angew. Chem., Int. Ed. Engl.* **1988**, 27, 226; b) P. B. Venuto, *Microporous Mater.* **1994**, 2, 297; c) V. V. Speybroeck, K. Hemelsoet, L. Joos, M. Waroquier, R. G. Bell, C. R. A. Catlow, *Chem. Soc. Rev.* **2015**, 44, 7044; d) W. Vermeiren, J.-P. Gilson, *Top. Catal.* **2009**, 52, 1131.
- [30] a) J. J. Pluth, J. V. Smith, *J. Am. Chem. Soc.* **1983**, 105, 1192; b) J. J. Pluth, J. V. Smith, *J. Am. Chem. Soc.* **1980**, 102, 4704; c) J. J. Pluth, J. V. Smith, *J. Phys. Chem.* **1979**, 83, 741.
- [31] J. Gascon, F. Kapteijn, B. Zornoza, V. Sebastián, C. Casado, J. Coronas, *Chem. Mater.* **2012**, 24, 2829.
- [32] a) M. Y. Jeon, D. Kim, P. Kumar, P. S. Lee, N. Rangnekar, P. Bai, M. Shete, B. Elyassi, H. S. Lee, K. Narasimharao, S. N. Basahel, S. Al-Thabaiti, W. Xu, H. J. Cho, E. O. Fetisov, R. Thyagarajan, R. F. DeJaco, W. Fan, K. A. Mkhoyan, J. I. Siepmann, M. Tsapatsis, *Nature* **2017**, 543, 690; b) G.-E. Wang, G. Xu, B.-W. Liu, M.-S. Wang, M.-S. Yao, G.-C. Guo, *Angew. Chem., Int. Ed.* **2015**, 55, 514; c) S. V. Krivovichev, V. Kahlenberg, R. Kaindl, E. Mersdorf, I. G. Tananaev, B. F. Myasoedov, *Angew. Chem., Int. Ed.* **2005**, 44, 1134; d) C. D. Malliakas, M. G. Kanatzidis, *J. Am. Chem. Soc.* **2006**, 128, 6538; e) A. Choudhury, P. K. Dorhout, *J. Am. Chem. Soc.* **2007**, 129, 9270; f) S. P. Albu, A. Ghicov, J. M. Macak, R. Hahn, P. Schmuki, *Nano Lett.* **2007**, 7, 1286.
- [33] O. M. Yaghi, G. Li, H. Li, *Nature* **1995**, 378, 703.
- [34] K. S. Park, Z. Ni, A. P. Côté, J. Y. Choi, R. Huang, F. J. Uribe-Romo, H. K. Chae, M. O’Keeffe, O. M. Yaghi, *Proc. Natl. Acad. Sci. USA* **2006**, 103, 10186.
- [35] a) M. O’Keeffe, O. M. Yaghi, *Chem. Rev.* **2012**, 112, 675; b) N. W. Ockwig, O. Delgado-Friedrichs, M. O’Keeffe, O. M. Yaghi, *Acc. Chem. Res.* **2005**, 38, 176.
- [36] a) Z. Wang, S. M. Cohen, *Chem. Soc. Rev.* **2009**, 38, 1315; b) S. M. Cohen, *Chem. Rev.* **2012**, 112, 970.
- [37] O. K. Farha, I. Eryazici, N. C. Jeong, B. G. Hauser, C. E. Wilmer, A. A. Sarjeant, R. Q. Snurr, S. T. Nguyen, A. Ö. Yazaydin, J. T. Hupp, *J. Am. Chem. Soc.* **2012**, 134, 15016.
- [38] H. Furukawa, N. Ko, Y. B. Go, N. Aratani, S. B. Choi, E. Choi, A. Ö. Yazaydin, R. Q. Snurr, M. O’Keeffe, J. Kim, O. M. Yaghi, *Science* **2010**, 329, 424.
- [39] B. Chen, S. Xiang, G. Qian, *Acc. Chem. Res.* **2010**, 43, 1115.
- [40] M. Eddaoudi, J. Kim, N. Rosi, D. Vodak, J. Wachter, M. O’Keeffe, O. M. Yaghi, *Science* **2002**, 295, 469.
- [41] a) S. Ma, H.-C. Zhou, *Chem. Commun.* **2010**, 46, 44; b) L. J. Murray, M. Dincă, J. R. Long, *Chem. Soc. Rev.* **2009**, 38, 1294.
- [42] a) L. E. Kreno, K. Leong, O. K. Farha, M. Allendorf, R. P. Van Duyne, J. T. Hupp, *Chem. Rev.* **2012**, 112, 1105; b) M.-S. Yao, W.-X. Tang, G.-E. Wang, B. Nath, G. Xu, *Adv. Mater.* **2016**, 28, 5229; c) W.-T. Koo, S.-J. Choi, S.-J. Kim, J.-S. Jang, H. L. Tuller, I.-D. Kim, *J. Am. Chem. Soc.* **2016**, 138, 13431; d) M. G. Campbell, M. Dincă, *Sensors* **2017**, 17, 1108; e) M. G. Campbell, D. Sheberla, S. F. Liu, T. M. Swager, M. Dincă, *Angew. Chem., Int. Ed.* **2015**, 54, 4349.
- [43] J.-R. Li, J. Sculley, H.-C. Zhou, *Chem. Rev.* **2012**, 112, 869.
- [44] J.-R. Li, R. J. Kuppler, H.-C. Zhou, *Chem. Soc. Rev.* **2009**, 38, 1477.
- [45] D. J. Tranchemontagne, J. R. Hunt, O. M. Yaghi, *Tetrahedron* **2008**, 64, 8553.
- [46] A. P. Côté, A. I. Benin, N. W. Ockwig, M. O’Keeffe, A. J. Matzger, O. M. Yaghi, *Science* **2005**, 310, 1166.
- [47] J. Fu, S. Das, G. Xing, T. Ben, V. Valtchev, S. Qiu, *J. Am. Chem. Soc.* **2016**, 138, 7673.
- [48] H. Furukawa, O. M. Yaghi, *J. Am. Chem. Soc.* **2009**, 131, 8875.
- [49] a) C. R. DeBlase, K. Hernández-Burgos, K. E. Silberstein, G. G. Rodríguez-Calero, R. P. Bisbey, H. D. Abruña, W. R. Dichtel, *ACS Nano* **2015**, 9, 3178; b) C. R. DeBlase, K. E. Silberstein, T.-T. Truong, H. D. Abruña, W. R. Dichtel, *J. Am. Chem. Soc.* **2013**, 135, 16821; c) C. R. Mulzer, L. Shen, R. P. Bisbey, J. R. McKone, N. Zhang, H. D. Abruña, W. R. Dichtel, *ACS Cent. Sci.* **2016**, 2, 667; d) J.-S. M. Lee, T.-H. Wu, B. M. Alston, M. E. Briggs, T. Hasell, C.-C. Hu, A. I. Cooper, *J. Mater. Chem. A* **2016**, 4, 7665.
- [50] a) Z. Xiang, D. Cao, *J. Mater. Chem. A* **2013**, 1, 2691; b) S.-Y. Ding, W. Wang, *Chem. Soc. Rev.* **2013**, 42, 548.
- [51] a) S. Iijima, *Nature* **1991**, 354, 56; b) J. Hone, M. Whitney, C. Piskoti, A. Zettl, *Phys. Rev. B* **1999**, 59, R2514.
- [52] a) H. Dai, E. W. Wong, C. M. Lieber, *Science* **1996**, 272, 523; b) T. W. Ebbesen, H. J. Lezec, H. Ghaemi, T. Thio, P. Wolff, *Nature* **1998**, 391, 667.
- [53] M. M. J. Treacy, T. W. Ebbesen, J. M. Gibson, *Nature* **1996**, 381, 678.
- [54] a) H. Kanzow, C. Lenski, A. Ding, *Phys. Rev. B* **2001**, 63, 125402; b) H. Ago, T. Komatsu, S. Ohshima, Y. Kuriki, M. Yumura, *Appl. Phys. Lett.* **2000**, 77, 79.

- [55] a) K. Balasubramanian, M. Burghard, *Small* **2005**, *1*, 180; b) D. Tasis, N. Tagmatarchis, A. Bianco, M. Prato, *Chem. Rev.* **2006**, *106*, 1105; c) S. S. Wong, E. Joselevich, A. T. Woolley, C. L. Cheung, C. M. Lieber, *Nature* **1998**, *394*, 52.
- [56] S. K. Bhatia, H. Chen, D. S. Sholl, *Mol. Simul.* **2005**, *31*, 643.
- [57] C. Y. Lee, W. Choi, J.-H. Han, M. S. Strano, *Science* **2010**, *329*, 1320.
- [58] H. Liu, J. He, J. Tang, H. Liu, P. Pang, D. Cao, P. Krstic, S. Joseph, S. Lindsay, C. Nuckolls, *Science* **2010**, *327*, 64.
- [59] D. Cohen-Tanugi, J. C. Grossman, *Nano Lett.* **2012**, *12*, 3602.
- [60] H. Suda, K. Haraya, *J. Phys. Chem. B* **1997**, *101*, 3988.
- [61] J. Koresh, A. Soffer, *J. Chem. Soc., Faraday Trans. 1* **1980**, *76*, 2457.
- [62] a) J.-i. Hayashi, M. Yamamoto, K. Kusakabe, S. Morooka, *Ind. Eng. Chem. Res.* **1995**, *34*, 4364; b) C. W. Jones, W. J. Koros, *Carbon* **1994**, *32*, 1419; c) M. G. Sedigh, L. Xu, T. T. Tsotsis, M. Sahimi, *Ind. Eng. Chem. Res.* **1999**, *38*, 3367.
- [63] A. B. Fuertes, D. M. Nevskaia, T. A. Centeno, *Microporous Mesoporous Mater.* **1999**, *33*, 115.
- [64] D. Q. Vu, W. J. Koros, S. J. Miller, *Ind. Eng. Chem. Res.* **2002**, *41*, 367.
- [65] H. Hatori, Y. Yamada, M. Shiraishi, H. Nakata, S. Yoshitomi, *Carbon* **1992**, *30*, 305.
- [66] a) A. J. Bird, D. L. Trimm, *Carbon* **1983**, *21*, 177; b) Y. D. Chen, R. T. Yang, *Ind. Eng. Chem. Res.* **1994**, *33*, 3146.
- [67] W. Shusen, Z. Meiyun, W. Zhizhong, *J. Membr. Sci.* **1996**, *109*, 267.
- [68] T. A. Centeno, A. B. Fuertes, *Carbon* **2000**, *38*, 1067.
- [69] a) W. N. W. Salleh, A. F. Ismail, *Sep. Purif. Technol.* **2012**, *88*, 174; b) A. B. Fuertes, *Carbon* **2001**, *39*, 697; c) W. N. W. Salleh, A. F. Ismail, T. Matsuura, M. S. Abdullah, *Sep. Purif. Rev.* **2011**, *40*, 261.
- [70] A. F. Ismail, L. I. B. David, *J. Membr. Sci.* **2001**, *193*, 1.
- [71] Y. Rong, D. He, A. Sanchez-Fernandez, C. Evans, K. J. Edler, R. Malpass-Evans, M. Carta, N. B. McKeown, T. J. Clarke, S. H. Taylor, A. J. Wain, J. M. Mitchels, F. Marken, *Langmuir* **2015**, *31*, 12300.
- [72] V. Percec, A. E. Dulcey, V. S. K. Balagurusamy, Y. Miura, J. Smidrkal, M. Peterca, S. Nummelin, U. Edlund, S. D. Hudson, P. A. Heiney, H. Duan, S. N. Magonov, S. A. Vinogradov, *Nature* **2004**, *430*, 764.
- [73] J. T. Davis, G. P. Spada, *Chem. Soc. Rev.* **2007**, *36*, 296.
- [74] a) D. A. Hines, E. R. Darzi, E. S. Hirst, R. Jasti, P. V. Kamat, *J. Phys. Chem. A* **2015**, *119*, 8083; b) M. R. Golder, R. Jasti, *Acc. Chem. Res.* **2015**, *48*, 557.
- [75] D. Zhao, J. S. Moore, *Chem. Commun.* **2003**, *0*, 807.
- [76] M. R. Ghadiri, J. R. Granja, R. A. Milligan, D. E. McRee, N. Khazanovich, *Nature* **1993**, *366*, 324.
- [77] R. Hourani, C. Zhang, R. van der Weegen, L. Ruiz, C. Li, S. Keten, B. A. Helms, T. Xu, *J. Am. Chem. Soc.* **2011**, *133*, 15296.
- [78] C. Reiriz, M. Amorín, R. García-Fandiño, L. Castedo, J. R. Granja, *Org. Biomol. Chem.* **2009**, *7*, 4358.
- [79] T. Xu, N. Zhao, F. Ren, R. Hourani, M. T. Lee, J. Y. Shu, S. Mao, B. A. Helms, *ACS Nano* **2011**, *5*, 1376.
- [80] a) J. Sánchez-Quesada, M. P. Isler, M. R. Ghadiri, *J. Am. Chem. Soc.* **2002**, *124*, 10004; b) S. Fernandez-Lopez, H.-S. Kim, E. C. Choi, M. Delgado, J. R. Granja, A. Khasanov, K. Kraehenbuehl, G. Long, D. A. Weinberger, K. M. Wilcoxon, M. R. Ghadiri, *Nature* **2001**, *412*, 452.
- [81] L. Zang, Y. Che, J. S. Moore, *Acc. Chem. Res.* **2008**, *41*, 1596.
- [82] V. P. Shantarovich, I. B. Kevdina, Y. P. Yampolskii, A. Y. Alentiev, *Macromolecules* **2000**, *33*, 7453.
- [83] P. M. Budd, E. S. Elabas, B. S. Ghanem, S. Makhseed, N. B. McKeown, K. J. Msayib, C. E. Tattershall, D. Wang, *Adv. Mater.* **2004**, *16*, 456.
- [84] W. S. Drisdell, R. Poloni, T. M. McDonald, T. A. Pascal, L. F. Wan, C. D. Pemmaraju, B. Vlasisavljevich, S. O. Odoh, J. B. Neaton, J. R. Long, D. Prendergast, J. B. Kortright, *Phys. Chem. Chem. Phys.* **2015**, *17*, 21448.
- [85] H. B. Park, C. H. Jung, Y. M. Lee, A. J. Hill, S. J. Pas, S. T. Mudie, E. Van Wagner, B. D. Freeman, D. J. Cookson, *Science* **2007**, *318*, 254.
- [86] Z.-A. Qiao, S.-H. Chai, K. Nelson, Z. Bi, J. Chen, S. M. Mahurin, X. Zhu, S. Dai, *Nat. Commun.* **2014**, *5*, 3705.
- [87] L. M. Robeson, *J. Membr. Sci.* **2008**, *320*, 390.
- [88] L. Setiawan, R. Wang, K. Li, A. G. Fane, *J. Membr. Sci.* **2011**, *369*, 196.
- [89] a) K. K. Tanabe, S. M. Cohen, *Chem. Soc. Rev.* **2011**, *40*, 498; b) M. Dincă, J. R. Long, *J. Am. Chem. Soc.* **2007**, *129*, 11172.
- [90] S. Wang, X. Li, H. Wu, Z. Tian, Q. Xin, G. He, D. Peng, S. Chen, Y. Yin, Z. Jiang, M. D. Guiver, *Energy Environ. Sci.* **2016**, *9*, 1863.
- [91] D. T. Hallinan Jr., N. P. Balsara, *Annu. Rev. Mater. Res.* **2013**, *43*, 503.
- [92] C. Zhang, R. P. Lively, K. Zhang, J. R. Johnson, O. Karvan, W. J. Koros, *J. Phys. Chem. Lett.* **2012**, *3*, 2130.
- [93] Y. Pan, T. Li, G. Lestari, Z. Lai, *J. Membr. Sci.* **2012**, *390–391*, 93.
- [94] V. Bon, N. Kavooosi, I. Senkovska, P. Muller, J. Schaber, D. Wallacher, D. M. Tobbens, U. Mueller, S. Kaskel, *Dalton Trans.* **2016**, *45*, 4407.
- [95] W. Ogieglo, B. Ghanem, X. Ma, I. Pinnau, M. Wessling, *J. Phys. Chem. B* **2016**, *120*, 10403.
- [96] C. Li, A. L. Ward, S. E. Doris, T. A. Pascal, D. Prendergast, B. A. Helms, *Nano Lett.* **2015**, *15*, 5724.
- [97] S. E. Doris, A. L. Ward, A. Baskin, P. D. Frischmann, N. Gavvalapalli, E. Chénard, C. S. Sevov, D. Prendergast, J. S. Moore, B. A. Helms, *Angew. Chem., Int. Ed.* **2017**, *56*, 1595.
- [98] J. G. Wijmans, R. W. Baker, *J. Membr. Sci.* **1995**, *107*, 1.
- [99] B. Smit, J. A. Reimer, C. M. Oldenburg, I. C. Bourg, *Introduction to Carbon Capture and Sequestration*, Vol. 1, Imperial College Press, London **2014**.
- [100] a) I. Pinnau, L. G. Toy, *J. Membr. Sci.* **1996**, *116*, 199; b) A. W. Thornton, J. M. Hill, A. J. Hill, in *Modeling Gas Separation in Porous Membranes in Membrane Gas Separation*, (Eds: Y. Yampolskii, B. Freeman), John Wiley & Sons, Ltd, Chichester, UK **2010**, p. 85; c) E. L. Cussler, in *Diffusion: Mass Transfer in Fluid Systems*, Cambridge University Press, Cambridge, UK **2009**, p. 190.
- [101] R. Srinivasan, S. R. Auvil, P. M. Burban, *J. Membr. Sci.* **1994**, *86*, 67.
- [102] S. A. Reinecke, B. E. Sleep, *Water Resour. Res.* **2002**, *38*, 16.
- [103] R. Barrer, T. Gabor, *Proc. R. Soc. London, Ser. A* **1960**, *271*, 1.
- [104] R. Barrer, T. Gabor, *Proc. R. Soc. London, Ser. A* **1960**, *271*, 19.
- [105] K. L. Gleason, Z. P. Smith, Q. Liu, D. R. Paul, B. D. Freeman, *J. Membr. Sci.* **2015**, *475*, 204.
- [106] Q.-H. Wei, C. Bechinger, P. Leiderer, *Science* **2000**, *287*, 625.
- [107] E. Tajkhorshid, P. Nollert, M. Ø. Jensen, L. J. Miercke, J. O'Connell, R. M. Stroud, K. Schulten, *Science* **2002**, *296*, 525.
- [108] a) A. Striolo, *Nano Lett.* **2006**, *6*, 633; b) A. Berezhkovskii, G. Hummer, *Phys. Rev. Lett.* **2002**, *89*, 064503; c) A. Das, S. Jayanthi, H. S. M. V. Deepak, K. V. Ramanathan, A. Kumar, C. Dasgupta, A. K. Sood, *ACS Nano* **2010**, *4*, 1687.
- [109] a) V. Kukla, J. Kornatowski, D. Demuth, I. Girmus, *Science* **1996**, *272*, 702; b) J. Kärger, in *Adsorption and Diffusion* (Eds: H. G. Karge, J. Weitkamp), Springer, Berlin **2008**, p. 329.
- [110] P. Grathwohl, *Diffusion in Natural Porous Media: Contaminant Transport, Sorption/Desorption and Dissolution Kinetics*, Springer Science, New York **1998**.
- [111] E. P. Barrett, L. G. Joyner, P. P. Halenda, *J. Am. Chem. Soc.* **1951**, *73*, 373.
- [112] S. Eslava, M. R. Baklanov, C. E. A. Kirschhock, F. Iacopi, S. Aldea, K. Maex, J. A. Martens, *Langmuir* **2007**, *23*, 12811.
- [113] J. R. Izzo, A. S. Joshi, K. N. Grew, W. K. S. Chiu, A. Tkachuk, S. H. Wang, W. Yun, *J. Electrochem. Soc.* **2008**, *155*, B504.

- [114] W. R. Vieth, J. M. Howell, J. H. Hsieh, *J. Membr. Sci.* **1976**, *1*, 177.
- [115] G. K. Fleming, W. J. Koros, *Macromolecules* **1986**, *19*, 2285.
- [116] W. J. Koros, S. K. Burgess, Z. Chen, in *Encyclopedia of Polymer Science and Technology* (Ed: H. F. Mark), John Wiley & Sons, Inc., Hoboken, NJ **2015**, p. 1.
- [117] I. C. Sanchez, R. H. Lacombe, *Macromolecules* **1978**, *11*, 1145.
- [118] F. Doghieri, G. C. Sarti, *Macromolecules* **1996**, *29*, 7885.
- [119] P. M. Budd, N. B. McKeown, D. Fritsch, *J. Mater. Chem.* **2005**, *15*, 1977.
- [120] W. J. Koros, D. R. Paul, *J. Polym. Sci., Polym. Phys. Ed.* **1978**, *16*, 1947.
- [121] T. C. Merkel, V. Bondar, K. Nagai, B. D. Freeman, *J. Polym. Sci., Part B: Polym. Phys.* **2000**, *38*, 273.
- [122] a) Z. P. Smith, R. R. Tiwari, T. M. Murphy, D. F. Sanders, K. L. Gleason, D. R. Paul, B. D. Freeman, *Polymer* **2013**, *54*, 3026; b) P. Li, T. Chung, D. Paul, *J. Membr. Sci.* **2014**, *450*, 380.
- [123] S. Kim, H. J. Jo, Y. M. Lee, *J. Membr. Sci.* **2013**, *441*, 1.
- [124] Z. P. Smith, D. F. Sanders, C. P. Ribeiro Jr., R. Guo, B. D. Freeman, D. R. Paul, J. E. McGrath, S. Swinnea, *J. Membr. Sci.* **2012**, *416*, 558.
- [125] P. Li, T. S. Chung, D. R. Paul, *J. Membr. Sci.* **2013**, *432*, 50.
- [126] P. Bernardo, E. Drioli, G. Golemme, *Ind. Eng. Chem. Res.* **2009**, *48*, 4638.
- [127] H. B. Park, S. H. Han, C. H. Jung, Y. M. Lee, A. J. Hill, *J. Membr. Sci.* **2010**, *359*, 11.
- [128] W. Koros, D. Paul, G. Huvar, *Polymer* **1979**, *20*, 956.
- [129] D. W. Breck, in *Zeolite Molecular Sieves: Structure, Chemistry, and Use*, John Wiley & Sons, New York **1973**, p. 636.
- [130] T. C. Merkel, V. I. Bondar, K. Nagai, B. D. Freeman, I. Pinnau, *J. Polym. Sci., Part B: Polym. Phys.* **2000**, *38*, 415.
- [131] P. Pandey, *Prog. Polym. Sci.* **2001**, *26*, 853.
- [132] K. Tanaka, H. Kita, M. Okano, K.-i. Okamoto, *Polymer* **1992**, *33*, 585.
- [133] H. Eyring, *J. Chem. Phys.* **1936**, *4*, 283.
- [134] M. H. Cohen, D. Turnbull, *J. Chem. Phys.* **1959**, *31*, 1164.
- [135] H. Fujita, in *Diffusion in Polymer-Diluent Systems in Fortschritt Der Hochpolymeren-Forschung* (Eds: J. D. Ferry, W. Kern, G. Natta, C. G. Overberger, G. V. Schulz, A. J. Staverman, H. A. Stuart), Springer, Berlin, West Germany **1961**, p. 1.
- [136] a) A. Bondi, *Physical Properties of Molecular Crystals, Liquids and Glasses*, John Wiley & Sons, Inc., New York **1968**; b) A. Bondi, *J. Phys. Chem.* **1964**, *68*, 441; c) D. W. Van Krevelen, *Properties of Polymers: Their Correlation with Chemical Structure*, 3rd ed., Elsevier, Amsterdam **1997**; d) J. Y. Park, D. R. Paul, *J. Membr. Sci.* **1997**, *125*, 23; e) N. R. Horn, *J. Membr. Sci.* **2016**, *518*, 289.
- [137] Y. Jean, P. Mallon, D. Schrader, *Principles and Applications of Positron @ Positronium Chemistry*, World Scientific, Singapore **2003**.
- [138] R. Barrer, E. K. Rideal, *Trans. Faraday Soc.* **1939**, *35*, 644.
- [139] P. Meares, *J. Am. Chem. Soc.* **1954**, *76*, 3415.
- [140] L. M. Robeson, *J. Membr. Sci.* **1991**, *62*, 165.
- [141] a) B. D. Freeman, *Macromolecules* **1999**, *32*, 375; b) A. Y. Alentiev, Y. P. Yampolskii, *J. Membr. Sci.* **2000**, *165*, 201.
- [142] J. Su, H. Guo, *J. Phys. Chem. B* **2012**, *116*, 5925.
- [143] Z. Qin, M. J. Buehler, *Nano Lett.* **2015**, *15*, 3939.
- [144] M. E. Suk, N. R. Aluru, *J. Phys. Chem. Lett.* **2010**, *1*, 1590.
- [145] D. Konatham, J. Yu, T. A. Ho, A. Striolo, *Langmuir* **2013**, *29*, 11884.
- [146] a) I. Hanasaki, A. Nakatani, *J. Chem. Phys.* **2006**, *124*, 174714; b) M. C. Gordillo, J. Martí, *Chem. Phys. Lett.* **2000**, *329*, 341.
- [147] S. Joseph, N. R. Aluru, *Nano Lett.* **2008**, *8*, 452.
- [148] J. Liu, J. Fan, M. Tang, M. Cen, J. Yan, Z. Liu, W. Zhou, *J. Phys. Chem. B* **2010**, *114*, 12183.
- [149] L. Ruiz, A. Benjamin, M. Sullivan, S. Keten, *J. Phys. Chem. Lett.* **2015**, *6*, 1514.
- [150] M. A. Alsina, J.-F. Gaillard, S. Keten, *Phys. Chem. Chem. Phys.* **2016**, *18*, 31698.
- [151] Sources of Greenhouse Gas Emissions, U.S. Environmental Protection Agency, <https://www.epa.gov/ghgemissions/sources-greenhouse-gas-emissions#ref2> (accessed: August, 2017).
- [152] T. C. Merkel, H. Q. Lin, X. T. Wei, R. R. Baker, *J. Membr. Sci.* **2010**, *359*, 126.
- [153] T. C. Drage, C. E. Snape, L. A. Stevens, J. Wood, J. Wang, A. I. Cooper, R. Dawson, X. Guo, C. Satterley, R. Irons, *J. Mater. Chem.* **2012**, *22*, 2815.
- [154] R. R. Bottoms, *US Patent 1834016*, **1930**.
- [155] P. D. Vaidya, E. Y. Kenig, *Chem. Eng. Technol.* **2007**, *30*, 1467.
- [156] G. T. Rochelle, *Science* **2009**, *325*, 1652.
- [157] D. M. D'Alessandro, B. Smit, J. R. Long, *Angew. Chem., Int. Ed.* **2010**, *49*, 6058.
- [158] *Chem. Eng. News* **1979**, *57*, 26.
- [159] D. F. Sanders, Z. P. Smith, R. Guo, L. M. Robeson, J. E. McGrath, D. R. Paul, B. D. Freeman, *Polymer* **2013**, *54*, 4729.
- [160] R. W. Baker, K. Lokhandwala, *Ind. Eng. Chem. Res.* **2008**, *47*, 2109.
- [161] a) D. R. Snow Jr., (The Boeing Company), *US Patent 20050247197*, **2005**; b) B. L. Moravec, R. E. Boggs, R. N. Graham, A. Grim, D. A. Adkins, D. Snow Jr., G. A. Haack, (The Boeing Company), *US Patent 7152635*, **2006**.
- [162] R. W. Baker, B. T. Low, *Macromolecules* **2014**, *47*, 6999.
- [163] T. L. Reynolds, T. I. Eklund, G. A. Haack, Onboard Inert Gas Generation System/Onboard Oxygen Gas Generation System (OBIGGS/OBOGS) Study. Part 2: Gas Separation Technology—State of the Art, NASA Technical Report, <https://ntrs.nasa.gov/search.jsp?R=20010092198>.
- [164] R. W. Baker, *Membrane Technology and Applications*, 2nd ed., John Wiley & Sons, Ltd., West Sussex **2004**.
- [165] a) B. T. Low, L. Zhao, T. C. Merkel, M. Weber, D. Stolten, *J. Membr. Sci.* **2013**, *431*, 139; b) G. Dong, H. Li, V. Chen, *J. Mater. Chem. A* **2013**, *1*, 4610.
- [166] a) D. Zacher, O. Shekhah, C. Woll, R. A. Fischer, *Chem. Soc. Rev.* **2009**, *38*, 1418; b) B. Liu, M. Ma, D. Zacher, A. Bétard, K. Yusenko, N. Metzler-Nolte, C. Wöll, R. A. Fischer, *J. Am. Chem. Soc.* **2011**, *133*, 1734.
- [167] N. Rangnekar, M. Shete, K. V. Agrawal, B. Topuz, P. Kumar, Q. Guo, I. Ismail, A. Alyoubi, S. Basahel, K. Narasimharao, C. W. Macosko, K. A. Mkhoyan, S. Al-Thabaiti, B. Stottrup, M. Tsapatsis, *Angew. Chem., Int. Ed.* **2015**, *54*, 6571.
- [168] a) E. Tocci, L. De Lorenzo, P. Bernardo, G. Clarizia, F. Bazzarelli, N. B. McKeown, M. Carta, R. Malpass-Evans, K. Friess, K. Pilnáček, M. Lanč, Y. P. Yampolskii, L. Strarannikova, V. Shantarovich, M. Mauri, J. C. Jansen, *Macromolecules* **2014**, *47*, 7900; b) I. Rose, M. Carta, R. Malpass-Evans, M.-C. Ferrari, P. Bernardo, G. Clarizia, J. C. Jansen, N. B. McKeown, *ACS Macro Lett.* **2015**, *4*, 912; c) M. Carta, P. Bernardo, G. Clarizia, J. C. Jansen, N. B. McKeown, *Macromolecules* **2014**, *47*, 8320.
- [169] a) P. M. Budd, K. J. Msayib, C. E. Tattershall, B. S. Ghanem, K. J. Reynolds, N. B. McKeown, D. Fritsch, *J. Membr. Sci.* **2005**, *251*, 263; b) B. S. Ghanem, N. B. McKeown, P. M. Budd, D. Fritsch, *Macromolecules* **2008**, *41*, 1640.
- [170] N. Du, H. B. Park, G. P. Robertson, M. M. Dal-Cin, T. Visser, L. Scoles, M. D. Guiver, *Nat. Mater.* **2011**, *10*, 372.
- [171] M. Carta, R. Malpass-Evans, M. Croad, Y. Rogan, J. C. Jansen, P. Bernardo, F. Bazzarelli, N. B. McKeown, *Science* **2013**, *339*, 303.
- [172] P. Budd, N. McKeown, B. Ghanem, K. Msayib, D. Fritsch, L. Starannikova, N. Belov, O. Sanfirova, Y. Yampolskii, V. Shantarovich, *J. Membr. Sci.* **2008**, *325*, 851.
- [173] S. Kim, Y. M. Lee, *Prog. Polym. Sci.* **2015**, *43*, 1.
- [174] N. Du, H. B. Park, M. M. Dal-Cin, M. D. Guiver, *Energy Environ. Sci.* **2012**, *5*, 7306.
- [175] Z. P. Smith, K. Czenkusch, S. Wi, K. L. Gleason, G. Hernández, C. M. Doherty, K. Konstas, T. J. Bastow, C. Álvarez, A. J. Hill, A. E. Lozano, D. R. Paul, B. D. Freeman, *Polymer* **2014**, *55*, 6649.

- [176] S. H. Han, N. Misdan, S. Kim, C. M. Doherty, A. J. Hill, Y. M. Lee, *Macromolecules* **2010**, *43*, 7657.
- [177] a) D. F. Sanders, R. Guo, Z. P. Smith, Q. Liu, K. A. Stevens, J. E. McGrath, D. R. Paul, B. D. Freeman, *Polymer* **2014**, *55*, 1636; b) D. F. Sanders, R. Guo, Z. P. Smith, K. A. Stevens, Q. Liu, J. E. McGrath, D. R. Paul, B. D. Freeman, *J. Membr. Sci.* **2014**, *463*, 73.
- [178] R. Guo, D. F. Sanders, Z. P. Smith, B. D. Freeman, D. R. Paul, J. E. McGrath, *J. Mater. Chem. A* **2013**, *1*, 262.
- [179] Z. P. Smith, G. Hernández, K. L. Gleason, A. Anand, C. M. Doherty, K. Konstas, C. Alvarez, A. J. Hill, A. E. Lozano, D. R. Paul, B. D. Freeman, *J. Membr. Sci.* **2015**, *493*, 766.
- [180] a) S. Kim, S. H. Han, Y. M. Lee, *J. Membr. Sci.* **2012**, *403*, 169; b) K. T. Woo, J. Lee, G. Dong, J. S. Kim, Y. S. Do, W.-S. Hung, K.-R. Lee, G. Barbieri, E. Drioli, Y. M. Lee, *J. Membr. Sci.* **2015**, *490*, 129.
- [181] Y. Jiang, F. T. Willmore, D. F. Sanders, Z. P. Smith, C. P. Ribeiro, C. M. Doherty, A. Thornton, A. J. Hill, B. D. Freeman, I. C. Sanchez, *Polymer* **2011**, *52*, 2244.
- [182] a) R. Guo, D. F. Sanders, Z. P. Smith, B. D. Freeman, D. R. Paul, J. E. McGrath, *J. Mater. Chem. A* **2013**, *1*, 6063; b) M. Calle, Y. Chan, H. J. Jo, Y. M. Lee, *Polymer* **2012**, *53*, 2783; c) S. Li, H. J. Jo, S. H. Han, C. H. Park, S. Kim, P. M. Budd, Y. M. Lee, *J. Membr. Sci.* **2013**, *434*, 137.
- [183] a) S. Han, H. Kwon, K. Kim, J. Seong, C. Park, S. Kim, C. M. Doherty, A. Thornton, A. J. Hill, A. Lozano, K. Berchtold, Y. Lee, *Phys. Chem. Chem. Phys.* **2012**, *14*, 4365; b) A. Kushwaha, M. E. Dose, Z. P. Smith, S. Luo, B. D. Freeman, R. Guo, *Polymer* **2015**, *78*, 81; c) M. Calle, A. E. Lozano, Y. M. Lee, *Eur. Polym. J.* **2012**, *48*, 1313.
- [184] N. Du, G. P. Robertson, J. Song, I. Pinnau, S. Thomas, M. D. Guiver, *Macromolecules* **2008**, *41*, 9656.
- [185] N. Du, G. P. Robertson, J. Song, I. Pinnau, M. D. Guiver, *Macromolecules* **2009**, *42*, 6038.
- [186] H.-Y. Zhao, Y.-M. Cao, X.-L. Ding, M.-Q. Zhou, J.-H. Liu, Q. Yuan, *J. Membr. Sci.* **2008**, *320*, 179.
- [187] N. Du, G. P. Robertson, I. Pinnau, M. D. Guiver, *Macromolecules* **2010**, *43*, 8580.
- [188] M. Carta, M. Croad, R. Malpass-Evans, J. C. Jansen, P. Bernardo, G. Clarizia, K. Friess, M. Lanč, N. B. McKeown, *Adv. Mater.* **2014**, *26*, 3526.
- [189] L. C. E. Struik, *Physical Aging in Amorphous Polymers and Other Materials*, Elsevier Scientific Publication Co., Amsterdam **1978**.
- [190] R. D. Priestley, C. J. Ellison, L. J. Broadbelt, J. M. Torkelson, *Science* **2005**, *309*, 456.
- [191] Y. P. Yampol'Skii, S. Shishatskii, V. Shantorovich, E. Antipov, N. Kuzmin, S. Rykov, V. Khodjaeva, N. Plate, *J. Appl. Polym. Sci.* **1993**, *48*, 1935.
- [192] K. D. Dorkenoo, P. H. Pfromm, *Macromolecules* **2000**, *33*, 3747.
- [193] a) R. R. Tiwari, Z. P. Smith, H. Lin, B. D. Freeman, D. R. Paul, *Polymer* **2015**, *61*, 1; b) R. R. Tiwari, Z. P. Smith, H. Lin, B. D. Freeman, D. R. Paul, *Polymer* **2014**, *55*, 5788.
- [194] R. Swaidan, B. Ghanem, E. Litwiller, I. Pinnau, *Macromolecules* **2015**, *48*, 6553.
- [195] a) P. Lindemann, M. Tsotsalas, S. Shishatskiy, V. Abetz, P. Krolla-Sidenstein, C. Azucena, L. Monnereau, A. Beyer, A. Götzhäuser, V. Mugnaini, H. Gliemann, S. Bräse, C. Wöll, *Chem. Mater.* **2014**, *26*, 7189; b) G. Cheng, B. Bonillo, R. S. Sprick, D. J. Adams, T. Hasell, A. I. Cooper, *Adv. Funct. Mater.* **2014**, *24*, 5219.
- [196] A. I. Cooper, *Adv. Mater.* **2009**, *21*, 1291.
- [197] R. Barrer, T. Gabor, *Proc. R. Soc. London, Ser. A* **1960**, *256*, 267.
- [198] W. Koros, R. Mahajan, *J. Membr. Sci.* **2000**, *175*, 181.
- [199] R. L. Burns, W. J. Koros, *J. Membr. Sci.* **2003**, *211*, 299.
- [200] M. Rungta, C. Zhang, W. J. Koros, L. Xu, *AIChE J.* **2013**, *59*, 3475.
- [201] a) D. Bastani, N. Esmaeili, M. Asadollahi, *J. Ind. Eng. Chem.* **2013**, *19*, 375; b) F. Dorosti, M. R. Omidkhan, M. Z. Pedram, F. Moghadam, *Chem. Eng. J.* **2011**, *171*, 1469; c) H. Gong, S. S. Lee, T.-H. Bae, *Microporous Mesoporous Mater.* **2017**, *237*, 82; d) A. L. Khan, A. Cano-Odena, B. Gutierrez, C. Minguillon, I. F. J. Vankelecom, *J. Membr. Sci.* **2010**, *350*, 340; e) T. W. Pechar, S. Kim, B. Vaughan, E. Marand, M. Tsapatsis, H. K. Jeong, C. J. Cornelius, *J. Membr. Sci.* **2006**, *277*, 195; f) T. W. Pechar, M. Tsapatsis, E. Marand, R. Davis, *Desalination* **2002**, *146*, 3; g) C. M. Zimmerman, A. Singh, W. J. Koros, *J. Membr. Sci.* **1997**, *137*, 145.
- [202] T.-S. Chung, L. Y. Jiang, Y. Li, S. Kulprathipanja, *Prog. Polym. Sci.* **2007**, *32*, 483.
- [203] Y. Zhang, K. J. Balkus, I. H. Musselman, J. P. Ferraris, *J. Membr. Sci.* **2008**, *325*, 28.
- [204] J. E. Bachman, Z. P. Smith, T. Li, T. Xu, J. R. Long, *Nat. Mater.* **2016**, *15*, 845.
- [205] a) T.-H. Bae, J. S. Lee, W. Qiu, W. J. Koros, C. W. Jones, S. Nair, *Angew. Chem., Int. Ed.* **2010**, *49*, 9863; b) A. Car, C. Stropnik, K. V. Peinemann, *Desalination* **2006**, *200*, 424; c) J. Hu, H. Cai, H. Ren, Y. Wei, Z. Xu, H. Liu, Y. Hu, *Ind. Eng. Chem. Res.* **2010**, *49*, 12605; d) E. V. Perez, K. J. Balkus, J. P. Ferraris, I. H. Musselman, *J. Membr. Sci.* **2009**, *328*, 165; e) B. Seoane, J. Coronas, I. Gascon, M. E. Benavides, O. Karvan, J. Caro, F. Kapteijn, J. Gascon, *Chem. Soc. Rev.* **2015**, *44*, 2421; f) T. Yang, Y. Xiao, T.-S. Chung, *Energy Environ. Sci.* **2011**, *4*, 4171; g) B. Zornoza, C. Tellez, J. Coronas, J. Gascon, F. Kapteijn, *Microporous Mesoporous Mater.* **2013**, *166*, 67.
- [206] T.-H. Bae, J. R. Long, *Energy Environ. Sci.* **2013**, *6*, 3565.
- [207] T. Rodenas, I. Luz, G. Prieto, B. Seoane, H. Miro, A. Corma, F. Kapteijn, F. X. Llabrés i Xamena, J. Gascon, *Nat. Mater.* **2015**, *14*, 48.
- [208] C. Zhang, Y. Dai, J. R. Johnson, O. Karvan, W. J. Koros, *J. Membr. Sci.* **2012**, *389*, 34.
- [209] J. E. Bachman, J. R. Long, *Energy Environ. Sci.* **2016**, *9*, 2031.
- [210] a) J. Ahn, W.-J. Chung, I. Pinnau, M. D. Guiver, *J. Membr. Sci.* **2008**, *314*, 123; b) J. Ahn, W.-J. Chung, I. Pinnau, J. Song, N. Du, G. P. Robertson, M. D. Guiver, *J. Membr. Sci.* **2010**, *346*, 280; c) C. J. Cornelius, E. Marand, *J. Membr. Sci.* **2002**, *202*, 97; d) N. C. Su, Z. P. Smith, B. D. Freeman, J. J. Urban, *Chem. Mater.* **2015**, *27*, 2421; e) R. Xing, W. S. W. Ho, *J. Membr. Sci.* **2011**, *367*, 91.
- [211] W. A. W. Rafizah, A. F. Ismail, *J. Membr. Sci.* **2008**, *307*, 53.
- [212] D. Q. Vu, W. J. Koros, S. J. Miller, *J. Membr. Sci.* **2003**, *211*, 311.
- [213] a) A. F. Ismail, P. S. Goh, S. M. Sanip, M. Aziz, *Sep. Purif. Technol.* **2009**, *70*, 12; b) S. Kim, T. W. Pechar, E. Marand, *Desalination* **2006**, *192*, 330.
- [214] J. Liu, T.-B. Bae, W. Qiu, S. Husain, S. Nair, C. W. Jones, R. R. Chance, W. J. Koros, *J. Membr. Sci.* **2009**, *343*, 157.
- [215] T. H. Nguyen, H. Gong, S. S. Lee, T.-H. Bae, *ChemPhysChem* **2016**, *17*, 3165.
- [216] J. Ploegmakers, S. Japip, K. Nijmeijer, *J. Membr. Sci.* **2013**, *428*, 445.
- [217] a) W. L. Queen, M. R. Hudson, E. D. Bloch, J. A. Mason, M. I. Gonzalez, J. S. Lee, D. Gygi, J. D. Howe, K. Lee, T. A. Darwish, M. James, V. K. Peterson, S. J. Teat, B. Smit, J. B. Neaton, J. R. Long, C. M. Brown, *Chem. Sci.* **2014**, *5*, 4701; b) E. D. Bloch, W. L. Queen, R. Krishna, J. M. Zadrozny, C. M. Brown, J. R. Long, *Science* **2012**, *335*, 1606.
- [218] M. A. Shannon, P. W. Bohn, M. Elimelech, J. G. Georgiadis, B. J. Mariñas, A. M. Mayes, *Nature* **2008**, *452*, 301.
- [219] K. P. Lee, T. C. Arnot, D. Mattia, *J. Membr. Sci.* **2011**, *370*, 1.
- [220] G. M. Geise, D. R. Paul, B. D. Freeman, *Prog. Polym. Sci.* **2014**, *39*, 1.

- [221] a) G. M. Geise, H. B. Park, A. C. Sagle, B. D. Freeman, J. E. McGrath, *J. Membr. Sci.* **2011**, 369, 130; b) D. R. Paul, *J. Membr. Sci.* **2004**, 241, 371.
- [222] a) A. Kalra, S. Garde, G. Hummer, *Proc. Natl. Acad. Sci. USA* **2003**, 100, 10175; b) K. Falk, F. Sedlmeier, L. Joly, R. R. Netz, L. Bocquet, *Nano Lett.* **2010**, 10, 4067.
- [223] B. Corry, *J. Phys. Chem. B* **2008**, 112, 1427.
- [224] J. K. Holt, H. G. Park, Y. Wang, M. Stadermann, A. B. Artyukhin, C. P. Grigoropoulos, A. Noy, O. Bakajin, *Science* **2006**, 312, 1034.
- [225] M. Majumder, N. Chopra, B. J. Hinds, *ACS Nano* **2011**, 5, 3867.
- [226] F. Fornasiero, H. G. Park, J. K. Holt, M. Stadermann, C. P. Grigoropoulos, A. Noy, O. Bakajin, *Proc. Natl. Acad. Sci. USA* **2008**, 105, 17250.
- [227] D. Li, Y. Yan, H. Wang, *Prog. Polym. Sci.* **2016**, 61, 104.
- [228] T. Y. Cath, A. E. Childress, M. Elimelech, *J. Membr. Sci.* **2006**, 281, 70.
- [229] S. Zhao, L. Zou, C. Y. Tang, D. Mulcahy, *J. Membr. Sci.* **2012**, 396, 1.
- [230] Z. Song, Z. Xu, *Sci. Rep.* **2015**, 5, 10597.
- [231] N. Ma, J. Wei, R. Liao, C. Y. Tang, *J. Membr. Sci.* **2012**, 405–406, 149.
- [232] C. C. Coterillo, A. M. U. Mendia, I. O. Uribe, in *Membrane Science and Technology*, Vol. 13 (Eds: R. Mallada, M. Menéndez), Elsevier, Amsterdam, the Netherlands **2008**, p. 217.
- [233] Y. K. Ong, G. M. Shi, N. L. Le, Y. P. Tang, J. Zuo, S. P. Nunes, T.-S. Chung, *Prog. Polym. Sci.* **2016**, 57, 1.
- [234] F. Xiangli, Y. Chen, W. Jin, N. Xu, *Ind. Eng. Chem. Res.* **2007**, 46, 2224.
- [235] a) T. C. Bowen, R. D. Noble, J. L. Falconer, *J. Membr. Sci.* **2004**, 245, 1; b) J. Coronas, J. Santamaría, *Sep. Purif. Rev.* **1999**, 28, 127; c) D. Korelskiy, T. Leppäjärvi, H. Zhou, M. Grahn, J. Tanskanen, J. Hedlund, *J. Membr. Sci.* **2013**, 427, 381; d) A. Tavoraro, E. Drioli, *Adv. Mater.* **1999**, 11, 975; e) T. Bein, *Chem. Mater.* **1996**, 8, 1636.
- [236] Y. Morigami, M. Kondo, J. Abe, H. Kita, K. Okamoto, *Sep. Purif. Technol.* **2001**, 25, 251.
- [237] S. V. Adymkanov, Y. P. Yampol'skii, A. M. Polyakov, P. M. Budd, K. J. Reynolds, N. B. McKeown, K. J. Msayib, *Polym. Sci. Ser. A* **2008**, 50, 444.
- [238] P. Salehian, W. F. Yong, T.-S. Chung, *J. Membr. Sci.* **2016**, 518, 110.
- [239] W. F. Yong, P. Salehian, L. Zhang, T.-S. Chung, *J. Membr. Sci.* **2017**, 523, 430.
- [240] a) D. Hua, Y. K. Ong, Y. Wang, T. Yang, T.-S. Chung, *J. Membr. Sci.* **2014**, 453, 155; b) C.-H. Kang, Y.-F. Lin, Y.-S. Huang, K.-L. Tung, K.-S. Chang, J.-T. Chen, W.-S. Hung, K.-R. Lee, J.-Y. Lai, *J. Membr. Sci.* **2013**, 438, 105; c) G. M. Shi, T. Yang, T. S. Chung, *J. Membr. Sci.* **2012**, 415–416, 577; d) X.-L. Liu, Y.-S. Li, G.-Q. Zhu, Y.-J. Ban, L.-Y. Xu, W.-S. Yang, *Angew. Chem., Int. Ed.* **2011**, 50, 10636.
- [241] A. M. Marti, D. Tran, K. J. Balkus, *J. Porous Mater.* **2015**, 22, 1275.
- [242] K. Zhang, R. P. Lively, C. Zhang, R. R. Chance, W. J. Koros, D. S. Sholl, S. Nair, *J. Phys. Chem. Lett.* **2013**, 4, 3618.
- [243] X. Y. Qu, H. Dong, Z. J. Zhou, L. Zhang, H. L. Chen, *Ind. Eng. Chem. Res.* **2010**, 49, 7504.
- [244] a) A. Kasik, Y. S. Lin, *Sep. Purif. Technol.* **2014**, 121, 38; b) Z. Zhao, X. Ma, Z. Li, Y. S. Lin, *J. Membr. Sci.* **2011**, 382, 82; c) A. Ibrahim, Y. S. Lin, *Ind. Eng. Chem. Res.* **2016**, 55, 8652.
- [245] H. B. Awbi, *Renewable Sustainable Energy Rev.* **1998**, 2, 157.
- [246] M. R. H. Abdel-Salam, M. Fauchoux, G. Ge, R. W. Besant, C. J. Simonson, *Appl. Energy* **2014**, 127, 202.
- [247] M. R. H. Abdel-Salam, G. Ge, M. Fauchoux, R. W. Besant, C. J. Simonson, *Renewable Sustainable Energy Rev.* **2014**, 39, 700.
- [248] a) M. Khayet, *Adv. Colloid Interface Sci.* **2011**, 164, 56; b) J. Woods, *Renewable Sustainable Energy Rev.* **2014**, 33, 290.
- [249] W. F. Yong, Y. X. Ho, T.-S. Chung, *ChemSusChem* **2017**, 10, 4046.
- [250] Y. Shin, W. Liu, B. Schwenzer, S. Manandhar, D. Chase-Woods, M. H. Engelhard, R. Devanathan, L. S. Fifield, W. D. Bennett, B. Ginovska, D. W. Gotthold, *Carbon* **2016**, 106, 164.
- [251] a) N. S. Lewis, D. G. Nocera, *Proc. Natl. Acad. Sci. USA* **2006**, 103, 15729; b) J. M. Carrasco, L. G. Franquelo, J. T. Bialasiewicz, E. Galvan, R. C. P. Guisado, M. A. M. Prats, J. I. Leon, N. Moreno-Alfonso, *IEEE Trans. Ind. Electron.* **2006**, 53, 1002; c) J. P. Barton, D. G. Infield, *IEEE Trans. Energy Convers.* **2004**, 19, 441.
- [252] D. E. Fenton, J. M. Parker, P. V. Wright, *Polymer* **1973**, 14, 589.
- [253] P. Lightfoot, M. A. Mehta, P. G. Bruce, *Science* **1993**, 262, 883.
- [254] K.-D. Kreuer, S. J. Paddison, E. Spohr, M. Schuster, *Chem. Rev.* **2004**, 104, 4637.
- [255] J. Chen, X.-Z. Li, Q. Zhang, A. Michaelides, E. Wang, *Phys. Chem. Chem. Phys.* **2013**, 15, 6344.
- [256] M. Eigen, *Angew. Chem., Int. Ed.* **1964**, 3, 1.
- [257] G. Zundel, J. Fritsch, in *The Chemical Physics of Solvation*, Vol. 2 (Eds: R. R. Dogonadze, E. Kálmán, A. A. Kornyshev, J. Ulstrup), Elsevier, Amsterdam **1986**.
- [258] S. Cukierman, *Biochim. Biophys. Acta Bioenerg.* **2006**, 1757, 876.
- [259] C. de Grotthuss, *Ann. Chim.* **1806**, 58, 54.
- [260] O. Markovitch, H. Chen, S. Izvekov, F. Paesani, G. A. Voth, N. Agmon, *J. Phys. Chem. B* **2008**, 112, 9456.
- [261] D. Marx, *ChemPhysChem* **2006**, 7, 1848.
- [262] A. Hassanali, F. Giberti, J. Cuny, T. D. Kühne, M. Parrinello, *Proc. Natl. Acad. Sci. USA* **2013**, 110, 13723.
- [263] M. L. Brewer, U. W. Schmitt, G. A. Voth, *Biophys. J.* **2001**, 80, 1691.
- [264] Z. Cao, Y. Peng, T. Yan, S. Li, A. Li, G. A. Voth, *J. Am. Chem. Soc.* **2010**, 132, 11395.
- [265] F. I. Allen, L. R. Comolli, A. Kusoglu, M. A. Modestino, A. M. Minor, A. Z. Weber, *ACS Macro Lett.* **2015**, 4, 1.
- [266] a) Y. Sone, P. Ekdunge, D. Simonsson, *J. Electrochem. Soc.* **1996**, 143, 1254; b) K. A. Mauritz, R. B. Moore, *Chem. Rev.* **2004**, 104, 4535.
- [267] S. J. Paddison, R. Paul, *Phys. Chem. Chem. Phys.* **2002**, 4, 1158.
- [268] C. Dellago, M. M. Naor, G. Hummer, *Phys. Rev. Lett.* **2003**, 90, 105902.
- [269] T. J. Day, A. V. Soudackov, M. Čuma, U. W. Schmitt, G. A. Voth, *J. Chem. Phys.* **2002**, 117, 5839.
- [270] J. Wu, K. Gerstandt, H. Zhang, J. Liu, B. J. Hinds, *Nat. Nanotechnol.* **2012**, 7, 133.
- [271] G. A. Pilgrim, J. W. Leadbetter, F. Qiu, A. J. Siitonen, S. M. Pilgrim, T. D. Krauss, *Nano Lett.* **2014**, 14, 1728.
- [272] R. H. Baughman, A. A. Zakhidov, W. A. de Heer, *Science* **2002**, 297, 787.
- [273] B. J. Hinds, N. Chopra, T. Rantell, R. Andrews, V. Gavalas, L. G. Bachas, *Science* **2004**, 303, 62.
- [274] X. Zhou, G. Liu, K. Yamato, Y. Shen, R. Cheng, X. Wei, W. Bai, Y. Gao, H. Li, Y. Liu, F. Liu, D. M. Czajkowsky, J. Wang, M. J. Dabney, Z. Cai, J. Hu, F. V. Bright, L. He, X. C. Zeng, Z. Shao, B. Gong, *Nat. Commun.* **2012**, 3, 949.
- [275] M. S. Kaucher, M. Peterca, A. E. Dulcey, A. J. Kim, S. A. Vinogradov, D. A. Hammer, P. A. Heiney, V. Percec, *J. Am. Chem. Soc.* **2007**, 129, 11698.
- [276] P. De Santis, S. Morosetti, R. Rizzo, *Macromolecules* **1974**, 7, 52.
- [277] M. R. Ghadiri, J. R. Granja, L. Buehler, *Nature* **1994**, 369, 301.
- [278] J. Montenegro, M. R. Ghadiri, J. R. Granja, *Acc. Chem. Res.* **2013**, 46, 2955.
- [279] G. K. H. Shimizu, J. M. Taylor, S. Kim, *Science* **2013**, 341, 354.
- [280] J. A. Hurd, R. Vaidyanathan, V. Thangadurai, C. I. Ratcliffe, I. L. Moudrakovski, G. K. H. Shimizu, *Nat. Chem.* **2009**, 1, 705.
- [281] P. Ramaswamy, R. Matsuda, W. Kosaka, G. Akiyama, H. J. Jeon, S. Kitagawa, *Chem. Commun.* **2013**, 50, 1144.
- [282] S. Horike, Y. Kamitsubo, M. Inukai, T. Fukushima, D. Umeyama, T. Itakura, S. Kitagawa, *J. Am. Chem. Soc.* **2013**, 135, 4612.

- [283] S. Bureekaew, S. Horike, M. Higuchi, M. Mizuno, T. Kawamura, D. Tanaka, N. Yanai, S. Kitagawa, *Nat. Mater.* **2009**, *8*, 831.
- [284] G. K. H. Shimizu, R. Vaidhyanathan, J. M. Taylor, *Chem. Soc. Rev.* **2009**, *38*, 1430.
- [285] M. G. Goesten, J. Juan-Alcañiz, E. V. Ramos-Fernandez, K. B. Sai Sankar Gupta, E. Stavitski, H. van Bekkum, J. Gascon, F. Kapteijn, *J. Catal.* **2011**, *281*, 177.
- [286] a) J. M. Taylor, K. W. Dawson, G. K. H. Shimizu, *J. Am. Chem. Soc.* **2013**, *135*, 1193; b) R. M. P. Colodrero, P. Olivera-Pastor, E. R. Losilla, D. Hernández-Alonso, M. A. G. Aranda, L. Leon-Reina, J. Rius, K. D. Demadis, B. Moreau, D. Villemin, M. Palomino, F. Rey, A. Cabeza, *Inorg. Chem.* **2012**, *51*, 7689.
- [287] S. Li, Z. Zhou, Y. Zhang, M. Liu, W. Li, *Chem. Mater.* **2005**, *17*, 5884.
- [288] M. Yoon, K. Suh, S. Natarajan, K. Kim, *Angew. Chem., Int. Ed.* **2013**, *52*, 2688.
- [289] A. Morozan, F. Jaouen, *Energy Environ. Sci.* **2012**, *5*, 9269.
- [290] P. Arora, Z. J. Zhang, *Chem. Rev.* **2004**, *104*, 4419.
- [291] a) Z. Jin, K. Xie, X. Hong, Z. Hu, X. Liu, *J. Power Sources* **2012**, *218*, 163; b) L. Su, R. M. Darling, K. G. Gallagher, W. Xie, J. L. Thelen, A. F. Badel, J. L. Barton, K. J. Cheng, N. P. Balsara, J. S. Moore, F. R. Brushett, *J. Electrochem. Soc.* **2016**, *163*, A5253; c) X. Yu, J. Joseph, A. Manthiram, *J. Mater. Chem. A* **2015**, *3*, 15683.
- [292] a) L. Li, C. Liu, G. He, D. Fan, A. Manthiram, *Energy Environ. Sci.* **2015**, *8*, 3274; b) Y. Lu, J. B. Goodenough, *J. Mater. Chem.* **2011**, *21*, 10113; c) L. Wang, Y. Zhao, M. L. Thomas, A. Dutta, H. R. Byon, *ChemElectroChem* **2016**, *3*, 152.
- [293] a) M. S. Kim, L. Ma, S. Choudhury, L. A. Archer, *Adv. Mater. Interfaces* **2016**, *3*, 1600450; b) H. Yao, K. Yan, W. Li, G. Zheng, D. Kong, Z. W. Seh, V. K. Narasimhan, Z. Liang, Y. Cui, *Energy Environ. Sci.* **2014**, *7*, 3381; c) Z. Zhang, Y. Lai, Z. Zhang, K. Zhang, J. Li, *Electrochim. Acta* **2014**, *129*, 55.
- [294] R. Darling, K. Gallagher, W. Xie, L. Su, F. Brushett, *J. Electrochem. Soc.* **2016**, *163*, A5029.
- [295] K. Xu, *Chem. Rev.* **2004**, *104*, 4303.
- [296] Y. Jiang, F. Chen, Y. Gao, Y. Wang, S. Wang, Q. Gao, Z. Jiao, B. Zhao, Z. Chen, *J. Power Sources* **2017**, *342*, 929.
- [297] A. L. Ward, S. E. Doris, L. Li, M. A. Hughes, X. Qu, K. A. Persson, B. A. Helms, *ACS Cent. Sci.* **2017**, *3*, 399.
- [298] M. T. Ong, O. Vernalers, E. W. Draeger, A. C. T. van Duin, V. Lordi, J. E. Pask, *J. Phys. Chem. B* **2015**, *119*, 1535.
- [299] T. Li, P. B. Balbuena, *J. Electrochem. Soc.* **1999**, *146*, 3613.
- [300] J.-C. Soetens, C. Millot, B. Maignet, *J. Phys. Chem. A* **1998**, *102*, 1055.
- [301] M. D. Bhatt, M. Cho, K. Cho, *Modell. Simul. Mater. Sci. Eng.* **2012**, *20*, 065004.
- [302] O. Borodin, G. D. Smith, *J. Phys. Chem. B* **2006**, *110*, 4971.
- [303] B. M. Wiers, M.-L. Foo, N. P. Balsara, J. R. Long, *J. Am. Chem. Soc.* **2011**, *133*, 14522.
- [304] R. Ameloot, M. Aubrey, B. M. Wiers, A. P. Gómora-Figueroa, S. N. Patel, N. P. Balsara, J. R. Long, *Chem. Eur. J.* **2013**, *19*, 5533.
- [305] M. L. Aubrey, R. Ameloot, B. M. Wiers, J. R. Long, *Energy Environ. Sci.* **2014**, *7*, 667.
- [306] J. H. Park, K. Suh, M. R. Rohman, W. Hwang, M. Yoon, K. Kim, *Chem. Commun.* **2015**, *51*, 9313.
- [307] F.-S. Ke, Y.-S. Wu, H. Deng, *J. Solid State Chem.* **2015**, *223*, 109.
- [308] J. F. Van Humbeck, M. L. Aubrey, A. Alsaibee, R. Ameloot, G. W. Coates, W. R. Dichtel, J. R. Long, *Chem. Sci.* **2015**, *6*, 5499.
- [309] S. Bai, X. Liu, K. Zhu, S. Wu, H. Zhou, *Nat. Energy* **2016**, *1*, 16094.
- [310] S. E. Doris, A. L. Ward, P. D. Frischmann, L. Li, B. A. Helms, *J. Mater. Chem. A* **2016**, *4*, 16946.
- [311] a) L. Cheng, R. S. Assary, X. Qu, A. Jain, S. P. Ong, N. N. Rajput, K. Persson, L. A. Curtiss, *J. Phys. Chem. Lett.* **2015**, *6*, 283; b) A. Jain, Y. Shin, K. A. Persson, *Nat. Rev. Mater.* **2016**, *1*, 15004; c) X. Qu, A. Jain, N. N. Rajput, L. Cheng, Y. Zhang, S. P. Ong, M. Brafman, E. Maginn, L. A. Curtiss, K. A. Persson, *Comput. Mater. Sci.* **2015**, *103*, 56.
- [312] a) M. Burgess, J. S. Moore, J. Rodríguez-López, *Acc. Chem. Res.* **2016**, *49*, 2649; b) E. C. Montoto, G. Nagarjuna, J. Hui, M. Burgess, N. M. Sekerak, K. Hernández-Burgos, T.-S. Wei, M. Kneer, J. Grolman, K. J. Cheng, J. A. Lewis, J. S. Moore, J. Rodríguez-López, *J. Am. Chem. Soc.* **2016**, *138*, 13230; c) G. Nagarjuna, J. Hui, K. J. Cheng, T. Lichtenstein, M. Shen, J. S. Moore, J. Rodríguez-López, *J. Am. Chem. Soc.* **2014**, *136*, 16309.
- [313] M. Burgess, E. Chénard, K. Hernández-Burgos, G. Nagarjuna, R. S. Assary, J. Hui, J. S. Moore, J. Rodríguez-López, *Chem. Mater.* **2016**, *28*, 7362.
- [314] a) D. Liu, T.-F. Liu, Y.-P. Chen, L. Zou, D. Feng, K. Wang, Q. Zhang, S. Yuan, C. Zhong, H.-C. Zhou, *J. Am. Chem. Soc.* **2015**, *137*, 7740; b) J. A. Mason, J. Oktawiec, M. K. Taylor, M. R. Hudson, J. Rodriguez, J. E. Bachman, M. I. Gonzalez, A. Cervellino, A. Guagliardi, C. M. Brown, P. L. Llewellyn, N. Masciocchi, J. R. Long, *Nature* **2015**, *527*, 357; c) S. Tominaka, F.-X. Coudert, T. D. Dao, T. Nagao, A. K. Cheetham, *J. Am. Chem. Soc.* **2015**, *137*, 6428.
- [315] M. K. Taylor, T. Run evski, J. Oktawiec, M. I. Gonzalez, R. L. Siegelman, J. A. Mason, J. Ye, C. M. Brown, J. R. Long, *J. Am. Chem. Soc.* **2016**, *138*, 15019.
- [316] T. M. McDonald, J. A. Mason, X. Kong, E. D. Bloch, D. Gygi, A. Dani, V. Crocella, F. Giordanino, S. O. Odoh, W. S. Drisdell, B. Vlaisavljevich, A. L. Dzubak, R. Poloni, S. K. Schnell, N. Planas, K. Lee, T. Pascal, L. F. Wan, D. Prendergast, J. B. Neaton, B. Smit, J. B. Kortright, L. Gagliardi, S. Bordiga, J. A. Reimer, J. R. Long, *Nature* **2015**, *519*, 303.
- [317] D.-e. Jiang, V. R. Cooper, S. Dai, *Nano Lett.* **2009**, *9*, 4019.
- [318] S. P. Surwade, S. N. Smirnov, I. V. Vlasiouk, R. R. Unocic, G. M. Veith, S. Dai, S. M. Mahurin, *Nat. Nanotechnol.* **2015**, *10*, 459.
- [319] L. Huang, M. Zhang, C. Li, G. Shi, *J. Phys. Chem. Lett.* **2015**, *6*, 2806.
- [320] G. Liu, W. Jin, N. Xu, *Chem. Soc. Rev.* **2015**, *44*, 5016.
- [321] a) S. P. Koenig, L. Wang, J. Pellegrino, J. S. Bunch, *Nat. Nanotechnol.* **2012**, *7*, 728; b) L. Wang, L. W. Draushuk, L. Cantley, S. P. Koenig, X. Liu, J. Pellegrino, M. S. Strano, J. S. Bunch, *Nat Nano* **2015**, *10*, 785.
- [322] K. Celebi, J. Buchheim, R. M. Wyss, A. Droudian, P. Gasser, I. Shorubalko, J.-I. Kye, C. Lee, H. G. Park, *Science* **2014**, *344*, 289.
- [323] a) S. C. O'Hern, D. Jang, S. Bose, J.-C. Idrobo, Y. Song, T. Laoui, J. Kong, R. Karnik, *Nano Lett.* **2015**, *15*, 3254; b) S. C. O'Hern, M. S. H. Boutilier, J.-C. Idrobo, Y. Song, J. Kong, T. Laoui, M. Atieh, R. Karnik, *Nano Lett.* **2014**, *14*, 1234.
- [324] D. Chen, H. Feng, J. Li, *Chem. Rev.* **2012**, *112*, 6027.
- [325] L. Huang, Y. Li, Q. Zhou, W. Yuan, G. Shi, *Adv. Mater.* **2015**, *27*, 3797.
- [326] a) R. R. Nair, H. A. Wu, P. N. Jayaram, I. V. Grigorieva, A. K. Geim, *Science* **2012**, *335*, 442; b) D. W. Boukhalvalov, M. I. Katsnelson, Y.-W. Son, *Nano Lett.* **2013**, *13*, 3930.
- [327] Q. Zhang, H. Zheng, Z. Geng, S. Jiang, J. Ge, K. Fan, S. Duan, Y. Chen, X. Wang, Y. Luo, *J. Am. Chem. Soc.* **2013**, *135*, 12468.
- [328] R. K. Joshi, P. Carbone, F. C. Wang, V. G. Kravets, Y. Su, I. V. Grigorieva, H. A. Wu, A. K. Geim, R. R. Nair, *Science* **2014**, *343*, 752.
- [329] L. Qiu, X. Zhang, W. Yang, Y. Wang, G. P. Simon, D. Li, *Chem. Commun.* **2011**, *47*, 5810.
- [330] a) M. Hu, B. Mi, *Environ. Sci. Technol.* **2013**, *47*, 3715; b) Y. Han, Y. Jiang, C. Gao, *ACS Appl. Mater. Interfaces* **2015**, *7*, 8147; c) W.-S. Hung, C.-H. Tsou, M. De Guzman, Q.-F. An, Y.-L. Liu, Y.-M. Zhang, C.-C. Hu, K.-R. Lee, J.-Y. Lai, *Chem. Mater.* **2014**, *26*,

- 2983; d) G. Srinivas, J. W. Burrell, J. Ford, T. Yildirim, *J. Mater. Chem.* **2011**, *21*, 11323.
- [331] H. W. Kim, H. W. Yoon, S.-M. Yoon, B. M. Yoo, B. K. Ahn, Y. H. Cho, H. J. Shin, H. Yang, U. Paik, S. Kwon, J.-Y. Choi, H. B. Park, *Science* **2013**, *342*, 91.
- [332] Z. P. Smith, B. D. Freeman, *Angew. Chem., Int. Ed.* **2014**, *53*, 10286.
- [333] F. Perreault, A. Fonseca de Faria, M. Elimelech, *Chem. Soc. Rev.* **2015**, *44*, 5861.
- [334] Y. Zhao, Y. Xie, Z. Liu, X. Wang, Y. Chai, F. Yan, *Small* **2014**, *10*, 4521.
- [335] J. Sakamoto, J. van Heijst, O. Lukin, A. D. Schlüter, *Angew. Chem., Int. Ed.* **2009**, *48*, 1030.
- [336] K. S. Novoselov, A. K. Geim, S. V. Morozov, D. Jiang, Y. Zhang, S. V. Dubonos, I. V. Grigorieva, A. A. Firsov, *Science* **2004**, *306*, 666.
- [337] a) N. A. A. Zwaneveld, R. Pawlak, M. Abel, D. Catalin, D. Gigmes, D. Bertin, L. Porte, *J. Am. Chem. Soc.* **2008**, *130*, 6678; b) I. Berlanga, M. L. Ruiz-González, J. M. González-Calbet, J. L. G. Fierro, R. Mas-Ballesté, F. Zamora, *Small* **2011**, *7*, 1207; c) J. W. Colson, A. R. Woll, A. Mukherjee, M. P. Levendorf, E. L. Spitzer, V. B. Shields, M. G. Spencer, J. Park, W. R. Dichtel, *Science* **2011**, *332*, 228.
- [338] a) L. Grill, M. Dyer, L. Lafferentz, M. Persson, M. V. Peters, S. Hecht, *Nat. Nanotechnol.* **2007**, *2*, 687; b) M. Bieri, M. Treier, J. Cai, K. Ait-Mansour, P. Ruffieux, O. Gröning, P. Gröning, M. Kastler, R. Rieger, X. Feng, K. Müllen, R. Fasel, *Chem. Commun.* **2009**, *0*, 6919.
- [339] a) P. Amo-Ochoa, L. Welte, R. González-Prieto, P. J. Sanz Miguel, C. J. Gómez-García, E. Mateo-Martí, S. Delgado, J. Gómez-Herrero, F. Zamora, *Chem. Commun.* **2010**, *46*, 3262; b) M. Abel, S. Clair, O. Ourdjini, M. Mossoyan, L. Porte, *J. Am. Chem. Soc.* **2011**, *133*, 1203; c) T. Bauer, Z. Zheng, A. Renn, R. Enning, A. Stemmer, J. Sakamoto, A. D. Schlüter, *Angew. Chem., Int. Ed.* **2011**, *50*, 7879.
- [340] a) P. Kissel, R. Erni, W. B. Schweizer, M. D. Rossell, B. T. King, T. Bauer, S. Götzinger, A. D. Schlüter, J. Sakamoto, *Nat. Chem.* **2012**, *4*, 287; b) P. Kissel, D. J. Murray, W. J. Wulfstange, V. J. Catalano, B. T. King, *Nat. Chem.* **2014**, *6*, 774; c) M. J. Kory, M. Wörle, T. Weber, P. Payamyar, S. W. v. d. Poll, J. Dshemuchadse, N. Trapp, A. D. Schlüter, *Nat. Chem.* **2014**, *6*, 779.
- [341] a) A. Corma, V. Fornes, S. B. Pergher, T. L. M. Maesen, J. G. Buglass, *Nature* **1998**, *396*, 353; b) M. Choi, K. Na, J. Kim, Y. Sakamoto, O. Terasaki, R. Ryoo, *Nature* **2009**, *461*, 246.
- [342] K. Varoon, X. Zhang, B. Elyassi, D. D. Brewer, M. Gettel, S. Kumar, J. A. Lee, S. Maheshwari, A. Mittal, C.-Y. Sung, M. Cococcioni, L. F. Francis, A. V. McCormick, K. A. Mkhoyan, M. Tsapatsis, *Science* **2011**, *334*, 72.
- [343] K. V. Agrawal, B. Topuz, T. C. T. Pham, T. H. Nguyen, N. Sauer, N. Rangnekar, H. Zhang, K. Narasimharao, S. N. Basahel, L. F. Francis, C. W. Macosko, S. Al-Thabaiti, M. Tsapatsis, K. B. Yoon, *Adv. Mater.* **2015**, *27*, 3243.
- [344] K. V. Agrawal, B. Topuz, Z. Jiang, K. Nguenkam, B. Elyassi, L. F. Francis, M. Tsapatsis, M. Navarro, *AIChE J.* **2013**, *59*, 3458.
- [345] W.-g. Kim, S. Nair, *Chem. Eng. Sci.* **2013**, *104*, 908.
- [346] Y. Peng, Y. Li, Y. Ban, H. Jin, W. Jiao, X. Liu, W. Yang, *Science* **2014**, *346*, 1356.
- [347] N. Widjojo, T.-S. Chung, S. Kulprathipanja, *J. Membr. Sci.* **2008**, *325*, 326.
- [348] a) L. Y. Jiang, T. S. Chung, S. Kulprathipanja, *AIChE J.* **2006**, *52*, 2898; b) L. Y. Jiang, T. S. Chung, S. Kulprathipanja, *J. Membr. Sci.* **2006**, *276*, 113.
- [349] a) I. F. J. Vankelecom, S. Van den broeck, E. Merckx, H. Geerts, P. Grobet, J. B. Uytterhoeven, *J. Phys. Chem.* **1996**, *100*, 3753; b) H. H. Yong, H. C. Park, Y. S. Kang, J. Won, W. N. Kim, *J. Membr. Sci.* **2001**, *188*, 151; c) S. R. Venna, M. Lartey, T. Li, A. Spore, S. Kumar, H. B. Nulwala, D. R. Luebke, N. L. Rosi, E. Albenze, *J. Mater. Chem. A* **2015**, *3*, 5014.
- [350] P. S. Goh, A. F. Ismail, S. M. Sanip, B. C. Ng, M. Aziz, *Sep. Purif. Technol.* **2011**, *81*, 243.
- [351] M. J. C. Ordoñez, K. J. Balkus, J. P. Ferraris, I. H. Musselman, *J. Membr. Sci.* **2010**, *361*, 28.
- [352] S. M. Meckler, C. Li, W. L. Queen, T. E. Williams, J. R. Long, R. Buonsanti, D. J. Milliron, B. A. Helms, *Chem. Mater.* **2015**, *27*, 7673.
- [353] a) H. K. Arslan, O. Shekhah, J. Wohlgemuth, M. Franzreb, R. A. Fischer, C. Wöll, *Adv. Funct. Mater.* **2011**, *21*, 4228; b) L. Heinke, M. Tu, S. Wannapaiboon, R. A. Fischer, C. Wöll, *Microporous Mesoporous Mater.* **2015**, *216*, 200; c) B. Liu, O. Shekhah, H. K. Arslan, J. Liu, C. Wöll, R. A. Fischer, *Angew. Chem., Int. Ed.* **2012**, *51*, 807; d) M. Tsotsalas, J. Liu, B. Tettmann, S. Grosjean, A. Shahnas, Z. Wang, C. Azucena, M. Addicoat, T. Heine, J. Lahann, J. Overhage, S. Bräse, H. Gliemann, C. Wöll, *J. Am. Chem. Soc.* **2014**, *136*, 8.
- [354] R. Ameloot, F. Vermoortele, W. Vanhove, M. B. Roeffaers, B. F. Sels, D. E. De Vos, *Nat. Chem.* **2011**, *3*, 382.
- [355] A. J. Brown, N. A. Brunelli, K. Eum, F. Rashidi, J. R. Johnson, W. J. Koros, C. W. Jones, S. Nair, *Science* **2014**, *345*, 72.
- [356] a) A. Dong, X. Ye, J. Chen, Y. Kang, T. Gordon, J. M. Kikkawa, C. B. Murray, *J. Am. Chem. Soc.* **2011**, *133*, 998; b) E. L. Rosen, R. Buonsanti, A. Llordes, A. M. Sawvel, D. J. Milliron, B. A. Helms, *Angew. Chem., Int. Ed.* **2012**, *51*, 684; c) S. E. Doris, J. J. Lynch, C. Li, A. W. Wills, J. J. Urban, B. A. Helms, *J. Am. Chem. Soc.* **2014**, *136*, 15702.
- [357] A. Dąbrowski, *Adv. Colloid Interface Sci.* **2001**, *93*, 135.
- [358] H. B. Tanh Jeazet, C. Staudt, C. Janiak, *Dalton Trans.* **2012**, *41*, 14003.
- [359] R. Lin, L. Ge, L. Hou, E. Strounina, V. Rudolph, Z. Zhu, *ACS Appl. Mater. Interfaces* **2014**, *6*, 5609.
- [360] a) R. Semino, N. A. Ramsahye, A. Ghoufi, G. Maurin, *ACS Appl. Mater. Interfaces* **2016**, *8*, 809; b) I. Erucar, S. Keskin, *Chem. Rec.* **2016**, *16*, 703; c) M. Benzaqui, R. Semino, N. Menguy, F. Carn, T. Kundu, J.-M. Guigner, N. B. McKeown, K. J. Msayib, M. Carta, R. Malpass-Evans, C. Le Guillouzer, G. Clet, N. A. Ramsahye, C. Serre, G. Maurin, N. Steunou, *ACS Appl. Mater. Interfaces* **2016**, *8*, 27311.
- [361] R. Pelton, *Langmuir* **2014**, *30*, 15373.
- [362] J. Kundu, T. Pascal, D. Prendergast, S. Whitelam, *Phys. Chem. Chem. Phys.* **2016**, *18*, 21760.